Pisias, N.G., Mayer, L.A., Janecek, T.R., Palmer-Julson, A., and van Andel, T.H. (Eds.), 1995
Proceedings of the Ocean Drilling Program, Scientific Results, Vol. 138

12. PLEISTOCENE THROUGH MIOCENE CALCAREOUS NANNOFOSSILS FROM EASTERN EQUATORIAL PACIFIC OCEAN (LEG 138)[1]

Isabella Raffi[2] and José-Abel Flores[3]

ABSTRACT

The calcareous nannofossil biostratigraphy of the sediments retrieved during Leg 138 in the eastern equatorial Pacific Ocean is presented and discussed. The sedimentary sequences stidoed, at 10 of the 11 sites drilled, span the stratigraphic interval from Pleistocene to upper (Sites 847 and 848) and middle Miocene (Sites 851, 852, and 853), and three extend to the upper part of the lower Miocene (Sites 844, 845, and 846). Most of the zonal boundaries of the 1973 zonation of Bukry and standard 1971 zonation of Martini are recognized and used for the biostratigraphic classification of these low-latitude sediments. Additional biostratigraphic events are discussed and in some intervals are used as secondary criteria for improving the biostratigraphic resolution. A further subdivision of upper Miocene Subzone CN9b of Okada and Bukry (1980) is proposed using the lowest and highest occurrences of *Amaurolithus amplificus.*

Comments on the biochronology of calcareous nannofossils are given, with special reference to Miocene events, taking advantage of the very good magnetostratigraphy and orbitally tuned time scale produced for the Leg 138 sites.

INTRODUCTION

During Ocean Drilling Program (ODP) Leg 138, the Neogene sediments of the eastern equatorial Pacific Ocean were sampled. This leg was the fifth in a series designed to recover high-quality sedimentary sections in the tropical oceans for detailed studies of global climate change during late Cenozoic time. During previous cruises sediments were drilled in the western equatorial Pacific (Leg 130), the western tropical Indian Ocean (Leg 117), the Peru Current region (Leg 112), and the equatorial Atlantic Ocean (Leg 108). The major scientific objective of Leg 138 was to study Neogene paleoceanographic evolution in the highly productive waters of this region. Continuous sedimentary records, suitable for high-resolution paleoceanographic studies, were constructed by splicing together stratigraphic sections recovered by drilling adjacent and offset holes with the advanced hydraulic piston corer (APC) and the extended core barrel (XCB). Along two complementary north-south transects (95°W and 110°W), 11 sites (42 holes) were drilled and more than 5500 m of cores was recovered (Fig. 1 and Table 1). Complete recovery of the stratigraphic section occurred at 8 of the 11 sites, and composite depth sections were constructed by using multiple measurements of sediment density (GRAPE) and other sedimentary parameters (see Hagelberg et al., in Mayer, Pisias, Janecek, et al., 1992). The sediments recovered range in age from the Miocene to Pleistocene. In six of the recovered sequences, high-quality magnetostratigraphic data were obtained (Leg 138 *Init. Repts.* volume; Schneider, this volume), and these provide an excellent stratigraphic framework (e.g., Site 845; Schneider, this volume). This allows us to calibrate several nannofossil events to the magnetic polarity time scale and provides new biochronologic data for the Miocene (Table 2).

In this study, we comment on (1) the Pleistocene-to-Miocene calcareous nannofossil biostratigraphy and biostratigraphic resolution in the eastern equatorial Pacific; (2) the biostratigraphic classification and age assignment of 10 of the 11 sites drilled during Leg 138; and (3) some aspects of the late Neogene chronostratigraphy and calcareous nannofossil biochronology.

Details about the distribution patterns and biomagnetostratigraphy of some middle and late Miocene calcareous nannofossil index species are reported and discussed in Raffi et al. (this volume), who collected quantitative data from some of the Leg 138 sections.

METHODS

Smear slides of each sample were prepared from unprocessed material and were examined with a light microscope at ×1400 magnification under cross-polarized and transmitted light. Approximately 2400 samples were examined. We examined approximately 200 fields of view in each slide, primarily those areas where the sample material had optimum density and where no appreciable piling of specimens had occurred (with an average number of 50 specimens per field). In each slide, the nannofossil assemblage was characterized, and the abundance of nannofossils was estimated in a semiquantitative fashion. To check for the presence or absence of index species in critical stratigraphic intervals, we used the quantitative counting techniques of Thierstein et al. (1977), Backman and Shackleton (1983), Rio et al. (1990a, 1990b), and Fornaciari et al. (1990). To detect index species events, we counted variable numbers of nannofossils, depending on the abundance of all nannofossils in the assemblage and on the abundance of the specific index species. For example, the presence or absence of index species belonging to discoasterids, helicoliths, sphenoliths, and ceratolithids was evaluated by counting a fixed number of forms belonging to the group (100–200 discoasterids, 100 helicoliths and sphenoliths, and 20–30 ceratolithids).

All the biostratigraphic events (Fig. 2) reported in Tables 3–12 and Figures 3–12 have been quantitatively defined.

In the range charts that we present of selected sites, only selected samples have been plotted. Abundance and preservation have been semiquantitatively and qualitatively evaluated, respectively. The abundance code is as follows:

A (abundant) = usually >10 specimens observed per field;
C (common) = 1–10 specimens per field;
F (few) = 1 specimen per 1–10 fields; and
R (rare) = <1 specimen per 10 fields.

[1] Pisias, N.G., Mayer, L.A., Janecek, T.R., Palmer-Julson, A., and van Andel, T.H. (Eds.), 1995. *Proc. ODP, Sci. Results,* 138: College Station, TX (Ocean Drilling Program).

[2] Istituto di Geologia, Università di Parma, c/o Villa Cybo, 00040 Castelgandolfo, Italy. (Current address: Università degli Studi "G. D'Annunzio," Chieti - Facoltà di Scienze Matematiche, Fisiche e Naturali, Italy.)

[3] Universidad de Salamanca, Departamento de Geologia, Paleontologia, 37008 Salamanca, Spain.

Table 1. Summary of Leg 138 sites.

Site	Latitude	Longitude	Water depth (m)
844	7°55.28N	90°28.85W	3425.0
845	9°34.95N	94°35.45W	3715.9
846	3°5.70N	90°49.08W	3295.6
847	0°11.59S	95°19.23W	3346.0
848	2°59.63S	110°28.79W	3867.3
849	0°10.98N	110°31.18W	3850.8
850	1°17.83N	110°31.29W	3797.8
851	2°46.22N	110°34.31W	3772.0
852	5°17.57N	110°4.58W	3871.6
853	7°12.66N	109°45.08W	3727.2

Table 2. Calcareous nannofossil events and age estimates.

Event	Zone (base)	Adopted age (Ma)	Reference
B acme *Emiliania huxleyi*		0.085–0.073	1
B *Emiliania huxleyi*	CNs15	0.26	1
T *Pseudoemiliania lacunosa*	CN14b	0.461	1
Reentrance medium *Gephyrocapsa* spp.	CN14a (?)	1.028	2
T large *Gephyrocapsa* spp.		1.24	2
B large *Gephyrocapsa* spp.		1.457	2
T *Calcidiscus macintyrei*		1.597	2
B medium *Gephyrocapsa* spp.	CN13b (?)	1.67	2
T *Discoaster brouweri*	CN13a	1.96–0.11	3
T *Discoaster pentaradiatus*	CN12d	2.44–0.06	3
T *Discoaster surculus*	CN12c	2.61–0.09	3
T *Discoaster tamalis*	CN12b	2.76–0.01	3
T *Sphenolithus* spp.	CN12aB	3.65–0.05	3
T *Reticulofenestra pseudoumbilicus*	CN12aA	3.804–0.003	3
B *Ceratolithus rugosus*	CN10c	5.04–0.03	3
B *Ceratolithus acutus*	CN10b	5.34– 0.02	3
T *Triquetrorhabdulus rugosus*		5.34– 0.02	3
T *Discoaster quinqueramus*	CN10a	5.56–0.04	3
T *Amaurolithus amplificus*	CN9bC	5.88–0.02	3
B *Amaurolithus amplificus*	CN9bB	6.50–0.06	3
T absence interval *R. pseudoumbilicus*		6.80–0.2	3
B *Amaurolithus primus*	CN9bA	7.24–0.12	3
B *Discoaster berggrenii*	CN9a	8.35–0.11	3
B *Discoaster loeblichii*	CN8b	8.43–0.08	3
B absence interval *R. pseudoumbilicus*		8.85–0.3	3
B *Minylitha convallis*		9.43–0.04	3
T *Discoaster hamatus*	CN8a	9.36–0.12	3
B *Discoaster neohamatus*		9.56–0.11	3
B *Discoaster hamatus*	CN7	10.39–0.12	3
T *Coccolithus miopelagicus*		10.39–0.1	3
B *Catinaster coalitus*	CN6	10.71–0.01	3
T c *Discoaster kugleri*		11.34–0.03	3
B c *Discoaster kugleri*		11.74–0.04	3
B *Discoaster kugleri*	CN5b	12.20–0.2	3
T *Coronocyclus nitescens*		12.12–0.01	3
T *Calcidiscus macintyrei*		12.34–0.01	3
T *Calcidiscus premacintyrei*		12.65–0.02	3
B *Triquetrorhabdulus rugosus*		12.62–0.02	3
T *Discoaster signus*		12.73–0.01	3
T *Cyclicargolithus floridanus*		13.19–0.01	3
T *Sphenolithus heteromorphus*	CN5a	13.57–0.05	3
T *Helicosphaera ampliaperta*	CN4	15.83	4
B *Discoaster signus*		16.19–0.01	3
End acme *Discoaster deflandrei*		16.21–0.01	3

Notes: T = top occurrence, B = bottom occurrence, T c = top occurrence of common and continuous species, and B c = bottom occurrence of common and continuous species. References are as follows: 1 = Thierstein et al. (1977), 2 = Raffi et al. (1993), 3 = this study, and Shackleton et al. (this volume), and 4 = reestimated from Backman et al. (1990).

The qualitative evaluation of the state of preservation of the calcareous nannofossils found within each sample was made with the following criteria:

G (good) = specimens exhibit little or no dissolution and/or overgrowth;

M–G (moderate to good) = specimens exhibit slight to moderate dissolution and/or overgrowth, and the identification of some species is hampered;

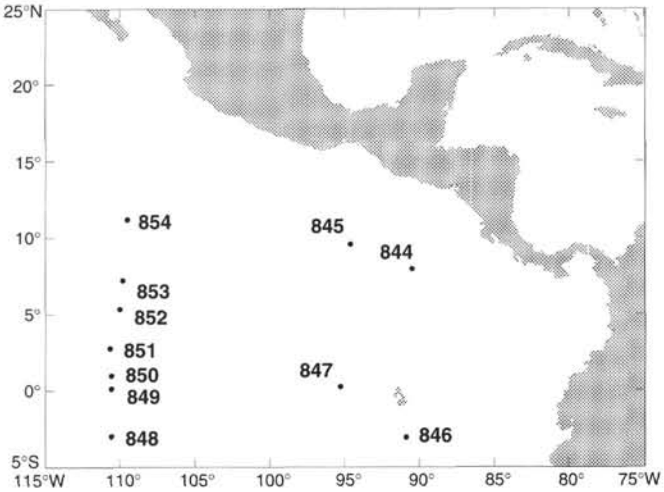

Figure 1. Location map for Leg 138 sites.

M (moderate) = specimens exhibit moderate dissolution and/or overgrowth, and identification is difficult at the specific level; and

P (poor) = specimens exhibit extreme dissolution and/or overgrowth.

These categories were determined on the basis of the "average" state of preservation of the calcareous nannofossils examined on the smear slides. Considerable variation in the state of preservation of the individual specimens can be observed in the same sample.

In the range charts, the degree of etching (E) and overgrowth (O) is also reported, following the criteria proposed by Roth and Thierstein (1972) and modified by Roth (1983), as follows:

E=0 and O=0: no sign of dissolution and overgrowth;
E=1 and O=1: slight dissolution and overgrowth;
E=2 and O=2: moderate dissolution and overgrowth; and
E=3 and O=3: severe effects of dissolution and overgrowth.

The taxa we consider here are reported in alphabetic order and by generic epithets in Appendix A. Bibliographic references for these species are given in Loeblich and Tappan (1966, 1968, 1969, 1970a, 1970b, 1971, 1973) and Aubry (1984, 1988, 1989, 1990). The taxonomic concepts we used in this study primarily followed those of Rio et al. (1990a) and are summarized below (see "Taxonomic Notes" section, this chapter).

BIOSTRATIGRAPHY

Here, we give a general discussion on the biostratigraphy obtained in the sedimentary sequences recovered during Leg 138. We refer to the zonal schemes of Martini (1971) and Bukry (1973, 1978), which were code numbered by Okada and Bukry (1980) and are regarded as the "standard" for the biostratigraphic classification of Cenozoic marine sediments. These zonations have been applied to all the stratigraphic intervals with relative ease. In addition to the known zonal boundaries in the Pleistocene and upper Miocene, we record other bioevents that improve the biostratigraphic resolution of the two standard zonations. In Figure 2, we report the recognized nannofossil events, the zones, and the adopted definitions, together with the adopted biochronology and chronostratigraphy. Details on the biostratigraphic results of each section are reported in the individual site chapters below.

Pleistocene

The Pleistocene biostratigraphic classification is based on the biozonation of Gartner (1977) and on recent data from a biochronologic study of low- and mid-latitude, deep-sea records (Raffi et al., 1993).

Table 3. Position of calcareous nannofossil events at Site 844.

Event	Interval (cm)	Depth (mcd)	Interval (cm)	Depth (mcd)
T *Pseudoemiliania lacunosa*	844B-1H-CC/2H-1, 120	4.53–6.83		
Reentrance medium *Gephyrocapsa* spp.	844B-2H-4, 120/2H-5, 120	11.13–12.63		
T large *Gephyrocapsa* spp.	844B-2H-5, 120/2H-6, 120	12.63–14.13		
B large *Gephyrocapsa* spp.	844B-2H-7, 47/2H-CC	14.90–15.61		
T *Calcidiscus macintyrei*	844B-2H-CC/3H-1, 120	15.61–17.45		
B medium *Gephyrocapsa* spp.	844B-3H-2, 60/3H-2, 120	18.35–18.95		
T *Discoaster brouweri*	844B-3H-3, 85/3H-3, 120	20.10–20.45		
T *Discoaster pentaradiatus*	844C-3H-1, 83/3H-2, 83	21.78–23.28		
T *Discoaster surculus*	844C-3H-2, 83/3H-3, 83	23.28–24.78		
B *Ceratolithus acutus*	844C-4H-1, 30/4H-1, 50	32.55–32.75	844D-1H-3, 75/1H-3, 100	32.45–32.70
T *Discoaster quinqueramus*	844C-4H-1, 75/4H-1, 100	33.00–33.25	844D-1H-3, 125/1H-3, 150	32.95–33.20
T *Amaurolithus amplificus*	844C-4H-2, 125/4H-2, 145	35.00–35.20		
B *Amaurolithus amplificus*	844B-5H-2, 60/5H-2, 90	39.04–39.34		
T absence interval *R. pseudoumbilicus*	844B-5H-3, 90/5H-3, 120	40.84–41.14		
B *Amaurolithus primus*	844B-5H-4, 120/5H-5, 29	42.35–42.94		
T *Minylitha convallis*	844C-5H-3, 2/5H-3, 50	45.87–46.35		
B *Discoaster berggrenii*	844B-6H-4, 60/6H-4, 150	51.70–52.60	844C-5H-7, 30/6H-1, 70	52.15–54.45
B *Discoaster pentaradiatus*	844B-6H-4, 150/6H-5, 60	52.60–53.20		
B *Discoaster loeblichii*	844B-6H-5, 60/6H-6, 60	53.20–54.70		
B absence interval *R. pseudoumbilicus*	844C-6H-2, 70/6H-2, 90	55.95–56.15		
B *Minylitha convallis*	844C-6H-5, 5/6H-5, 30	59.80–60.05		
T *Discoaster hamatus*	844B-7H-1, 100/7H-1, 120	59.90–60.10	844C-6H-5, 5/6H-5, 30	59.80–60.05
B *Discoaster hamatus*	844B-8H-1, 60/8H-2, 60	69.26–70.76	844C-7H-5, 2/7H-5, 25	70.27–70.50
T *Coccolithus miopelagicus*	844B-8H-2, 60/8H-3, 60	70.76–72.26	844C-7H-5, 125/7H-6, 2	71.50–71.77
B *Catinaster coalitus*	844B-8H-4, 120/8H-5, 60	74.36–75.26		
T c *Discoaster kugleri*	844B-10H-1, 60/10H-2, 60	91.73–93.23		
B c *Discoaster kugleri*	844B-11H-4, 60/11H-4, 120	108.60–109.20		
B *Discoaster kugleri*	844B-13H-4, 60/13H-4, 120	127.90–128.50		
T *Coronocyclus nitescens*	844B-13H-4, 120/13H-5, 60	128.50–129.40		
T *Calcidiscus premacintyrei*	844B-14H-5, 120/14H-6, 120	140.53–142.03		
B *Triquetrorhabdulus rugosus*	844B-15H-4, 120/15H-5, 60	148.70–149.60		
T *Discoaster signus*	844B-15H-7, 40/16H-1, 120	152.40–154.88		
T *Cyclicargolithus floridanus*	844B-17H-6, 120/17H-7, 60	171.30–172.20		
T *Sphenolithus heteromorphus*	844B-19H-4, 65/19H-4, 120	188.35–188.90		
B *Reticulofenestra pseudoumbilicus*	844B-19H-4, 65/19H-4, 120	188.35–188.90		
T *Helicosphaera ampliaperta*	844B-26X-3, 120/26X-4, 90	256.13–258.46		
B *Discoaster signus*	844B-28X-2, 60/28X-2, 122	273.33–273.95		

Notes: T = top occurrence, B = bottom occurrence, T c = top occurrence of common and continuous species, and B c = bottom occurrence of common and continuous species. Depths in meters composite depth (mcd).

Table 4. Position of calcareous nannofossil events at Site 845.

Event	Interval (cm)	Depth (mcd)	Interval (cm)	Depth (mcd)
T *Pseudoemiliania lacunosa*	845A-2H-CC/3H-1, 42	18.09–18.38		
Reentrance medium *Gephyrocapsa* spp.	845A-3H-4, 42/3H-5, 42	22.88–24.38		
T large *Gephyrocapsa* spp.	845A-3H-7, 42/3H-CC	27.38–27.85		
B large *Gephyrocapsa* spp.	845A-4H-1, 42/4H-2, 42	29.15–30.65		
T *Calcidiscus macintyrei*	845A-4H-3, 42/4H-4, 42	32.15–33.65		
B medium *Gephyrocapsa* spp.	845A-4H-6, 43/4H-7, 42	36.66–38.15		
T *Discoaster brouweri*	845A-5H-3, 42/5H-3, 150	43.03–44.38		
T *Discoaster pentaradiatus*	845A-5H-7, 50/5H-CC	49.11–49.60		
B *Ceratolithus acutus*	845A-8H-5, 94/8H-5, 120	77.84–78.10		
T *Discoaster quinqueramus*	845A-8H-6, 120/8H-7, 12	79.60–80.01		
B *Amaurolithus amplificus*	845A-10H-3, 120/10H-4, 13	96.28–96.71		
T absence interval *R. pseudoumbilicus*	845A-10H-5, 90/10H-5, 145	98.98–99.53		
B *Amaurolithus primus*	845A-11H-2, 32/11H-4, 32	104.68–107.68		
B *Discoaster berggrenii*	845A-13H-1, 145/13H-2, 45	126.16–126.66	845B-12H-4, 150/12H-5, 150	125.08–126.58
B *Discoaster hamatus*	845A-15H-7, 50/16H-1, 42	156.46–158.85	845B-15H-2, 120/15H-2, 145	157.10–157.35
T *Coccolithus miopelagicus*	845A-16H-1, 42/16H-1, 120	158.75–159.53	845B-15H-4, 20/15H-4, 40	159.10–159.30
B *Catinaster coalitus*	845A-16H-4, 32/16H-4, 78	163.15–163.61		
T c *Discoaster kugleri*			845B-16H-6, 120/16H-7, 20	174.00–174.50
B c *Discoaster kugleri*			845B-17H-5, 10/17H-5, 42	181.00–181.32
T *Coronocyclus nitescens*	845A-19H-1, 78/19H-2, 42	190.54–191.68	845B-18H-5, 10/18H-5, 78	190.50–191.18
B *Discoaster kugleri*			845B-18H-5, 78/18H-5, 120	191.18–191.60
B *Calcidiscus macintyrei* (?)	845A-19H-1, 78/19H-2, 42	190.54–191.68	845B-18H-5, 78/18H-5, 120	191.18–191.60
T *Calcidiscus premacintyrei*			1845B-8H-7, 23/18H-7, 50	194.00–194.99
B *Triquetrorhabdulus rugosus*	845A-20H-4, 78/20H-5, 42	206.21–207.35		
T *Discoaster signus*	845A-20H-6, 42/20H-6, 78	208.85–209.21		
T *Cyclicargolithus floridanus*	845A-22H-1, 78/22H-1, 143	223.61–224.26		
T *Sphenolithus heteromorphus*	845A-23X-4, 46/23X-4, 86	237.29–237.69		
B *Reticulofenestra pseudoumbilicus*	845A-23X-4, 46/23X-4, 86	237.29–237.69		
T *Helicosphaera ampliaperta*	845A-27X-6, 42/27X-6, 118	278.95–279.71		
B *Discoaster signus*	845A-29X-4, 40/29X-4, 120	294.73–295.53		
T acme *Discoaster deflandrei*	845A-29X-4, 120/29X-5, 120	295.53–297.03		

Note: See note to Table 3.

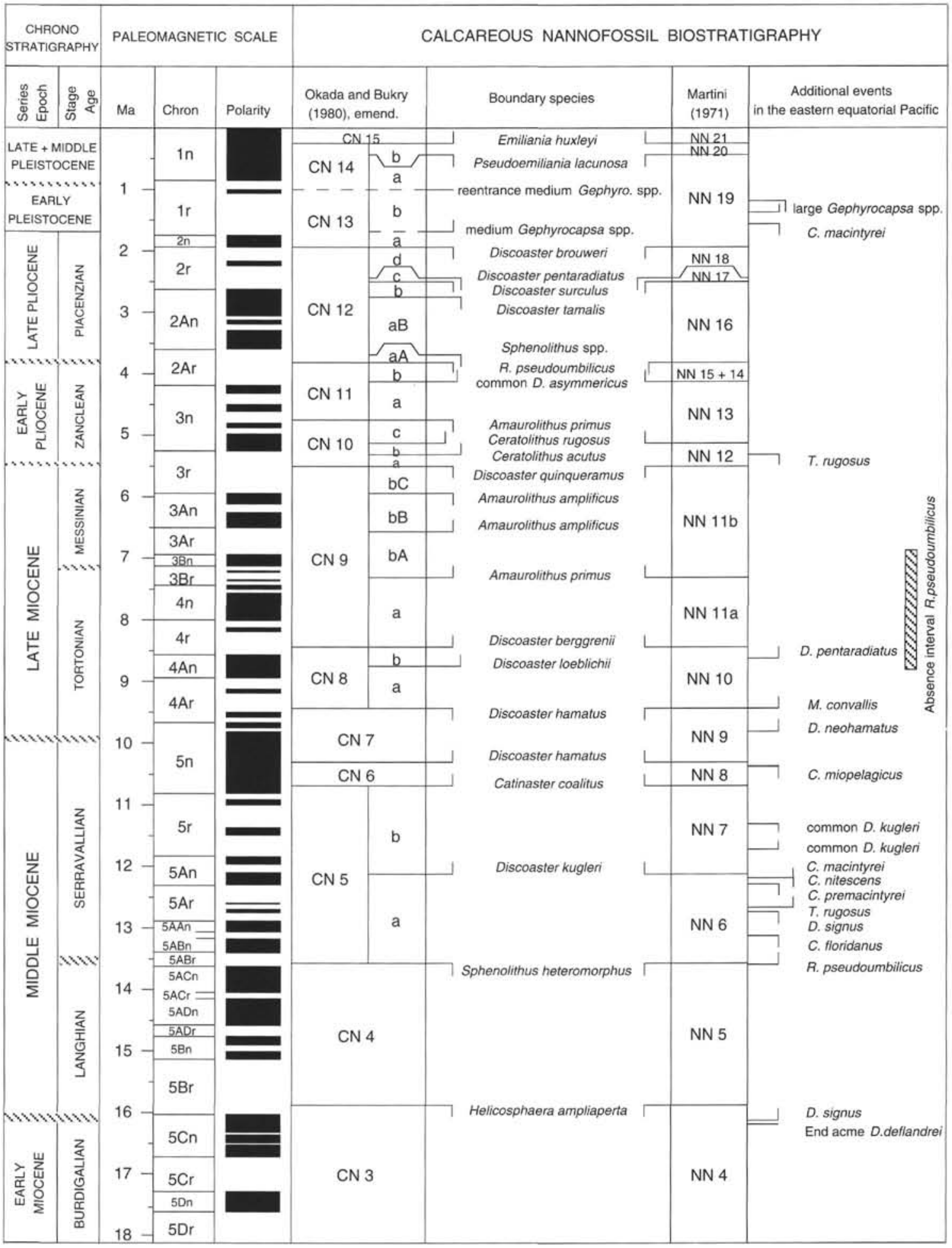

Figure 2. Adopted chronostratigraphy and calcareous nannofossil biostratigraphy and biochronology. Geomagnetic polarity time scale after Cande and Kent (1992), with revised ages after Shackleton et al. (this volume).

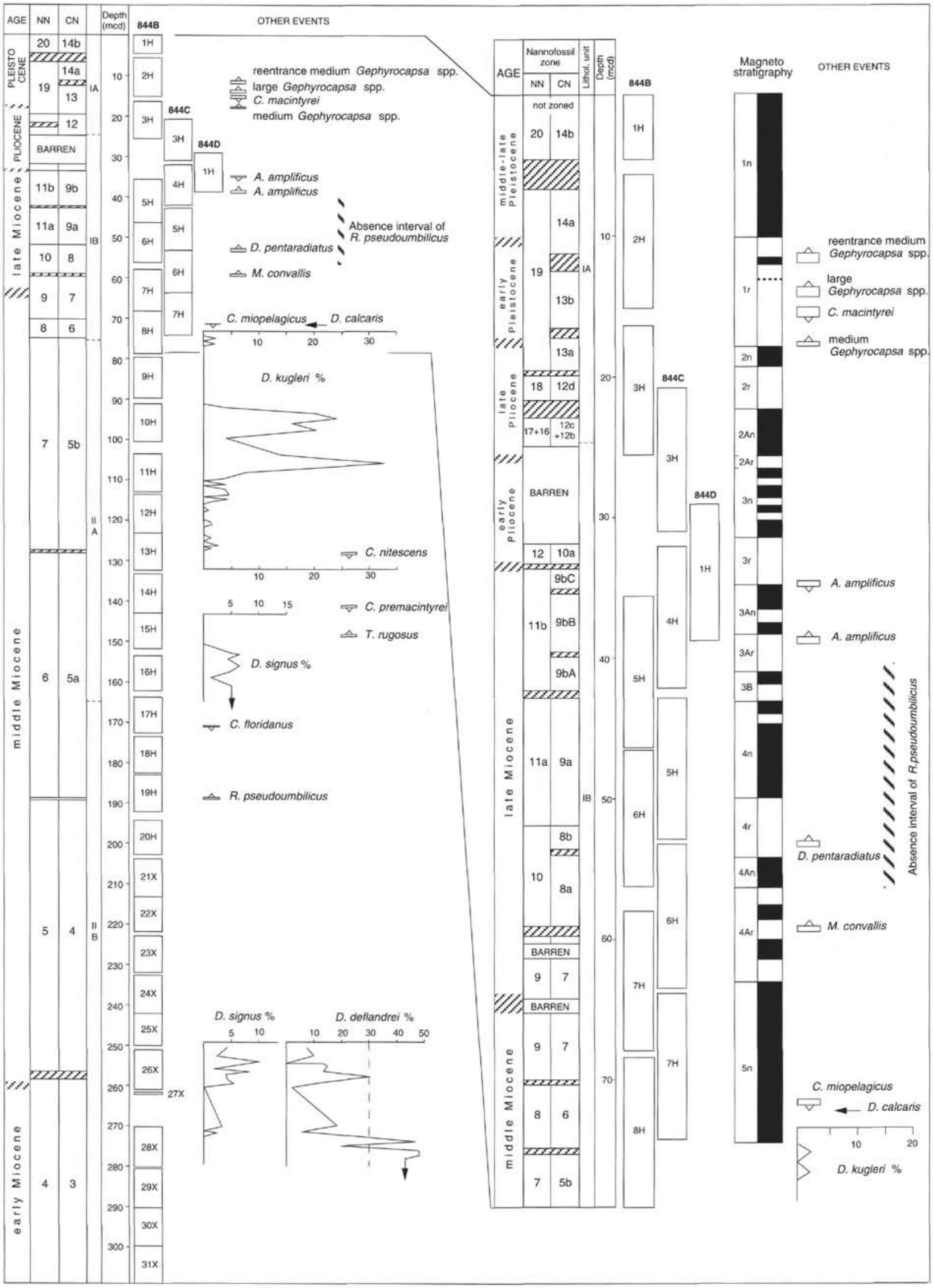

Figure 3. Chronostratigraphy and calcareous nannofossil biostratigraphy at Site 844. Magnetostratigraphy from site chapters in Mayer, Pisias, Janecek, et al. (1992) and Schneider et al. (this volume). "Striped" areas at zonal boundaries represent intervals (sample spacing) within which biostratigraphic events occur.

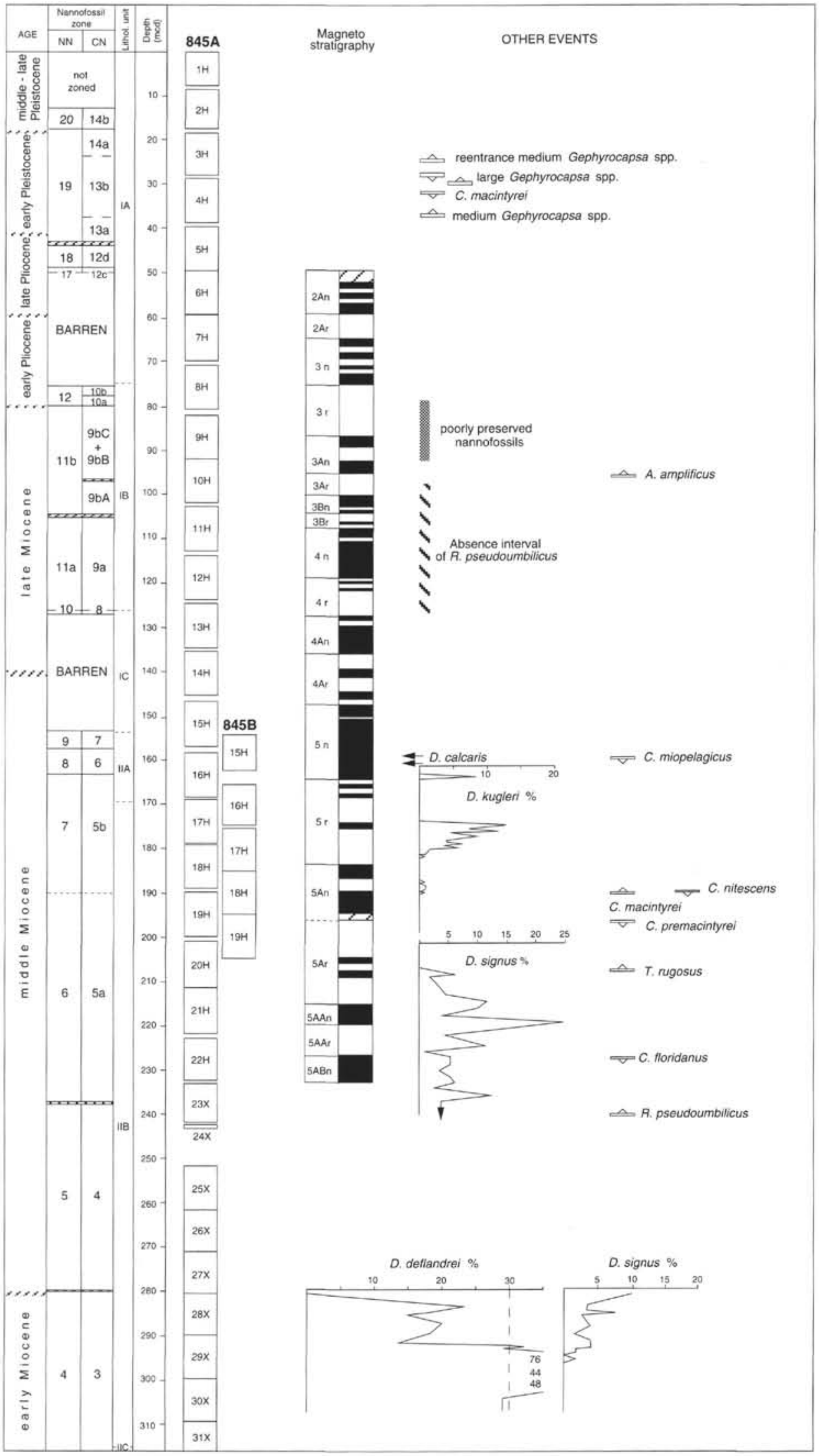

Figure 4. Chronostratigraphy and calcareous nannofossil biostratigraphy at Site 845. Notation as specified in Figure 3.

Table 5. Position of calcareous nannofossil events at Site 846.

Event	Interval (cm)	Depth (mcd)
Pseudoemiliania lacunosa	846B-2H-7, 20/2H-CC, 5	16.80–17.39
Reentrance medium *Gephyrocapsa* spp.	846B-4H-6, 45/4H-6, 120	37.10–37.85
T large *Gephyrocapsa* spp.	846B-5H-3, 120/5H-4, 40	44.90–45.60
B large *Gephyrocapsa* spp.	846B-6H-3, 120/6H-4, 39	55.70–56.39
T *Calcidiscus macintyrei*	846B-6H-5, 40/6H-5, 120	57.90–58.70
B medium *Gephyrocapsa* spp.	846B-6H-6, 40/6H-CC, 5	59.40–60.04
T *Discoaster brouweri*	846B-8H-3, 43/8H-3, 120	77.13–77.90
T *Discoaster surculus*	846B-10H-1, 60/10H-1, 135	96.15–96.90
T *Discoaster tamalis*	846B-12H-2, 120/12H-3, 60	118.00–120.40
T *Sphenolithus* spp.	846B-14H-4, 120/14H-5, 60	143.85–144.75
T *Reticulofenestra pseudoumbilicus*	846B-14H-CC, 13/15H-1, 60	147.71–150.80
B c *Discoaster asymmetricus*	846B-15H-CC/16H-1, 60	160.32–160.80
T *Amaurolithus primus*	846B-17H-1, 120/17H-2, 50	171.95–172.75
T *Ceratolithus acutus*	846B-19H-1, 40/19H-1, 120	192.70–193.50
B *Ceratolithus rugosus*	846B-19H-3, 120/19H-4, 40	196.50–197.20
B *Ceratolithus acutus*	846B-20H-3, 120/20H-4, 50	207.80–208.60
T *Discoaster quinqueramus*	846B-21H-4, 50/21H-4, 120	219.45–220.15
T circular reticulofenestrids	846B-23X-2, 120/23X-3, 50	243.20–244.00
T *Amaurolithus amplificus*	846B-23X-3, 50/23X-3, 120	244.00–244.70
B *Amaurolithus amplificus*	846B-23X-CC, 10/24X-1, 40	250.15–252.00
B circular reticulofenestrids	846B-25X-2, 39/25X-3, 50	262.69–264.30
T absence interval *R. pseudoumbilicus*	846D-26X-4, 120/26X-5, 50	279.30–280.10
B *Amaurolithus primus*	849D-26X-6, 120/26X-7, 23	282.30–282.83
T *Minylitha convallis*	846B-29X-2, 60/29X-3, 60	301.40–302.90
B *Discoaser berggrenii*	846B-29X-5, 60/29X-5, 120	305.90–306.50
B *Discoaster loeblichii*	846B-30X-3, 60/30X-4, 60	312.60–314.10
B absence interval *R. pseudoumbilicus*	846B-30X-5, 60/30X-6, 60	315.60–317.10
B *Minylitha convallis*	846B-32X-1, 60/32X-2, 60	328.80–330.30
T *Discoaster hamatus*	846B-32X-5, 60/32X-5, 120	334.80–335.40
B *Discoaster hamatus*	846B-33X-4, 120/33X-5, 60	343.60–344.50
T *Coccolithus miopelagicus*	846B-33X-5, 120/33X-6, 60	345.10–346.00
B *Catinaster coalitus*	846B-33X-6, 120/33X-7, 34	346.60–347.24
T c *Discoaster kugleri*	846B-35X-2, 60/35X-2, 120	359.20–359.80
B c *Discoaster kugleri*	846B-36X-1, 36/36X-2, 60	367.16–368.90
B *Discoaster kugleri*	846B-38X-6, 50/38X-6, 120	394.10–394.80
T *C. floridanus* + *C. nitescens*	846B-38X-CC, 10/40X-1, 40	395.11–405.80
T *Sphenolithus heteromorphus*	846B-38X-CC, 10/40X-1, 40	395.11–405.80
B *Reticulofenestra pseudoumbilicus*	846B-38X-CC, 10/40X-1, 40	395.11–405.80
T *Helicosphaera ampliaperta*	846B-41X-CC, 9/42X-1, 79	421.87–425.49
T acme *Discoaster deflandrei*	846B-42X-CC, 12/43X-CC, 3	426.00–434.33
Discoaster signus	846B-42X-CC, 12/43X-CC, 3	426.00–434.33

Note: See note to Table 3.

Almost all the known Pleistocene nannofossil events have been observed. Because we only used the light microscope technique to examine the nannofossils, we were not able to record the appearance (CN15/CN14b and NN21/NN20 boundary) and the increase in abundance of *Emiliania huxleyi* in the upper Pleistocene interval. Detection of the other Pleistocene events follows the rationale in Rio et al. (1990b) and Raffi et al. (1993), which is primarily based on morphometric studies of gephyrocapsids. This group represents an important component of Pleistocene nannofossil assemblages (see discussion on taxonomy of gephyrocapsids in Raffi et al., 1993). A biometrically based definition of the group provides a precise tool in the correlation of lower Pleistocene sequences (Raffi et al., 1993; Rio et al., in press).

In the interval from the Chron 1n/1r.1r boundary (Brunhes/Matuyama boundary) to the top of Chron 2n (Olduvai), the nannofossil events recorded are (1) the reentrance of medium *Gephyrocapsa* spp. (mainly composed of *G. omega–G. parallela* morphotypes); (2) the disappearance of large and medium *Gephyrocapsa* spp.; (3) the first occurrence (FO) of large *Gephyrocapsa* spp.; (4) the last occurrence (LO) of *Calcidiscus macintyrei*; and (5) the FO of medium *Gephyrocapsa* spp.

The use of these events in the biostratigraphic classification of the lower–middle Pleistocene improves the stratigraphic resolution in this time interval. Note that some events correspond to the boundary definitions of the "standard" zones, and most events are isochronous over wide areas (Raffi et al., 1993). The reentrance of medium *Gephyrocapsa* spp. probably corresponds to boundary CN14a/CN13b, defined by the appearance of *G. oceanica* s.s. by Bukry (1973), who recorded *G. omega* as occurring close to this boundary.

The appearance of medium-sized *Gephyrocapsa* spp. (≥4 µm) has been used to recognize the CN13b/CN13a boundary, originally defined (Bukry, 1973) by the FO of *Gephyrocapsa caribbeanica,* a species difficult to recognize in the optical microscope. The use of the appearance of medium-sized *Gephyrocapsa* spp. allows one to define more easily the CN13b/CN13a boundary. This event occurs in the same stratigraphic interval as the FO of *G. caribbeanica* (after the LO of *Discoaster brouweri* and before the LO of *Calcidiscus macintyrei*). The appearance of medium *Gephyrocapsa* spp. represents the best approximation of the Pliocene/Pleistocene boundary, as defined in the boundary stratotype section of Vrica (southern Italy) (Aguirre and Pasini, 1985).

Table 6. Position of calcareous nannofossil events at Site 847B.

Event	Interval (cm)	Depth (mcd)
B *Emiliania huxleyi*	1H-3, 120/1H-4, 120	3.20–4.70
T *Pseudoemiliania lacunosa*	2H-5, 120/2H-6, 51	13.83–14.64
Reentrance medium *Gephyrocapsa* spp.	4H-2, 60/4H-2, 120	30.43–31.03
T large *Gephyrocapsa* spp.	5H-1, 60/5H-1, 120	38.40–39.00
B large *Gephyrocapsa* spp.	5H-7, 40/5H-CC	47.20–47.70
T *Calcidiscus macintyrei*	6H-1, 60/6H-1, 19	50.18–50.77
B medium *Gephyrocapsa* spp.	6H-3, 120/6H-4, 60	55.28–56.18
T *Discoaster brouweri*	7H-6, 60/7H-6, 120	68.85–69.45
T *Discoaster surculus*	9H-3, 60/9H-3, 120	86.08–86.68
T *Discoaster tamalis*	9H-6, 120/9H-7, 15	91.18–91.63
T *Sphenolithus* spp.	12H-3, 60/12H-3, 120	118.13–118.73
T *Reticulofenestra pseudoumbilicus*	12H-5, 60/12H-5, 120	121.13–121.73
B c *Discoaster asymmetricus*	14H-5, 60/14H-5, 124	140.58–141.22
T *Amaurolithus primus*	14H-5, 124/14H-6, 60	141.22–142.08
T *Ceratolithus acutus*	17X-3, 60/17X-4, 60	168.75–170.25
B *Ceratolithus rugosus*	17X-5, 123/17X-6, 60	172.38–173.25
B *Ceratolithus acutus*	18X-7, 3/18X-7, 15	183.78–183.90
T *Discoaster quinqueramus*	20X-3, 93/20X-4, 60	197.18–198.35

Note: See note to Table 3.

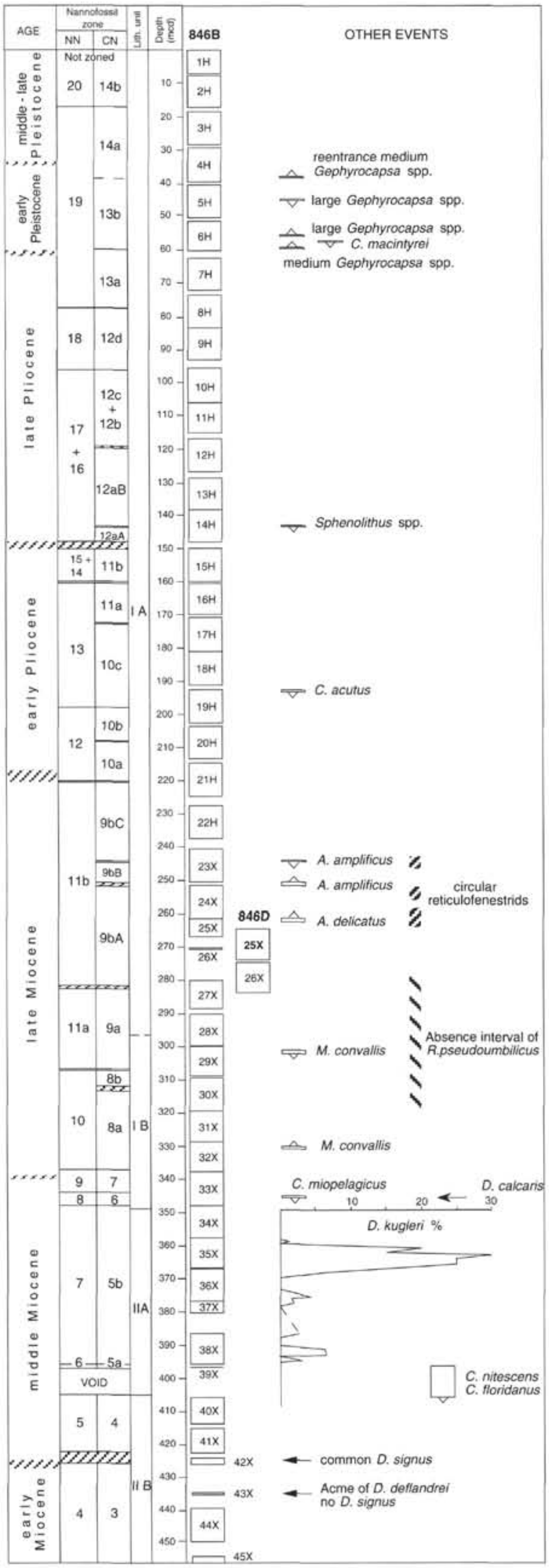

Figure 5. Chronostratigraphy and calcareous nannofossil biostratigraphy at Site 846. "Striped" areas at zonal boundaries represent intervals (sample spacing) within which biostratigraphic events occur.

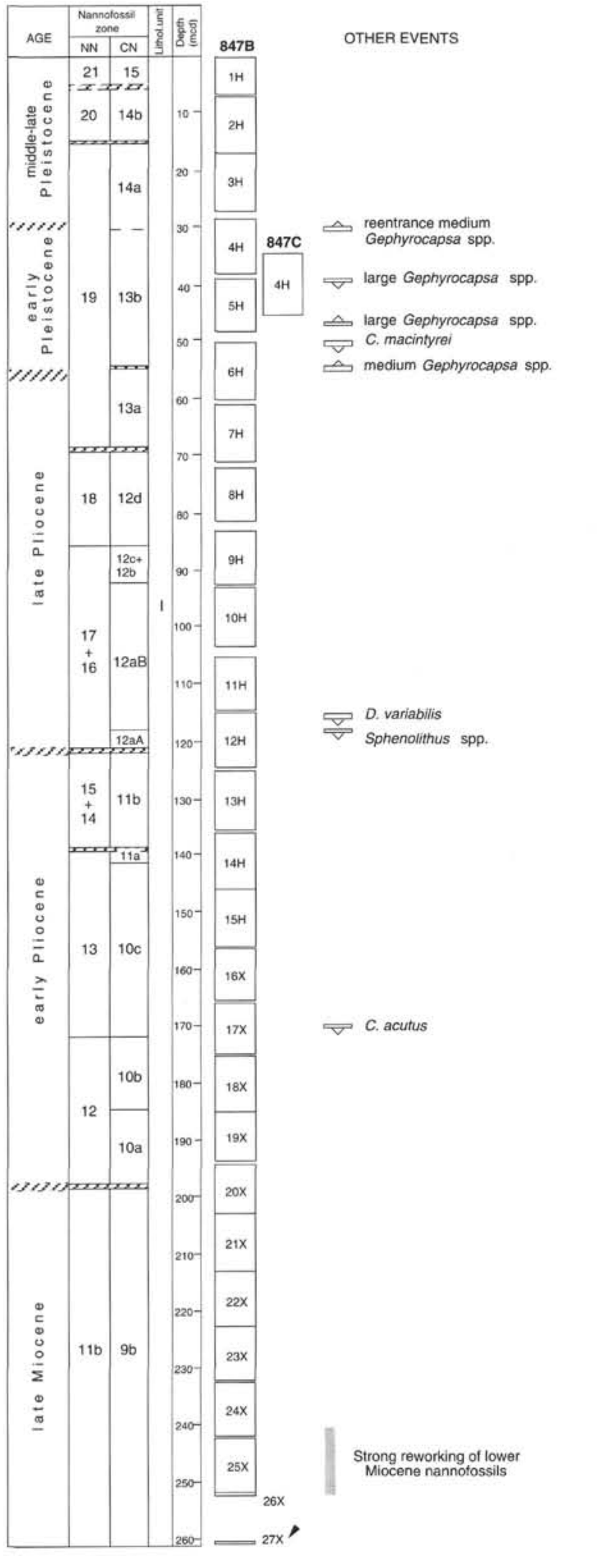

Figure 6. Chronostratigraphy and calcareous nannofossil biostratigraphy at Site 847. Notation as specified in Figure 5.

The extinction of *Helicosphaera sellii* is confirmed to be an unreliable event in the Pacific, based on the diachroneity clearly demonstrated by Backman and Shackleton (1983) and Raffi et al. (1993), who compared Pacific Ocean records with those from the Atlantic Ocean and the Mediterranean Sea (e.g., Takayama and Sato, 1987; Rio et al., 1990b). In the Leg 138 sites, this species is rare and is

Table 7. Position of calcareous nannofossil events at Site 848.

Event	Interval (cm)	Depth (mcd)
T *Pseudoemiliania lacunosa*	848A-1H-4, 60/1H-5, 60	5.3–6.8
Reentrance medium *Gephyrocapsa* spp.	848B-3H-1, 70/3H-1, 80	16.35–16.40
T large *Gephyrocapsa* spp.	848B-3H-3, 60/3H-3, 120	19.25–19.85
B large *Gephyrocapsa* spp.	848B-3H-5, 120/3H-6, 40	22.85–23.55
T *Calcidiscus macintyrei*	848C-3H-5, 20/3H-5, 40	24.22–24.42
B medium *Gephyrocapsa* spp.	848C-3H-5, 40/3H-5, 50	24.42–24.52
T *Discoaster brouweri*	848C-3H-6, 120/3H-7, 10	26.72–27.12
T *Discoaster pentaradiatus*	848B-4H-4, 40/4H-4, 80	30.45–30.85
T *Discoaster surculus*	848B-4H-4, 40/4H-4, 80	30.45–30.85
T *Discoaster tamalis*	848B-4H-5, 23/4H-5, 85	31.78–32.40
T *Sphenolithus* spp.	848B-4H-CC/5H-1, 42	35.52–36.77
T *Reticulofenestra pseudoumbilicus*	848B-5H-1, 95/5H-1, 120	37.30–37.55
B c *Discoaster asymmetricus*	848B-5H-2, 50/5H-2, 120	38.35–39.05
T *Amaurolithus primus*	848B-5H-2, 127/5H-3, 62	39.12–39.97
T *Ceratolithus acutus*	848B-6H-1, 75/6H-2, 35	46.65–47.75
B *Ceratolithus rugosus*	848B-6H-4, 35/6H-4, 65	50.75–51.05
B *Ceratolithus acutus*	848B-6H-5, 35/6H-5, 75	52.25–52.65
T *Discoaster quinqueramus*	848B-7H-1, 50/7H-1, 95	56.90–57.35
T *Amaurolithus amplificus*	848C-7H-2, 25/7H-2, 50	62.54–62.79
B *Amaurolithus amplificus*	848C-7H-6, 145/7H-7, 20	69.74–69.99
T absence interval *R. pseudoumbilicus*	848C-8H-6, 40/8H-6, 60	75.00–75.20
B *Amaurolithus primus*	848C-8H-6, 80/8H-6, 140	79.94–80.54
T *Minylitha convallis*	848B-9H-5, 85/9H-5, 119	85.15–85.89
B *Discoaster berggrenii* (?)	848B-9H-5, 119/9H-6, 40	85.89–86.60
B absence interval *R. pseudoumbilicus*	848B-9H-6, 119/9H-7, 10	86.99–87.40
B *Discoaster loeblichii*	848B-9H-6, 119/9H-7, 10	86.99–87.40
B *Minylitha convallis*	848B-10H-2, 120/10H-2, 150	91.50–91.80
T *Discoaster hamatus*	848C-10H-1, 100/10H-1, 125	93.32–93.57
T *Discoaster neohamatus*	848C-10H-2, 75/10H-2, 100	94.57–94.82
B *Discoaster hamatus*	848C-10H-5, 30/10H-5, 50	98.62–98.82
T *Coccolithus miopelagicus*	848C-10H-5, 50/10H-5, 75	98.82–99.03

Note: See note to Table 3.

Table 8. Position of calcareous nannofossil events at Site 849.

Event	Interval (cm)	Depth (mcd)	Interval (cm)	Depth (mcd)
T *Pseudoemiliania lacunosa*	849B-2H-3, 120/2H-4, 60	12.85–13.75		
Reentrance medium *Gephyrocapsa* spp.	849B-3H-6, 60/3H-CC	28.35–29.26		
T large *Gephyrocapsa* spp.	849B-4H-2, 120/4H-3, 60	33.45–34.35		
B large *Gephyrocapsa* spp.	849B-4H-6, 120/4H-7, 52	39.45–40.27		
T *Calcidiscus macintyrei*	849B-5H-2, 60/5H-2, 120	43.75–44.35	849C-4H-6, 100/4H-6, 140	45.10–45.50
B medium *Gephyrocapsa* spp.	849B-5H-4, 60/5H-4, 120	46.75–47.35	849C-5H-1, 13/5H-1, 80	47.28–47.95
T *Discoaster brouweri*	849D-5H-6, 130/5H-7, 0	59.25–59.45		
T *Discoaster surculus*	849B-7H-5, 60/7H-6, 60	70.25–71.75		
T *Discoaster tamalis*	849C-7H-6, 60/7H-6, 90	77.05–77.35		
T *Sphenolithus* spp.	849B-10H-5, 60/10H-6, 60	101.10–102.60		
T *Reticulofenestra pseudoumbilicus*	849C-10H-3, 120/10H-3, 140	105.15–105.35		
B *Ceratolithus rugosus*	849B-15X-5, 120/15X-6, 60	156.80–157.70		
T *Triquetrorhabdulus rugosus*	849B-17X-1, 120/17X-2, 60	173.85–174.75		
B *Ceratolithus acutus*	849B-17X-1, 120/17X-2, 60	173.85–174.75		
T *Discoaster quinqueramus*	849B-18X-4, 60/18X-4, 120	189.35–189.95		
T *Amaurolithus amplificus*	849B-21X-5, 120/21X-6, 60	224.40–225.30		
B *Amaurolithus amplificus*	849B-22X-1, 120/22X-2, 60	229.35–230.25		
T absence interval *R. pseudoumbilicus*	849B-23X-1, 60/23X-1, 120	239.30–239.90		
B *Amaurolithus primus*	849B-27X-3, 60/27X-4, 60	280.70–282.20		
B *Discoaster berggrenii*	849B-29X-4, 40/29X-4, 80	304.00–304.40		
B absence interval *R. pseudoumbilicus*	849B-32X-5, 120/32X-6, 92	337.80–339.02		
B *Minylitha convallis*	849B-32X-5, 120/32X-6, 92	337.80–339.02		
T *Discoaster hamatus*	849B-32X-CC/33X-1, 60	340.37–341.80		
B *Discoaster neohamatus*	849B-33X-4, 45/33X-4, 130	346.75–347.60		
B *Discoaster hamatus*	849B-34X-3, 60/34X-4, 61	355.40–356.91		
T *Coccolithus miopelagicus*	849B-34X-5, 62/34X-6, 56	358.42–359.86		
T c *Discoaster kugleri*	849B-36X-CC/37X-1, 60	381.86–382.25		

Note: See note to Table 3.

scattered in the upper part of its range. *Helicosphaera sellii* shows a peak in abundance close to (just above and just below) the appearance of medium *Gephyrocapsa* spp.

Pliocene

All the zones of Bukry (1973) and Martini (1971) can be differentiated in the Pliocene sections at all sites, except Sites 844 and 845, where nannofossil barren zones represent episodes of severe carbonate dissolution. Subzonal boundaries within Zones CN12 and CN11 are not easily recognized because of the scarcity of markers such as discoasterid and ceratolithid species.

Zone CN12 (Zones NN18–NN17–NN16)

The LO of *Discoaster brouweri* (CN13/CN12 and NN19/NN18 boundary) was recorded in all Leg 138 sites. The boundary is characterized by the LO of *Discoaster triradiatus,* a species that occurs in abundance only at the end of the range of *D. brouweri* (Takayama, 1970). This event was not clearly detected because *D. triradiatus* is

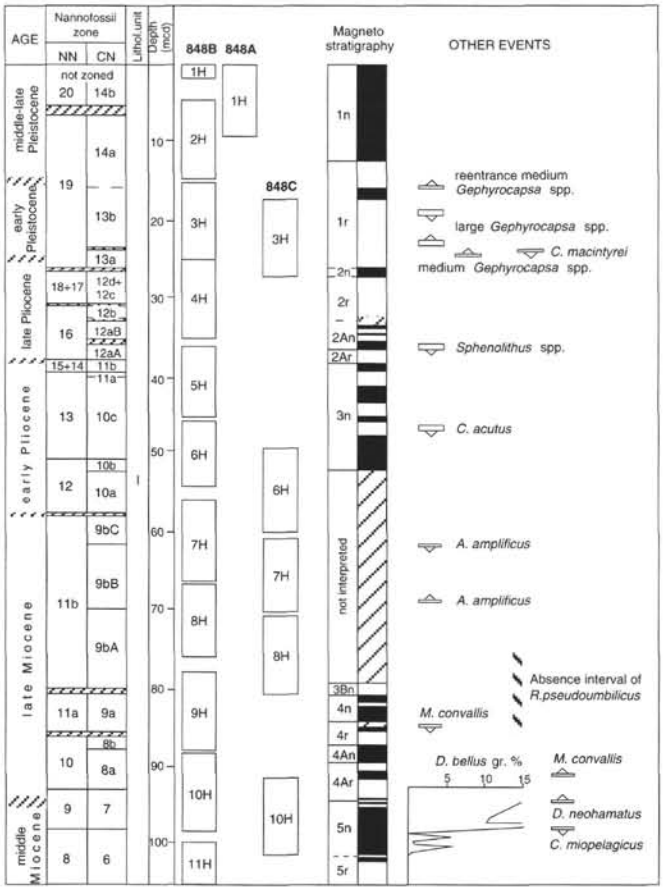

Figure 7. Chronostratigraphy and calcareous nannofossil biostratigraphy at Site 848. Notation as specified in Figure 3.

never present abundantly and consistently in the sections studied. This pattern of distribution also prevents the recognition of the increase in proportion (>20%) of *D. triradiatus* relative to *D. brouweri*, a datum introduced by Backman and Shackleton (1983).

The successive and closely spaced extinctions of *Discoaster pentaradiatus* and *Discoaster surculus* define the boundaries between Subzones CN12d–CN12c (Zones NN18–NN17) and Subzones CN12c–CN12b (Zones NN17–NN16), respectively. The two events are often recorded together (Backman and Pestiaux, 1986; Rio et al., 1990b). In the Leg 138 sites, *D. surculus* and *D. pentaradiatus* are generally rare or absent in the late Pliocene section. In all sites except Sites 852 and 853, *D. pentaradiatus,* when present, leaves the stratigraphic record together with *D. surculus.*

Note that the highly variable distribution and generally low abundance or absence of discoasterids, and thus their unreliability as biostratigraphic markers in the upper Pliocene, are particularly evident at sites strongly influenced by upwelling (such as Sites 849, 850, and 851 in the western transect and Sites 844, 845, and 846 in the eastern transect). Similar low abundances and scattered occurrences of other marker species of discoasterids and other nannofossils have been observed at various levels in Leg 138 holes. These distribution patterns may have been influenced by varying productivity pressures, as suggested by Chepstow-Lusty et al. (1989, 1992), who showed that regions of high productivity are associated with lower discoasterid abundance.

Discoaster tamalis becomes extinct before *D. surculus,* thus defining the boundary between Subzones CN12b and CN12a. In the material studied, *D. tamalis,* together with *D. asymmetricus* and members of the *Discoaster variabilis* group, have an irregular distribution, being more common in sites located out of the equatorial zone.

In the lower part of Subzone CN12a (Zone NN16), we record the LO of the last representatives of the genus *Sphenolithus* (*S. abies* and *S. neoabies*). This event occurs shortly above the LO of *Reticulofenestra pseudoumbilicus* and allows us to divide the CN12a Subzone further, defining Subzone "CN12aA" as proposed by Bukry (1991). A similar extinction of the last sphenoliths with respect to the final occurrence of *R. pseudoumbilicus* has been recorded in oceanic sediments (Backman and Shackleton, 1983; Rio et al., 1990a; Bukry, unpubl. data, 1990; Bukry, 1991) and by Rio et al. (1990b) in the Mediterranean.

Zone CN11

The LO of *R. pseudoumbilicus,* which defines the boundary of Zones CN12–CN11 (NN16–NN15), represents an easily recognized event at all the sites investigated except Site 845, where part of the Pliocene interval contains no nannofossils. To recognize this boundary, we refer to the taxonomic concept of *R. pseudoumbilicus* as expressed by Raffi and Rio (1979) and Backman and Shackleton (1983), and we consider the final exit of the large specimens of *R. pseudoumbilicus* (>7 μm). This event occurs in the upper part of Chron 2Ar (late Gilbert Chron) at Sites 848, 851, 852, and 853, as it does in many other areas (Rio, 1982; Backman and Shackleton, 1983; Rio et al., 1990a, 1990b).

Boundary CN11b/CN11a is defined by the beginning of the common and continuous occurrence of *D. asymmetricus,* a species that has a generally scattered distribution in the upper Miocene of the eastern equatorial Pacific, as well as other oceanic regions (Bukry, 1973), such as the western Indian Ocean (Roth, 1974; Rio et al., 1990b). Following Okada and Bukry's zonation, the *D. asymmetricus* event occurs above the LO of *Amaurolithus primus* and *Amaurolithus tricorniculatus,* which defines the boundary between Zones CN11 and CN10. In the lower Pliocene section of the eastern equatorial Pacific, the recognition of these two events has been hampered in some sequences because of (1) the low abundance of the two markers, (2) preservation problems, and (3) sediment reworking, which is particularly evident at western transect Sites 852 and 853. The continuous presence of *D. asymmetricus* and the disappearance of *A. primus* have been recognized at Sites 846, 847, 848, 851, 852, and 853; generally, the events are close each other.

Regarding the extinction datums of some ceratolithids species, such as representatives of the genus *Amaurolithus* (*A. primus, A. delicatus,* and *A. tricorniculatus*) and *C. acutus,* note that data from various authors (see Berggren et al., 1985) show some discrepancy in the age estimates for these events. The discrepancy may be attributed to a poorly documented extinction pattern of these ceratolithids and/or from usage of different criteria when identifying the species. Misidentification occurs in samples that contain nannofossils with calcite overgrowth and when specimens of different *Amaurolithus* and *Ceratolithus* species possess intergrade morphologic features. This is the case in most of the lower Pliocene sequences recovered during Leg 138. Ceratolithid species are irregularly distributed and are not easily differentiated because of the presence of overgrowth and intergrade morphotypes. Furthermore, at sites where ceratolithids are common and well preserved in the lower Pliocene interval (as at Sites 851, 852, and 853), it was not possible to obtain well-documented extinction patterns because of mixing in nannofossil assemblages caused by strong reworking of upper Miocene sediments.

The presence of *Discoaster tristellifer* within Zone CN11 is noteworthy because it is particularly common in the interval corresponding to the lower range of *D. asymmetricus.*

Zone CN10 (Zones NN13, pars-NN12)

Boundary CN10c/CN10b (NN12/NN13) is defined by the FO of *Ceratolithus rugosus.* This boundary is recognized at the first appearance of rare but typical specimens of *C. rugosus,* although the presence of forms intergrading between *C. rugosus* and its ancestor *Ceratolithus acutus* sometimes makes the recognition of the event difficult. This difficulty may explain the different position of the *C. rugosus* event with respect to Subchron 3n.4n (Thvera). In Site 852, the FO

Table 9. Position of calcareous nannofossil events at Hole 850B.

Event	Interval (cm)	Depth (mcd)
T *Pseudoemiliania lacunosa*	1H-4, 120/1H-5, 63	8.70–9.63
Reentrance medium *Gephyrocapsa* spp.	2H-4, 41/2H-4, 120	19.31–20.11
T large *Gephyrocapsa* spp.	3H-1, 120/3H-2, 54	24.85–25.69
B large *Gephyrocapsa* spp.	3H-3, 120/3H-4, 54	27.85–28.69
T *Calcidiscus macintyrei*	3H-5, 120/3H-6, 62	30.80–31.77
B medium *Gephyrocapsa* spp.	3H-CC/4H-1, 51	33.39–36.36
T *Discoaster brouweri*	4H-5, 50/4H-5, 65	42.45–42.60
T *Discoaster surculus*	5H-6, 20/5H-7, 65	53.10–55.05
T *Discoaster tamalis*	6H-1, 20/6H-1, 65	56.20–56.65
T *Sphenolithus* spp.	7H-CC/8H-1, 60	76.66–77.85
T *Reticulofenestra pseudoumbilicus*	8H-2, 80/8H-2, 100	79.55–79.75
T *Amaurolithus primus* (?)	10H-1, 59/10H-6, 150	96.84–105.23
T *Ceratolithus acutus* (?)	11X-CC/12X-1, 70	114.65–115.95
B *Ceratolithus rugosus*	12X-1, 70/12X-2, 120	115.95–116.45
B *Ceratolithus acutus*	13X-4, 120/13X-5, 60	130.55–131.45
T *Discoaster quinqueramus*	14X-7, 30/15X-1, 35	144.10–144.50
T *Amaurolithus amplificus*	17X-6, 58/18X-1, 42	171.00–173.17
T circular reticulofenestrids	19X-3, 60/19X-4, 60	185.55–187.05
B *Amaurolithus amplificus*	19X-6, 60/19X-7, 34	190.05–191.29
T absence interval *R. pseudoumbilicus*	20X-7, 43/21X-1, 60	201.28–201.85
B circular reticulofenestrids	23X-6, 61/23X-7, 20	227.84–228.95
B *Amaurolithus primus*	23X-7, 20/24X-1, 61	228.95–230.86
B *Discoaster berggrenii*	26X-3, 58/26X-4, 60	253.13–254.65
B *Discoaster loeblichii*	29X-6, 55/29X-7, 31	286.10–287.36
B absence interval *R. pseudoumbilicus*	30X-3, 60/30X-4, 60	300.92–302.42
T *Discoaster hamatus*	33X-2, 60/33X-3, 60	318.75–320.25
B *Discoaster neohamatus*	33X-2, 60/33X-3, 60	318.75–320.25
B *Minylitha convallis*	33X-3, 60/33X-4, 14	320.25–321.29
B *Discoaster hamatus*	36X-5, 47/36X-CC	352.05–352.42
T *Coccolithus miopelagicus*	37X-1, 60/37X-2, 61	355.85–357.36
T c *Discoaster kugleri*	40X-7, 20/41X-1, 60	393.35–394.45

Note: See note to Table 3.

of *Ceratolithus rugosus* is recorded above the Thvera (in Subchron 3n.3r); whereas in Sites 848 and 853, it apparently occurs within the Thvera. In this same position, the event was detected by Backman and Shackleton (1983) in the central equatorial Pacific, and by Rio et al. (1990a) in the western equatorial Indian Ocean. In some sections (Sites 846, 848, 850, and 853), we detected an overlap of *C. rugosus* with specimens of *C. acutus.* Although this observation agrees with that made by Rio et al. (1990a), most authors (see Berggren et al., 1985) do not report such an overlap.

The first appearance of *C. acutus* corresponds to the CN10b/CN10a boundary, as defined by Bukry (1973) together with the LO of *Triquetrorhabdulus rugosus.* Bukry noted that Subzone CN10a is of very short duration and can easily go undetected in sections with compressed sedimentation rates. In the Leg 138 sections, the FO of *C. acutus* has been consistently recorded at all sites. It occurs simultaneously with the extinctions of *T. rugosus* and *T. rioensis* at those sites where the two triquetrorhabdulids are present. We note that, in the Leg 138 sections, triquetrorhabdulids are generally rare in their final range, and have a discontinuous distribution within their range, from the middle Miocene upward.

The Subzone CN10a represents the best approximation for the recognition of the Miocene/Pliocene boundary by means of calcareous nannofossils.

Miocene

The zonal boundaries of the Miocene, as defined by Martini (1971) and Bukry (1973), have been recognized at all sites, with two exceptions: (1) the base of Zone CN6 (NN8) at western transect Sites 849 and 850; and (2) the top of CN7 (NN9) at eastern transect Site 845. In the upper Miocene, supplementary biostratigraphic events allow us to divide the rather long time interval (about 1.7 m.y.) corresponding to Subzone CN9b. Subzones CN7a–CN7b could not be differentiated.

Zone CN9 (NN11)

This zone is defined by the total range of the two related taxa *Discoaster quinqueramus* and *Discoaster berggrenii.* The LO of *D.*

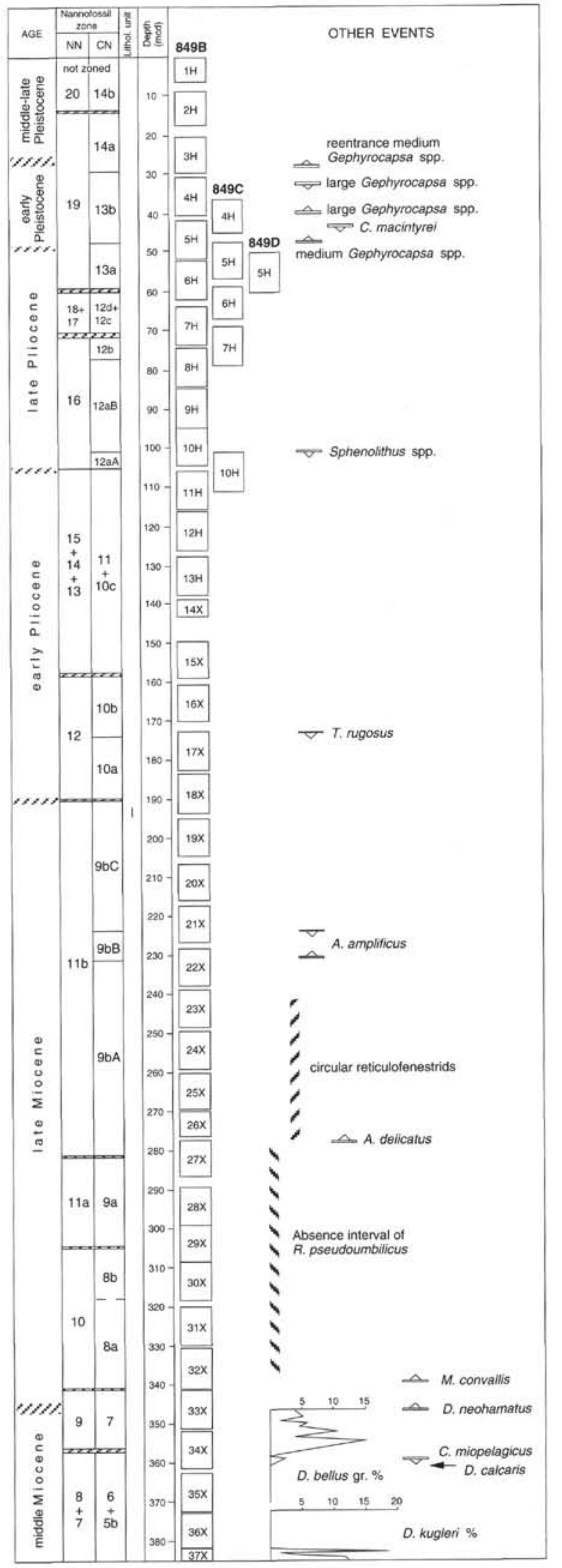

Figure 8. Chronostratigraphy and calcareous nannofossil biostratigraphy at Site 849. Notation as specified in Figure 5.

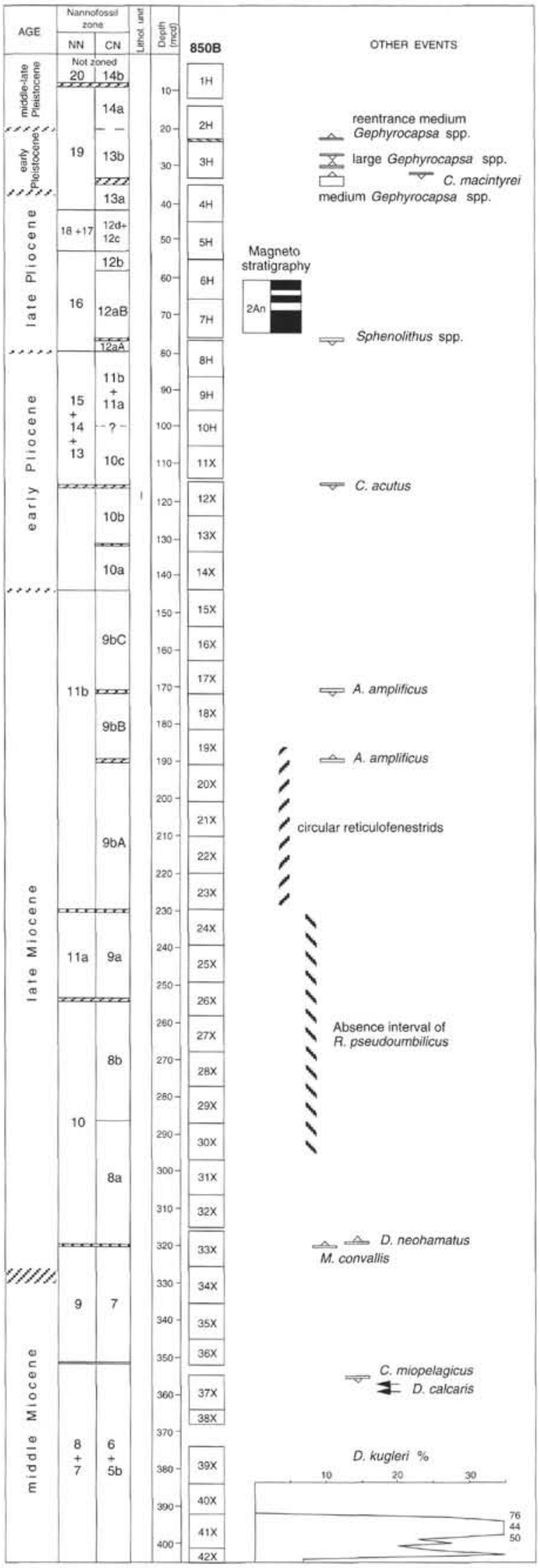

Figure 9. Chronostratigraphy and calcareous nannofossil biostratigraphy at Site 850. Notation as specified in Figure 5.

quinqueramus is used to mark the top of Zones CN9 and NN11, as *D. berggrenii* becomes extinct before *D. quinqueramus* (Bukry, 1973; Rio et al., 1990a). In our sections, the LO of *D. quinqueramus* was easily detected; it follows the extinction of *D. berggrenii,* as it does in other regions.

Boundary CN9b/CN9a is defined by the entrance in the stratigraphic record of the genus *Amaurolithus,* namely, by the FO of *A. primus.* Although ceratoliths are generally rare, their appearance at the base of Subzone CN9b was easily detected. The earlier forms, belonging to *A. primus* (see "Taxonomic Notes" section, this chapter), evolved rapidly, leading to the appearance of *A. delicatus* (which occurs shortly after the FO of *A. primus*). Intergrading forms between the two species are frequently found. *Amaurolithus tricorniculatus,* often recorded as appearing in Subzone CN9b (i.e., Berggren et al., 1985), is very rare and scattered in the material studied. Another species, *A. amplificus,* occurs after the FO of *A. delicatus.* The presence of intergrade forms between *Triquetrorhabdulus extensus–T. rugosus* and *A. amplificus* just below the appearance level of *A. amplificus* possibly proves the phylogenetic relationship between *Triquetrorhabdulus* and *Amaurolithus* previously suggested by other authors (Gartner, 1967; Perch-Nielsen, 1977, 1985).

The same observations on the *A. amplificus* distribution pattern have been made in the western equatorial Indian Ocean in Leg 115 successions (Rio et al., 1990a). In the eastern equatorial Pacific, *A. amplificus* becomes extinct within the upper part of Subzone CN9b, in agreement with the previous findings of Bergen (1984) and Rio et al. (1990a). Compared to the Leg 138 paleomagnetic stratigraphy, the FOs and LOs of *A. amplificus* occur at the base and the top of Chron 3An, respectively, and turn out to be isochronous events with records from the western equatorial Indian Ocean (Rio et al., 1990a). The stratigraphic relationship of the lowest and highest occurrences of *A. amplificus* relative to the lowest occurrence of *A. primus* and the highest occurrence of *D. quinqueramus* allows us to divide the Okada and Bukry (1980) Subzone CN9b further, as suggested by Rio et al. (1990a). We can use these additional events to divide Subzone CN9b into three biostratigraphic units, defined as follows:

CN9bA: from the FO of *A. primus* to the FO of *A. amplificus*;
CN9bB: from the FO of *A. amplificus* to the LO of *A. amplificus*; and
CN9bC: from the LO of *A. amplificus* to the LO of *D. quinqueramus.*

The definitions and occurrences of these three new biostratigraphic units are given in Appendix B in addition to any related remarks.

Within Subzone CN9b, the discoasterids are represented by several species, mainly *D. quinqueramus, D. berggreni, D. surculus,* and *D. pentaradiatus.* We note that in all CN9 zonal intervals, discoasterids fluctuate in abundance and their preservation varies widely in the different successions, sometimes preventing a precise identification of marker and secondary species. Following Rio et al. (1990a), we searched for a large form of *Discoaster* aff. *brouweri* (tabulated in Leg 115 range charts as *Discoaster* sp. 2), which seems to have a restricted stratigraphic distribution within the lower part of CN9b and the upper part of CN9a in the western equatorial Indian Ocean. In our cores, this discoasterid does not give the same clear biostratigraphic signal as in the Indian Ocean.

Regarding the CN9a and NN11a subzones, we use the appearance of *D. berggrenii* to define their lower boundary, as indicated by Bukry (1973). In fact, the *D. berggrenii* morphotypes (the five-rayed discoasterids with a stellar knob in a distinct central area; Plate 2, Figs. 1–2) appeared slightly earlier than *D. quinqueramus* morphotypes sensu Bukry (1971) (Plate 2, Figs. 4–5). Although it is useful to distinguish them for biostratigraphic purposes, *D. berggrenii* and *D. quinqueramus* have been considered as a single taxonomic unit in the range charts, as intergrades between them are common (Plate 2, Fig. 3). In the eastern equatorial Pacific, the appearance of *D. berggrenii* occurs

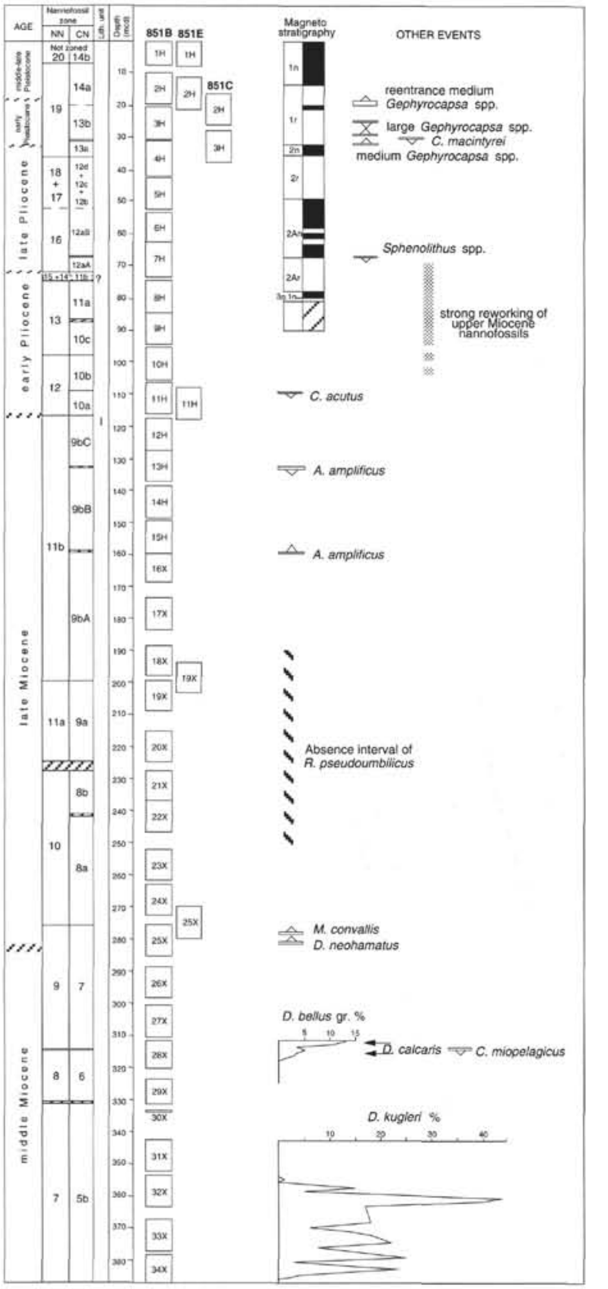

Figure 10. Chronostratigraphy and calcareous nannofossil biostratigraphy at Site 851. Notation as specified in Figure 3.

in the lowermost part of Chron 4r (Subchron 4r.2r), and it is isochronous with the western equatorial Indian Ocean (Rio et al., 1990a). The morphological development of *D. berggrenii* and *D. quinqueramus* was gradual; these discoasterids probably evolved from other five-rayed forms that belong to the *D. bellus* group (Bukry, 1973), and intergrades between the two discoasterid groups are common.

Within Subzone CN9a, we record the occurrence, but in low abundance, of *D. pentaradiatus* and *D. surculus*. Typical *D. bellus* and *Minylitha convallis*, present in the underlying intervals, disappear in the upper part of this subzone, whereas the rare *D. neohamatus*, *D. prepentaradiatus*, and *D. loeblichii* have their LOs in the lower part. Similar co-occurrences of *D. loeblichii* and *D. berggrenii* have been noted previously by Rio et al. (1990b) in the western equatorial Indian Ocean, and by Proto-Decima et al. (1978), Mazzei et al. (1979), and Parker et al. (1985) in the Atlantic Ocean.

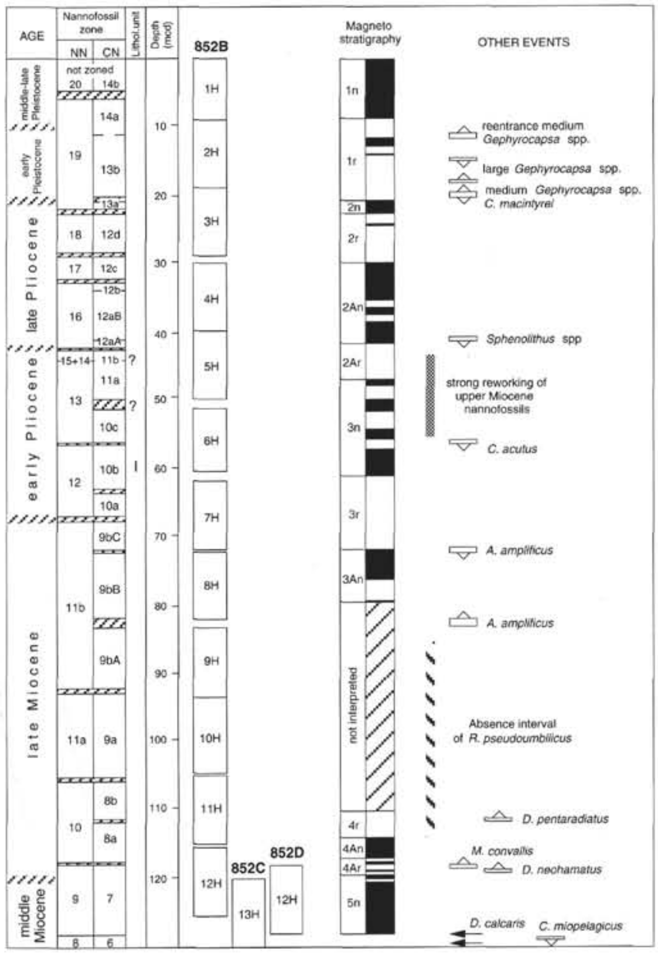

Figure 11. Chronostratigraphy and calcareous nannofossil biostratigraphy at Site 852. Notation as specified in Figure 3.

Zone CN8 (NN10)

The upper part of this biostratigraphic interval is characterized by the presence of *Discoaster loeblichii,* used by Bukry (1973), together with *D. neorectus,* as a marker for dividing Zone CN8 into Subzones CN8b and CN8a. *D. loeblichii* was recorded with great consistency in almost all Leg 138 sections, except those where the scarcity and/or poor preservation prevented recognition. At Sites 844, 846, 849, 850, 851, 852, and 853, we differentiate the two subzones, although *D. neorectus* was found only sporadically.

Close to the FO of *D. loeblichii,* we observed the lowest specimens of *D. pentaradiatus.* Other components of the discoasterid assemblage of CN8 are abundant or common (e.g., *D. brouweri* and *D. bellus* gr.) and scarce (*D. neohamatus*). In the lower part of the zone, where *D. bellus* gr. dominates, *D. prepentaradiatus* and *D. calcaris* are present in low abundances.

The lower boundary of Zone CN8 is defined by the LO of *Discoaster hamatus.* This form is generally rare in the uppermost part of the range; however, the event can be consistently recognized in Leg 138 material, with the exception of Site 845, where the corresponding stratigraphic interval is barren of nannofossils.

Just above the extinction of *D. hamatus,* the FO of *M. convallis* is recorded. This event can be used to recognize the boundary between Zones CN8/CN7 when *D. hamatus* is too rare (Rio et al., 1990a). In the Leg 138 material, the range of *M. convallis,* which encompasses Zones CN8 and CN9a, shows variability. At the eastern transect sites, the species is generally rare and occurs sporadically, whereas it is continuously present at other sites. This irregular distribution of *M.*

Table 10. Position of calcareous nannofossil events at Site 853.

Event	Interval (cm)	Depth (mcd)
T *Pseudoemiliania lacunosa*	851B-1H-5, 95/1H-5, 140	6.95–7.40
Reentrance medium *Gephyrocapsa* spp.	851E-2H-5, 15/2H-5, 45	19.15–19.45
T large *Gephyrocapsa* spp.	851C-2H-6, 25/2H-6, 70	23.75–24.20
B large *Gephyrocapsa* spp.	851B-3H-5, 30/3H-5, 60	27.45–27.75
T *Calcidiscus macintyrei*	851B-3H-6, 100/3H-7, 46	29.65–30.61
B medium *Gephyrocapsa* spp.	851C-3H-3, 70/3H-3, 140	31.25–31.95
T *Discoaster brouweri*	851B-4H-3, 100/4H-3, 150	35.90–36.40
T *Discoaster surculus*	851B-5H-7, 65/5H-CC	51.95–52.19
T *Discoaster tamalis*	851B-5H-7, 65/5H-CC	51.95–52.19
T *Sphenolithus* spp.	851B-7H-3, 58/7H-4, 60	67.03–68.55
T *Reticulofenestra pseudoumbilicus*	851B-7H-6, 25/7H-6, 60	71.20–71.55
B c *Discoaster asymmetricus* (?)	851B-7H-7, 45/8H-1, 60	72.90–75.00
T *Amaurolithus primus*	851B-09H-2, 60/9H-3, 60	86.50–88.00
B *Ceratolithus rugosus*	851B-10H-2, 25/10H-2, 60	97.20–97.55
T *Ceratolithus acutus*	851B-10H-2, 25/10H-2, 60	97.20–97.55
B *Ceratolithus acutus*	851B-11H-2, 60/11H-2, 110	108.25–108.75
T *Discoaster quinqueramus*	851E-11H-6, 44/11H-6, 90	116.24–116.70
T *Amaurolithus amplificus*	851B-13H-3, 68/13H-4, 70	131.48–133.00
B *Amaurolithus amplificus*	851B-15H-6, 69/15H-7, 63	157.54–158.98
T absence interval *R. pseudoumbilicus*	851B-18X-2, 60/18X-3, 60	190.35–191.85
B *Amaurolithus primus*	851E-19X-4, 25/19X-4, 60	199.25–199.60
T *Minylitha convallis*	851B-19X-1, 25/19X-1, 58	199.40–199.68
B *Discoaster berggrenii*	851B-20X-CC/21X-1, 25	224.88–227.90
B *Discoaster loeblichii*	851B-22X-3, 60/22X-4, 60	240.45–241.95
B absence interval *R. pseudoumbilicus*	851B-22X-7, 31/23X-1, 60	246.16–252.65
T *Discoaster hamatus*	851E-25X-4, 25/25X-4, 56	275.05–275.36
B *Minylitha convallis*	851B-25X-1, 60/25X-2, 60	276.10–277.60
B *Discoaster neohamatus*	851B-25X-4, 120/25X-5, 60	281.20–282.10
B *Discoaster hamatus*	851B-28X-2, 140/28X-3, 40	314.30–314.8
T *Coccolithus miopelagicus*	851B-28X-3, 40/28X-3, 80	314.80–315.20
B *Catinaster coalitus*	851B-29X-5, 71/29X-CC	330.21–331.23
T c *Discoaster kugleri*	851B-32X-4, 55/32X-4, 120	358.80–359.45
B c *Discoaster kugleri* (?)	851B-34X-3, 120/34X-4, 65	382.65–383.60

Note: See note to Table 3.

Table 11. Position of calcareous nannofossil events at Site 851.

Event	Interval (cm)	Depth (mcd)
T *Pseudoemiliania lacunosa*	852B-1H-3, 110/1H-4, 60	4.30–5.30
Reentrance medium *Gephyrocapsa* spp.	852B-2H-2, 65/2H-2, 140	11.30–12.05
T large *Gephyrocapsa* spp.	852B-2H-4, 65/2H-4, 140	14.30–15.05
B large *Gephyrocapsa* spp.	852B-2H-6, 140/2H-7, 40	18.05–18.55
T *Calcidiscus macintyrei*	852B-3H-1, 65/3H-1, 140	19.85–20.70
B medium *Gephyrocapsa* spp.	852B-3H-1, 65/3H-1, 140	19.85–20.70
T *Discoaster brouweri*	852B-3H-2, 65/3H-2, 140	21.35–22.10
T *Discoaster pentaradiatus*	852B-3H-7, 35/3H-CC	28.55–29.29
T *Discoaster surculus*	852B-4H-2, 65/4H-2, 140	32.45–33.20
T *Discoaster tamalis*	852B-4H-3, 65/4H-3, 140	33.95–34.70
T *Sphenolithus* spp.	852B-5H-1, 80/5H-1, 135	41.05–41.60
T *Reticulofenestra pseudoumbilicus*	852B-5H-2, 80/5H-2, 140	42.55–43.15
B c *Discoaster asymmetricus* (?)	852B-5H-3, 30/5H-3, 80	43.55–44.05
T *Amaurolithus primus*	852B-5H-7, 80/6H-1, 80	50.05–52.65
B *Ceratolithus rugosus*	852B-6H-3, 135/6H-4, 35	56.20–56.70
T *Ceratolithus acutus*	852B-6H-4, 35/6H-4, 80	56.70–57.15
B *Ceratolithus acutus*	852B-7H-1, 71/7H-1, 127	62.96–63.52
T *Discoaster quinqueramus*	852B-7H-3, 75/7H-3, 140	66.00–66.65
T *Amaurolithus amplificus*	852B-7H-CC/8H-1, 120	72.21–73.85
B *Amaurolithus amplificus*	852B-8H-CC/9H-1, 70	82.77–84.60
T absence interval *R. pseudoumbilicus*	852B-9H-1, 70/9H-2, 70	84.60–86.10
B *Amaurolithus primus*	852B-9H-6, 140/9H-7, 70	92.80–93.60
B *Discoaster berggrenii*	852B-11H-1, 40/11H-1, 80	105.80–106.20
B *Discoaster pentaradiatus*	852B-11H-4, 145/11H-5, 40	111.35–111.80
B *Discoaster loeblichii*	852B-11H-5, 40/11H-5, 80	111.80–112.20
B absence interval *R. pseudoumbilicus*	852B-11H-6, 140/11H-7, 83	114.30–115.23
B *Minylitha convallis*	852B-12H-2, 70/12H-2, 110	118.30–118.70
T *Discoaster hamatus*	852B-12H-2, 70/12H-2, 110	118.30–118.70
B *Discoaster neohamatus*	852B-12H-2, 120/12H-3, 143	118.80–119.03
B *Discoaster hamatus*	852C-13X-6, 40/13X-6, 50	128.80–128.90
T *Coccolithus miopelagicus*	852C-13X-6, 50/13X-6, 90	128.90–129.30

Note: See note to Table 3.

convallis seems to be influenced by variability in either the preservation of nannofossil assemblages or the productivity conditions, in that the form is rare and discontinuous at sites influenced by upwelling (i.e., 844 and 845).

A feature of the nannofossil assemblage of Zone CN8 is the turnover detected within the placolith group, namely, an almost total disappearance of large specimens (>7 µm) of *Reticulofenestra pseudoumbilicus.* This placolith enters the stratigraphic record in the middle Miocene, close to the top of Zone CN4 (NN5), and exits in the middle part of the Pliocene. The interval of absence of *R. pseudoumbilicus,* recorded in all the stratigraphic successions of Leg 138, starts from the lower upper Miocene (Zones CN8–NN10) and extends to the

Table 12. Position of calcareous nannofossil events at Site 853.

Event	Interval (cm)	Depth (mcd)
T *Pseudoemiliania lacunosa*	853B-1H-2, 120/1H-2, 130	2.70–2.80
Reentrance medium *Gephyrocapsa* spp.	853B-1H-3, 80/1H-CC	3.80–4.25
B large *Gephyrocapsa* spp.	853B-2H-1, 120/2H-2, 65	5.45–6.40
T *Calcidiscus macintyrei*	853B-2H-2, 65/2H-2, 120	6.40–6.95
B medium *Gephyrocapsa* spp.	853B-2H-2, 140/2H-3, 25	7.15–7.50
T *Discoaster brouweri*	853B-2H-3, 25/2H-3, 65	7.50–7.90
T *Discoaster pentaradiatus*	853B-2H-5, 65/2H-5, 120	10.90–11.45
T *Discoaster surculus*	853B-2H-6, 120/2H-6, 140	12.95–13.15
T *Discoaster tamalis*	853B-2H-7, 30/3H-1, 65	13.55–15.35
T *Sphenolithus spp.*	853B-3H-4, 120/3H-4, 140	20.40–20.60
T *Reticulofenestra pseudoumbilicus*	853B-3H-4, 120/3H-4, 140	20.40–20.60
B c *Discoaster asymmetricus*	853B-4H-1, 65/4H-2, 65	21.95–23.45
T *Amaurolithus primus*	853B-4H-3, 140/4H-4, 25	25.70–26.05
T *Ceratolithus acutus*	853B-4H-5, 140/4H-6, 80	28.70–29.60
B *Ceratolithus rugosus*	853B-4H-6, 80/4H-CC	29.60–29.89
B *Ceratolithus acutus*	853B-5H-1, 65/5H-1, 120	32.40–32.95
T *Discoaster quinqueramus*	853B-5H-1, 65/5H-1, 120	32.40–32.95
T *Amaurolithus amplificus*	853B-5H-5, 65/5H-5, 120	38.40–38.95
B *Amaurolithus amplificus*	853B-6H-4, 27/6H-4, 65	46.37–46.75
T absence interval *R. pseudoumbilicus*	853B-6H-5, 65/6H-6, 65	48.25–49.75
B *Amaurolithus primus*	853B-7H-2, 147/7H-3, 30	54.42–54.75
B *Discoaster berggrenii*	853D-7H-4, 120/7H-4, 140	69.47–69.67

Note: See note to Table 3.

lower part of Subzone CN9b. The bottom of this interval is characterized by the absence of all the representatives of genus *Reticulofenestra,* including the small (≤7 µm) morphotypes; large forms of *R. pseudoumbilicus* reenter, with low abundance, just below the appearance level of *A. amplificus.* This temporary disappearance has also been observed in the western equatorial Indian Ocean (Young, 1990; Rio et al., 1990a), and was interpreted as a regional stratigraphic feature, probably reflecting oceanographic-climatic instability (Rio et al., 1990a). Indications of the wider geographical extent of this "feature" in the *R. pseudoumbilicus* range are reported and discussed in Raffi et al. (this volume).

Zone CN7 (NN9)

The total range of *Discoaster hamatus* defines the CN7 (NN9) zonal interval. Despite the low abundance of discoasterids at some sites (Sites 846, 849, and 850) and the presence of barren intervals observed at others (Sites 844 and 845), the consistent occurrence of *D. hamatus* allows us to recognize this zonal interval in the material we investigated. Close to the FO of *D. hamatus,* other five-rayed discoasterids appear. They have straight, tapering arms and belong to the *Discoaster bellus* group. Their presence is useful in monitoring the base of the zone where *D. hamatus* is rare.

We have not divided Zone CN7 into two subzones ("a" and "b"), as suggested by Bukry (1973) on the basis of the first evolutionary appearance of *C. calyculus* from *C. coalitus.* In fact, in the Leg 138 sections, the genus *Catinaster* is represented mainly by *C. coalitus,* whereas very rare and scattered specimens of *C. calyculus* have been recorded in intervals below the appearance of *D. hamatus* (i.e., at Sites 844, 845, and 846). This finding agrees with the results from the western equatorial Indian Ocean (Rio et al., 1990a) and with the observation of Perch-Nielsen (1985), who questioned the subdivision of Zone CN7. Within this zone, the *D. variabilis* group and *D. bollii* are common; in the upper part, the last, rare representatives of *D. exilis* disappear, and *D. neohamatus* appears.

Zone CN6 (NN8)

The short CN6 (NN8) zonal interval is defined by the FO of *D. hamatus* (top) and the FO of *C. coalitus* plus the LO of *Discoaster kugleri* (bottom). In the material investigated, representatives of *Catinaster* are irregularly distributed. The zone is clearly recognized at Sites 844, 845, and 851, where *C. coalitus* is well represented, even

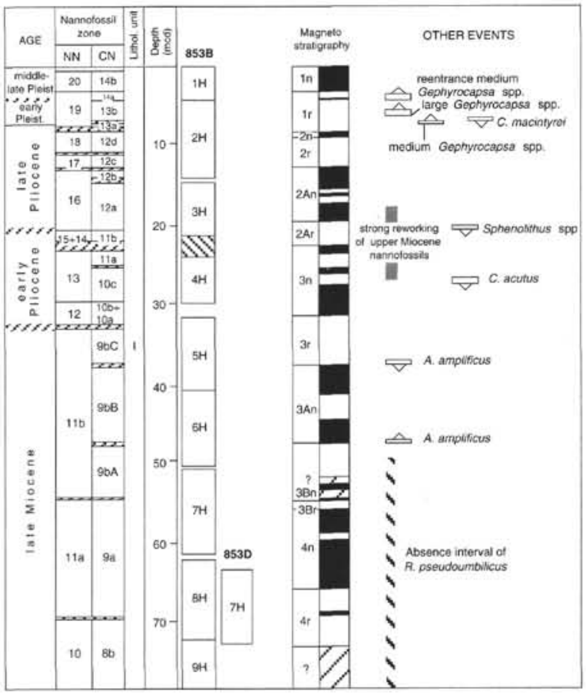

Figure 12. Chronostratigraphy and calcareous nannofossil biostratigraphy at Site 853. Notation as specified in Figure 3.

though *C. calyculus* is rare and scattered. At Site 846, the marker *C. coalitus* is very rare; and at Sites 849 and 850, it is found only in the biozone above (CN7). At these sites, fluctuating but low abundances also characterize the distributions of the other discoasterids. We failed to find the rare and scattered last specimens of *D. kugleri,* recorded at Sites 844 and 845, close to the *C. coalitus* appearance. These generally low abundances of discoasterids have been observed all along the interval encompassing Subzone CN5b (upper part)–CN6–CN7, corresponding to the time interval from 10.8 to 9.5 Ma. As already noted at other levels in the upper Miocene (Zone CN9) and Pliocene, high-productivity conditions influence these equatorial successions, the nannofossil content, and discoasterid abundance, as suggested by Chepstow-Lusty et al. (1989, 1992).

In the upper part of Zone CN6, and across the boundary between Zones CN7/CN6, a turnover in the nannofossil assemblage occurs, mainly within discoasterids. Besides the appearance of *D. bellus* gr., which becomes a dominant species in the overlying intervals, *D. calcaris* has a short and distinctive range. *D. exilis* declines gradually toward the extinction, and *D. brouweri* has a more continuous distribution. According to Bukry (1973), we recorded the extinction of *Coccolithus miopelagicus* within this zone, just below the upper boundary. In the eastern equatorial Pacific, this event seems to occur slightly later than at the mid-latitudes of the northern Atlantic (Olafsson, 1991) (see discussion in Raffi et al., this volume).

We detected a remarkable decline in the preservation state and composition of the nannofossil assemblages at Leg 138 sites in the interval from the top of CN5b to CN7. This interval, which is characterized by reduced sedimentation rates and increased carbonate dissolution, is comparable to other sites in the Pacific (Mayer et al., 1986) and may represent a dissolution event related to a general reorganization of Pacific circulation (Mayer, Pisias, Janecek, et al., 1992).

Zone CN5 (Zones NN7 and NN6)

The top of this zone is defined by the FO of *C. coalitus* and the LO of *Discoaster kugleri.* The bottom is defined by the LO of *Sphenolithus heteromorphus.* The zone spans a rather long time interval, over 2.5 m.y. In addition, Zone CN5 is divided into two subzones (CN5b and CN5a) by the FO of *Discoaster kugleri* (Bukry, 1973), which also defines the NN7/NN6 zonal boundary. The recognition of this boundary has been debated, as *D. kugleri* is considered a weak marker by many authors (e.g., Gartner and Chow, 1985; Gartner, 1992; Fornaciari et al., 1990). Substitute events suggested for dividing Zone CN5 are (1) the LO of *Cyclicargolithus floridanus,* proposed by Bukry (1973) as a secondary marker for the base of Subzone CN5b; (2) the FO of *Discoaster bollii,* proposed by Ellis (1981); and (3) the LO of *Coronocyclus nitescens,* proposed by Gartner and Chow (1985). Detailed documentation of these and other events can help to establish more reliable criteria for the definition of Subzones CN5b and CN5a (see discussion in Raffi et al., this volume). Among secondary biostratigraphic markers, Fornaciari et al. (1990) suggested that *C. nitescens* is more useful than *D. kugleri,* which is difficult to recognize in overgrown assemblages and which has a discontinuous distribution. In our sediments, we recorded some of these alternative potential markers, although the FO of *D. kugleri* was recognized and used to place the boundary between Subzones CN5b and CN5a. As expected, only through quantitative analysis on closely spaced samples has it been possible to determine the event precisely. *D. kugleri* is very rare in the lowermost range and is missing in many intervening samples. The distribution patterns at Sites 844, 845, and 846 (Figs. 3–5) provide evidence for the "appearance" of *D. kugleri*: (1) a first rare occurrence that is close to the extinction of *C. nitescens* (within Subchron 5An at Site 845) in the Leg 138 successions, as it is in the western equatorial Indian Ocean (Fornaciari et al., 1990); and (2) the beginning of common and continuous distribution, with a restricted stratigraphic extension, occurring at the base of Chron 5r. This latter event is probably the same event recorded as "*D. kugleri* lowest occurrence" by Gartner (1992) in DSDP Site 608 (North Atlantic), as suggested by the calibration to the magnetostratigraphy. The highest occurrence of *D. kugleri* is reported as occurring close to the appearance of *C. coalitus* (Bukry, 1973). In the material studied, we observed a clear event of "disappearance" for *D. kugleri,* which corresponds to the end of its common and continuous distribution and has been recorded in all the sequences that penetrated to Subzone CN5b. At Site 845, this event occurs within Chron 5r (just above Subchron 5r.2n). The last specimens of *D. kugleri,* known to disappear close to the appearance of *C. coalitus* (Bukry, 1973), have been observed only at Sites 844 and 845 as rare and scattered occurrences (Figs. 3–4).

Within Subzone CN5b in the equatorial Indian Ocean, large-sized *Calcidiscus* (≥11 μm), labeled as *C. macintyrei,* enter the stratigraphic record (Fornaciari et al., 1990). Detailed analyses performed on Leg 138 material to check this occurrence indicate that *C. macintyrei* is extremely rare and scattered. This species does not provide a useful biostratigraphic signal in this interval.

Within Subzone CN5a, in the middle part of Chron 5Ar at Site 845, we recorded the FO of *Triquetrorhabdulus rugosus.* This was recorded at a similar stratigraphic position in the mid-latitude North Atlantic (Olafsson, 1991). The biostratigraphic usefulness of this event has also been shown in the equatorial Atlantic, Pacific, and Indian oceans (Olafsson, 1989; Fornaciari et al., 1990, 1993).

In the lower part of Subzone CN5a, we record the highest occurrence of *C. floridanus,* within Chron 5AAr at Site 845. It is a distinct event that occurs well below the FO of *D. kugleri.* The final range of *C. floridanus* has been shown to be biogeographically controlled (Olafsson, 1991; Fornaciari et al., 1993). Therefore, the use of the extinction event of *C. floridanus* for recognizing the base of Subzone CN5b (base of Zone NN7) (Bukry, 1973) may cause confusion when correlating between different regions.

The nannofossil assemblage of Zone CN5 is dominated by helicoliths, placoliths, and sphenoliths. Discoasterids fluctuate in abundance and are generally overgrown. Besides *D. kugleri,* other groups that are well represented in Subzone CN5b include *D. exilis, D. musicus,* and *D. variabilis. D. bollii* and *D. brouweri* are very rare in Subzone CN5b and are scattered in the upper part. *D. signus* becomes extinct within Subzone CN5a, just below the lowest occurrence of *T. rugosus.* Among the placoliths of CN5, *R. pseudoumbilicus* (>7 μm) is dominant and representatives of genus *Calcidiscus* occur discontinuously in low abundance. Close to the transition between Subzones CN5b/CN5a (between the highest occurrence of *C. nitescens* and the lowest occurrence of *T. rugosus*), we observed the extinctions of *Triquetrorhabdulus serratus* and *Calcidiscus premacintyrei.* Additional investigations on the distribution of these taxa, and of *D. kugleri* and *C. floridanus,* may clarify their stratigraphic relationship and allow further subdivision of Zone CN5, at least on a regional scale.

Zone CN4 (NN5)

This zone is defined by the LO of *Sphenolithus heteromorphus* (top) and the FO of *Helicosphaera ampliaperta* (bottom).The CN5/CN4 boundary is characterized by another turnover in the nannofossil assemblage, also documented in the equatorial Indian Ocean (Rio et al., 1990a). Large *R. pseudoumbilicus,* which are dominant in the overlying interval, appears with rare specimens at the transition between CN5 and CN4.

The extinction of *S. heteromorphus* is a neat event in the successions studied. It marks the final occurrence of "spined" sphenoliths, which were dominant in the underlying intervals and have been replaced by small forms related to *Sphenolithus abies.* Helicoliths are common to abundant. In the discoasterid assemblage of Zone CN4, slender-armed forms like *D. exilis, D. variabilis,* and *D. signus* are present continuously, whereas the short-armed discoasterids of the *Discoaster deflandrei* group gradually disappear. Within this stratigraphic interval, the discoasterid assemblage was often strongly overgrown, thus preventing the recognition of the different species of discoasterids.

Zone CN3 (NN4)

Sediments belonging to this zone were recovered at eastern transect Sites 844, 845, and 846. The lowermost parts of these sequences fall within Zone CN3, that is, within the range of *S. heteromorphus.* This biostratigraphy provides the age control for the basement at these sites. The biostratigraphic basement age of 16.5 to 17 m.y. is older than the age previously estimated by tectonic subsidence or spreading models (Mayer, Pisias, Janecek, et al., 1992).

We used the highest occurrence of *Helicosphaera ampliaperta* to define the upper boundary of this zone, although Bukry (1975, 1978) considered this species a secondary marker, owing to its irregular distribution in many oceanic areas. He suggested the use of the appearance of *C. macintyrei* for the definition of the boundary between Zones CN4 and CN3. Moreover, Bukry (1978) "declassed" the end of the *D. deflandrei* acme (not quantitatively defined) as a secondary marker in his zonal scheme. This event was the primary criterion he proposed in 1973 for defining the CN4/CN3 zonal boundary. In fact, this event can be influenced by variable preservational and ecological factors and may vary from place to place (Bukry, 1978; Parker et al., 1985). In Leg 138 material, *H. ampliaperta* is rare in the upper part of the range, but its extinction is a rather clear event. Olafsson (1991) demonstrated that the disappearance of *H. ampliaperta* in the mid-latitude North Atlantic is also a distinct event. Interestingly, *H. ampliaperta* is absent in the western equatorial Pacific (Leg 130) (Fornaciari et al., 1993), thus confirming the regional character of this biostratigraphic marker. Other events have been proposed for the definition of boundary CN4/CN3. We have not considered them, such as the lowest occurrence of Bukry's *C. macintyrei,* as the application of different taxonomic concepts can lead to ambiguous biostratigraphic results (Fornaciari et al., 1990). Regarding the end of the *D. deflandrei* acme, we performed quantitative analyses on the discoasterid assemblages within the upper part of Zone CN3, following Rio et al. (1990a), to obtain the distribution pattern of *D. deflandrei.* Assuming the Rio et al. (1990a) definition for the end of the acme (i.e. a drop below a value of 30% relative to the total discoasterids), the event occurs before the LO of *H. ampliaperta* in the uppermost CN3. The *D. deflandrei* event coincides with the lowest occurrence of *Discoaster signus* (Figs. 3–4). Such concomitant events were detected also in the western equatorial Indian Ocean (Rio et al., 1990a) and were used to distinguish the CN4/CN3 boundary where *H. ampliaperta* was missing.

The nannofossil assemblage of this part of Zone CN3 is dominated by helicoliths, sphenoliths, and small placoliths as *Reticulofenestra* spp. and *Dictyococcites* spp. The distribution pattern of *S. heteromorphus* is characterized by peaks in abundance at discrete levels, where the species is the dominant component of the nannofossil assemblage.

BIOCHRONOLOGY

The biochronology adopted in this work is derived from a recalibration of the nannofossil events to the new time scale developed for Leg 138 sites (Shackleton et al., this volume). From 0 to 6 Ma, this new time scale is orbitally tuned and provides new ages for the magnetic reversals as well as the biostratigraphic events. Before 6 Ma, the Leg 138 time scale is based on the new calibrations obtained in the tuned interval, but it converges with the Cande and Kent (1992) paleomagnetic time scale by 14.8 Ma. In Table 2, we list the calcareous nannofossil events that define the zonal boundaries reported in Figure 2, as well as additional events, together with their assigned age estimates.

The nannofossil biochronology of the Pleistocene and Pliocene is well established, as demonstrated by a number of studies dealing with direct correlations of the events to magnetostratigraphies and high-resolution isotope stratigraphies (e.g., Backman and Shackleton, 1983; Berggren et al., 1985; Raffi et al., 1993). Therefore, the biochronologic data on Pleistocene and Pliocene nannofossil events reported in this work are derived from recent literature and from recalibration to an orbitally tuned time scale (Shackleton et al., this volume).

In the Miocene interval, the excellent magnetostratigraphies obtained at Sites 844, 845, 852, and 853 in the upper Miocene, and extending to the middle Miocene at Site 845 (see site reports in Mayer, Pisias, Janecek, et al., 1992, and Schneider, this volume), allow us to refine the nannofossil biochronology of this time interval. The resulting biochronology substantially agrees with that obtained in the equatorial Indian Ocean during ODP Leg 115 (Backman et al., 1990; Rio et al., 1990a). Differences between these low-latitude biochronologies include the B (bottom occurrence of) *C. coalitus.* In the Leg 138 material, this event was directly calibrated to magnetostratigraphy and occurs in the lower part of Chron 5n.2n (age estimate of 10.7 Ma). It is considerably younger than the date of 11.6 Ma (reestimated) obtained from Site 714 (Backman et al., 1990) by linear interpolation between B *D. hamatus* and T (top occurrence of) *S. heteromorphus.* Data from Site 845 provide calibration for some middle Miocene events. Among them, T *S. heteromorphus* has an estimated age of ca. 13.58 Ma, obtained by linear extrapolation from the base of Chrons 5AAn and 5ABn. This age estimate results slightly older than the age (reestimated) of 13.49 Ma obtained from DSDP Site 608 (Backman et al., 1990). More detailed discussion of Leg 138 Miocene nannofossil biomagnetostratigraphy and comparison with other low- and mid-latitude magnetobiochronologies is reported in Raffi et al. (this volume).

CHRONOSTRATIGRAPHY

The chronostratigraphic framework we adopt for this paper is that used by Rio et al. (1990a), which divides the Miocene and Pliocene into subseries-subsystems. This informal large-scale subdivision does not refer to European chronostratigraphic units of the Neogene. In fact, stage-age units designated in European sequences are often difficult to recognize outside the type regions. This is because they rarely have updated and detailed biostratigraphic and magnetostratigraphic age controls. On the other hand, reference to a correct chronostratigraphic framework is important, because the chronostratigraphy (precise definition of chronostratigraphic boundaries) is "a common language" for international communication and correlation. The procedures followed in defining the subseries-subsystems reported in Figure 2 are somewhat different from those adopted in the *Initial Reports* volume ("Explanatory Notes" chapter in Mayer, Pisias, Janecek, et al., 1992), for they take into account recent revisions and difficulties encountered in Neogene chronostratigraphy (Rio et al., 1990a, 1990c). The adopted definitions of the chronostratigraphic boundaries and units are briefly explained below.

The Pleistocene

The Pleistocene is divided into middle–late and early Pleistocene, following the chronostratigraphy of Berggren et al. (1985) and Rio et al. (1991).

The middle–late/early Pleistocene boundary (top of Selinuntian stage, as proposed by Rio et al., 1991) approximates the time of intensification of Pleistocene glaciations and the establishment of a strong 100,000-yr. eccentricity cycle in the ice-volume record. With reference to calcareous nannofossil biostratigraphy, this boundary approximates (slightly postdates) the reentrance in the stratigraphic record of medium-sized *Gephyrocapsa* spp. (Rio et al., 1990b, 1991) between the base of Chron 1n (Brunhes) and the top of Subchron 1r.1n (Jaramillo).

The definition of the Pleistocene/Pliocene boundary is based on the stratigraphic principle of establishing a boundary stratotype. The Vrica section (Calabria, Southern Italy) has been defined and accepted as the stratotype for the boundary (Aguirre and Pasini, 1985). Within this section, the top of the laminated level "e" in the Vrica section was selected as the marker horizon for the Pleistocene/Pliocene boundary (Aguirre and Pasini, 1985), and this level is just above the top of Chron 2n (Olduvai) (Tauxe et al., 1983; Hilgen, 1991a) at an age of ca. 1.81 Ma (revised to the astronomically calibrated chronology of Hilgen, 1991a).

In the present work, we have recognized the boundary by the FO of medium *Gephyrocapsa* spp., which occurs in the equatorial Pacific just above the top of the Olduvai Subchron, as it does at the boundary stratotype section in the Mediterranean (Rio et al., in press).

The Pliocene

We divide the Pliocene series into two intervals (early and late Pliocene), following the generally used procedure for which the boundary is approximated by means of calcareous nannofossils, namely, the highest occurrence of *Reticulofenestra pseudoumbilicus* within Chron 2Ar (close to the upper part of the Gilbert). It should be noted that Rio et al. (1991, 1994) have recently proposed a tripartite subdivision into lower (Zanclean stage), middle (Piacenzian stage), and upper (Gelasian stage) Pliocene, as the time interval between the top of the Piacenzian stage (ca. 2.6 Ma) and the Pliocene/Pleistocene boundary (ca. 1.81 Ma) is not represented by a formally designated chronostratigraphic unit (and stratotype section).

The Pliocene/Miocene Boundary

The recognition of the Pliocene/Miocene boundary was considered controversial, owing to the difficulty in correlating this boundary (defined in the Mediterranean) to the open-ocean record. Sometimes different procedures (magnetostratigraphy, planktonic foraminifers or calcareous nannofossils) are used for placing the boundary in the same sequence, and this can lead to controversial identification of it (see discussion in Rio et al., 1990a). New results from land sections in Calabria (Zijderveld et al., 1986; Channell et al., 1988; Hilgen and Langereis, 1988) suggest that the boundary occurs slightly below the Thvera Subchron (3n.4n) (in the upper part of Chron 3r), at an estimated age of about 5.32 Ma (Hilgen, 1991b). In this paper, we placed the Pliocene/Miocene boundary within nannofossil Subzone CN10a, between the appearance of *Ceratolithus acutus* (top) and the extinction of *Discoaster quinqueramus* (base), following Bukry (1973) who tentatively suggested the top of Subzone CN10a as the best approximation of this boundary, on the basis of correlations with Mediterranean stratotypes.

The Late/Middle Miocene Boundary

Berggren et al. (1985) defined the late/middle Miocene boundary (Tortonian/Serravallian boundary) at the base of the Tortonian stage and placed it within Zone CN6 (NN8), corresponding to the FO of *Neogloboquadrina acostaensis.* We have drawn the boundary in the upper part of nannofossil Zone CN7 (NN9), in agreement with the procedure followed by Rio et al. (1990a). Taking into account recent work in Italian sections (Rio et al., 1990c, and unpubl. data), Rio and co-workers saw that the bio- and magnetostratigraphic position of this boundary is unclear, owing to the poor quality of the data collected at the Mediterranean stratotype section of the Tortonian. Contradictions arise in the comparison and correlation of data from oceanic areas with the Mediterranean stratotype (see discussion in Rio et al., 1990a, for further details).

The Early/Middle Miocene Boundary

We followed the general criterion adopted by calcareous nannofossil paleontologists for recognizing the middle/early Miocene boundary and have drawn it at the top of Zone CN3 (NN4), just below the highest occurrence of *Helicosphaera ampliaperta.* With regard to chronostratigraphic units, the middle/early Miocene boundary is equivalent to the base of the Langhian stage (Berggren et al., 1985). This boundary is approximated by the FO of *Preorbulina glomerosa curva* (Cita and Premoli Silva, 1968), which is recorded above the FO of *Sphenolithus heteromorphus* in the stratotype section, just below the LO of *H. ampliaperta,* within the upper part of Zone NN4 (Martini, 1971).

SITE SUMMARIES

The preliminary biostratigraphic results included in the site chapters of the *Initial Reports* volume (Mayer, Pisias, Janecek, et al., 1992) show that the shipboard nannofossil biostratigraphy was sufficiently detailed to detect all major events. A general discussion of calcareous nannofossil biostratigraphy of the eastern equatorial Pacific, and a summary of the results at each site, are in the biostratigraphy chapter of this paper. We examined the middle and upper Miocene intervals by means of a new suite of more closely spaced samples. In this chapter, we report refinements to the on-board nannofossil biostratigraphy and discuss biostratigraphic details and problems that arose during our research. Biostratigraphic data were collected from composite depth sections constructed for each site (Hagelberg et al., 1992). These data are reported in Tables 3–12 and are illustrated in Figures 3–12. Depths of the data are reported in shipboard meters composite depth (mcd).

In the figures, we refer to the biostratigraphic scheme of Okada and Bukry (1980), which provides more resolution in some stratigraphic intervals. Details on the distribution patterns of stratigraphically indicative calcareous nannofossils in the middle and upper Miocene sections of some Leg 138 sites are reported in Raffi et al. (this volume). They collected quantitative data from many of the samples used in this study. We have excluded Site 854 from this report and refer the reader to the *Initial Reports* volume for Leg 138 for the nannofossil biostratigraphy of this sequence.

Eastern Transect: Sites 844, 845, 846, and 847

The eastern transect sites were drilled in the vicinity of 95°W (Fig. 1), in the area where the equatorial current system interacts with the Peru Current. The primary objective at these sites was the reconstruction of the paleoceanography in this area, namely, the history of the current system and of oceanic productivity under the influence of coastal upwelling. Additional objectives included (1) calibrating low-latitude biostratigraphies to the paleomagnetic time scale, by means of the anticipated magnetic stratigraphies at each site; (2) assisting in the reconstruction of the local tectonic history by providing biostratigraphic ages for previously undated magnetic anomalies in this region; and (3) determining the backtracked history of these sites.

Site 844

Site 844 is located in the Guatemala Basin, in an oceanographic region known as the Costa Rica Dome, a surface upwelling area with associated high open-ocean productivity. The site lies on the Cocos Plate, on basement formed at the East Pacific Rise approximately 17.5 m.y. ago (Mayer, Pisias, Janecek, et al., 1992).

The complete sediment sequence above the basalt basement was retrieved at Site 844, and two lithologic units were recognized. In the Pleistocene–upper Miocene interval, the recovered sediments are clay-rich and biogenic silica-rich oozes with minimal carbonate (Unit I). In the middle to lower Miocene interval, the sediment is microfossil (mainly nannofossil) ooze (Unit II). A good magnetostratigraphy was obtained in the late Neogene interval (Schneider, this volume).

The average sampling interval for nannofossil analysis was 60 cm in Holes 844B and 844D and in some cores from Hole 844C. The nannofossil events we recognized are listed in Table 3. In the upper part of the sequence (0–76 mcd), where siliceous microfossils (mainly diatoms) dominate, the relative abundance and preservation of calcareous nannofossils varies. Pleistocene nannofossil assemblages are diluted by siliceous microfossils and clay, but the major biostratigraphic events were recorded, despite the scarcity of nannofossils and the presence of barren intervals. A synthesis of the biostratigraphy at this site is presented in Figure 3.

Stratigraphic sections devoid of nannofossils are present within the Pliocene and upper Miocene intervals, and these sections are often characterized by reduced sedimentation rates. Consequently, in the lower Pliocene, we could not recognize Subzones CN12a, CN11b, CN11a, CN10c, and CN10b.

In the upper Miocene, we frequently encountered intervals containing few and strongly etched nannofossils. Barren intervals were observed within the CN7 (NN9) Zone. Nevertheless, the primary biostratigraphic events have been recognized by means of detailed analysis on short-spaced samples (about one sample every 0.048 m.y.). Nannofossils are abundant and well preserved in the middle and upper lower Miocene interval, except for discoasterids, which show strong overgrowths. The abundance of discoasterids varies throughout the

Miocene and is significantly low in some intervals (i.e., within CN7, CN6, and CN5). This discoasterid distribution pattern observed at Site 844, and at other Leg 138 sites, is typical beneath areas of strong upwelling and low abundances, and may be linked to enhanced upwelling conditions (Chepstow-Lusty et al., 1989, 1992). Within the middle Miocene Zone CN5 (NN7 and NN6), the following events were observed (Fig. 3): T (top occurrence of) common and continuous *D. kugleri;* B (bottom occurrence of) common and continuous *D. kugleri;* T *C. nitescens;* T *C. premacintyrei;* B *T. rugosus;* T *D. signus;* and T *C. floridanus.* These events provide additional biostratigraphic information that may be useful for increasing the stratigraphic resolution within the zonal subdivision of this time interval.

The lowermost part of Site 844 is placed within Zone CN3 (NN4), and is characterized by intervals of *S. heteromorphus* blooms.

Site 845

Three holes were drilled in the Guatemala Basin at Site 845, the northernmost site of the eastern transect. A continuous late Neogene record was constructed from these holes and a high-resolution magnetostratigraphy was obtained from the Pliocene to the middle Miocene (Schneider, this volume). This high-quality polarity record allows us to calibrate the biostratigraphies and to obtain new biomagnetostratigraphic data for the refinement of Miocene bioevents in a low-latitude environment (see also Raffi et al., this volume).

In the Pleistocene–upper Miocene interval, the sediments are diatom and radiolarian clays (lithologic Unit I) with isolated occurrences of pelagic carbonate. Below, in the middle–lower Miocene interval, the lithology is mostly nannofossil ooze (Unit II) with metalliferous sediments at the bottom, just above the basalt basement. Nannofossil data indicate a basement age of 17 m.y., which is older than the age estimated from plate reconstructions (see Mayer, Pisias, Janecek, et al., 1992).

We sampled Hole 845A and five cores of Hole 845B at an average interval of 70 cm. Detailed quantitative analyses were performed on closely spaced samples (about one sample every 0.025 m.y.) in the lowermost Pliocene–middle Miocene interval. The nannofossil events are summarized in Table 4 and Figure 4.

In the Pleistocene and upper Pliocene, the conventional biostratigraphic events were recognized. Nannofossil abundances are generally low throughout the interval because of clays and biosiliceous components. Most of the Pliocene section is barren of nannofossils, as the basal part of the upper Miocene corresponding to Zones CN8 and CN7 (NN10 and NN9). In the rest of the upper Miocene section (CN9–NN11), nannofossil assemblages are poorly preserved and show strong dissolution at some levels. In this interval, we could not detect T *A. amplificus.* Because discoasterids are considered a solution-resistant form of nannofossil (Ramsay, 1972, 1977; Ramsay et al., 1973), we expected their abundance to increase in the dissolved assemblages encountered in the upper Miocene (i.e., the upper part of Core 138-845A-13H, just above a barren interval; Fig. 4). On the contrary, we observed generally low abundances of discoasterids in this interval. In fact, abundances are low in some samples that contained strongly etched nannofossils. If this part of the Miocene was characterized by enhanced productivity, then our observation supports the contention (Chepstow-Lusty et al., 1989, 1992) that discoasterid abundances are reduced when productivity increases. Detailed quantitative analysis is needed to clarify this pattern and to understand the influence of environmental factors on nannofossils in the eastern equatorial Pacific (see Flores et al., this volume, for upper Pliocene interval).

In the middle and lower Miocene interval, the assemblages are rich with well-preserved nannofossils. Only discoasterids, whose abundance fluctuates even in this interval, are strongly overgrown in some samples. The excellent paleomagnetic record obtained at this site allowed us to calibrate directly the B of *C. coalitus* and the additional events within Zone CN5 (Zones NN7 and NN6) that are recorded in the same biostratigraphic interval at Site 844 (Figs. 3–4). Despite overgrowths that hamper the recognition of most of the discoasterids, we were able to identify the acme end of *D. deflandrei* in the lower Miocene section. By quantitative analysis, we were able to determine the appearance of *D. signus* in the upper part of CN3 (NN4). In the lowermost samples, we were able to find an acme in the abundance of *S. heteromorphus* (Plate 1, Fig. 7).

Site 846

Site 846 is located approximately 300 km south of the Galapagos Islands, where the South Equatorial Current interacts with the Peru Current. The four holes drilled at this site recovered a sedimentary sequence of more than 400 m, deposited since 16.5 Ma. The upper 200 m of the composite sedimentary section constructed at Site 846 is based on APC coring and is considered stratigraphically continuous. In the lower portion of the hole, recovered by XCB coring, small gaps occur in the composite section. The entire sedimentary section can be divided into two lithologic units: one consisting of alternating carbonate ooze (mostly nannofossil) and siliceous ooze (diatom and radiolarian) from 0 to about 350 mcd (Unit I); the other consisting of nannofossil ooze from about 350 to 455.3 mcd (Unit II).

We sampled Hole 846B and two cores of Hole 846D at an average interval of 70 cm. In these samples, we recognized almost all the conventional biostratigraphic events from the Pleistocene back to the upper part of the lower Miocene. These results are summarized in Table 5 and Figure 5. Range charts are reported in Tables 13 and 14. Reworking of upper Miocene nannofossils was observed in several intervals within the upper Pliocene. Nannofossils are generally abundant and well preserved throughout the section, with the exception of the lower part of the upper Miocene (CN8–CN7–CN6), where we observed poorly preserved assemblages. This interval corresponds to the dissolution event seen at other Leg 138 sites. This event was related to a major paleoceanographic event observed in the Pacific (Mayer et al., 1986; Mayer, Pisias, Janecek, et al., 1992). In the same interval, the abundances observed in discoasterid assemblage are remarkably low. These low abundances were also observed upward in the section, in intervals close to the first appearance of *Amaurolithus* spp. The occurrence of these discoasterid-depleted intervals appears linked to particularly high abundances of diatoms. The distribution of ceratolithids is also irregular, generally characterized as rare and scattered. After their entrance in the stratigraphic record, *A. primus* and *A. delicatus* are often missing from the samples. The scarcity of ceratolithids also effects the distribution of *A. amplificus,* which seems to have a shorter range at Site 846 than at Sites 844, 851, 852, and 853.

Although core recovery was poor in the lowermost part of the sedimentary sequence, the nannofossils from the few available samples of Cores 138-846B-42X and -43X allowed us to place these sediments in the upper part of Zone CN3. The assemblage in the dark reddish brown metalliferous sediments atop the basalt basement, is characterized by very high abundances of *S. heteromorphus.*

Site 847

This site, located 280 km west of the Galapagos Islands, is the equatorial divergence site of the eastern transect. The sedimentary sequence was deposited in a complex tectonic area, at the transition between crust formed at the Galapagos Spreading Center and the East Pacific Rise (Mayer, Pisias, Janecek, et al., 1992). The four holes drilled at Site 847 provide a continuous sequence spanning the last 7 m.y. that primarily consists of nannofossil ooze with abundant diatoms in some intervals. Estimated sedimentation rates are quite constant (around 30 m/m.y.), except in the early Pliocene time interval, when sedimentation rates increase (Mayer, Pisias, Janecek, et al., 1992). The average nannofossil sampling interval of 60 cm from Hole 847B provides a temporal resolution approximately 20 k.y.

In the Pleistocene and upper Pliocene, calcareous nannofossils are abundant and preservation is generally good. Most of the conventional biostratigraphic events were identified (Table 6 and Fig. 6; range chart reported in Table 15), although in some intervals nanno-

Table 13. Distrubution of calcareous nannofossil taxa in the Pleistocene-Pliocene interval at Site 846.

Zone (CN)	Core, section, interval (cm)	Depth (mbsf)	Depth (mcd)	Abundance	Preservation	Etching	Overgrowth	Small *Gephyrocapsa*	*P. lacunosa*	*G. omega*	*G. oceanica*	*Large Gephyrocapsa*	*H. sellii*
15 + 14B	2H-5, 60	13.6	14.2	A	G	1	0	A			cf.		
	2H-6, 54	15.04	15.64	A	G	1	0	A					
	2H-6, 120	15.7	16.3	A	G	1	0	A	R		F		
	2H-7, 20	16.2	16.8	A	G	1	0	A			F		
14a	2H-CC, 5	16.79	17.39	A	G	1	0	C	F		F		
	3H-1, 42	16.92	18.97	A	G	0	0	C	F		F		
	4H-1, 40	26.4	29.55	A	G	0	0	C	A	F			
	4H-5, 42	32.42	35.57	A	G	0	0	A	A	F	F		
	4H-5, 120	33.2	36.35	A	G	1	0	A	A	R	F		
	4H-6, 45	33.95	37.1	A	G	1	0	F	A	R	R		
13b	4H-6, 120	34.7	37.85	A	G	1	0	C	A				
	4H-7, 20	35.2	38.35	A	G	0	0	F	A				
	4H-7, 54	35.54	38.69	A	G	1	0	F	A				
	5H-1, 49	35.99	41.19	A	G	0	0	C	A		cf.		
	5H-3, 40	38.9	44.1	A	G	1	0		A			R	
	5H-3, 120	39.7	44.9	A	G	1	0		A			cf.	
	5H-4, 40	40.4	45.6	A	G	1	0		A			F	
	5H-6, 42	43.42	48.62	A	G	1	0	C	A		F	C	
	6H-1, 39	45.39	51.89	A	G	0	0	C	A		C	C	
	6H-3, 39	48.39	54.89	A	G	1	0	C	A		C	F	
	6H-3, 120	49.2	55.7	A	G	0	0	F	C		C	R	
	6H-4, 39	49.89	56.39	A	G	1	0	C	A		C		F
	6H-5, 40	52.4	58.9	C	G	1	0	A	C		C		F
	6H-6, 20	52.7	59.2	A	G	1	0	C	A		F		F
	6H-6, 40	52.9	59.4	A	G	1	0	F	A		F		F
13a	6H-CC, 5	53.74	60.24	A	G	1	0	F	C		cf.		F
	7H-5, 40	55.5	63.8	A	G	0	0		A				F
	8H-2, 120	66.7	76.4	A	G	1	0		C				C
	8H-3, 43	67.43	77.13	A	M	2	0		A				
12d + c	8H-3, 120	68.2	77.9	A	G	1	0		A				C
	8H-3, 140	68.4	78.1	C	M	2	0		A				F
	8H-4, 69	69.19	78.89	A	G	1	0		A				R
	9H-4, 60	78.6	88.75	A	G	1	0		C				
	10H-1, 60	83.6	96.15	A	G	0	0		A				
12b	10H-1, 135	84.35	96.9	A	G	1	0		A				
	10H-2, 60	85.1	97.65	A	G	0	1		A				
	10H-3, 60	86.6	99.15	A	G	0	0		C				
	10H-5, 60	89.6	102.15	A	G	1	0		C				
	11H-5, 60	99.1	112.6	A	G	0	0		C				
	12H-2, 120	103.2	118	A	M	1	1		C				
12ab	12H-3, 60	105.6	120.4	A	M	1	1		C				F
	12H-5, 60	108.6	123.4	A	G	0	0		C				
	13H-1, 60	112.1	128.55	A	G	0	0		A				R
	13H-7, 40	120.9	137.35	A	G	0	1		C				cf.
	14H-3, 60	124.6	141.75	A	M	1	2		C				F
	14H-3, 120	125.2	142.35	A	G	1	0		A				
	14H-4, 60	126.1	143.25	A	G	0	0		A				R
	14H-4, 120	126.7	143.85	A	M	1	0		C				F
12aA	14H-5, 60	127.6	144.75	A	M	0	0		C				
	14H-CC, 3	130.56	147.71	A	G	1	0		C				
11	15H-1, 60	131.1	150.8	A	G	1	0						
	15H-3, 60	134.1	153.8	A	G	1	0						
	15H-7, 40	139.9	159.6	A	G	1	0						
	15H-7, 63	140.13	158.83	A	M	1	1						
	15H-CC, 13	140.45	160.15	A	G	1	0						
	16H-1, 60	140.6	160.8	A	G	1	0						
	16H-4, 60	145.1	165.3	A	G	1	0						
	17H-1, 50	150	171.25	A	G	1	0						
	17H-1, 120	150.7	171.95	A	M	1	1						
10c	17H-2, 50	151.5	172.75	A	M	1	2						
	17H-2, 120	152.2	173.45	A	M	1	0						
	17H-5, 50	156	177.25	A	M	1	0						
	18H-1, 50	159.5	181.35	A	M	1	2						
	18H-3, 50	162.5	184.35	A	M	1	0						
	18H-6, 50	167	188.85	A	M	0	0						
	18H-7, 13	168.13	189.98	A	M	1	0						
	18H-CC, 13	168.97	190.82	A	M	1	0						
	19H-1, 40	168.9	192.7	A	G	0	0						
	19H-1, 120	169.7	193.5	A	M	1	0						
	19H-3, 40	171.9	195.7	A	G	0	0						
	19H-3, 120	172.7	196.5	A	G	0	0						
10b	19H-4, 40	173.4	197.2	A	M	1	0						
	20H-3, 50	181.5	207.1	A	G	0	0						
	20H-3, 120	182.2	207.8	A	M	1	2						
10a	20H-4, 50	183	208.6	A	M	1	2						
	20H-5, 50	184.5	210.1	A	M	1	1						
	21H-3, 50	191	217.95	A	M	1	2						
	21H-4, 50	192.5	219.45	A	G	1	0						

Notes: For an explanation of the abundance and preservation codes, see text. For genus names, see Appendix A.

Table 13 (continued).

C. macintyrei	*D. brouweri*	*D. triradiatus*	*D. pentaradiatus*	*D. surculus*	*D. tamalis*	*D. asymmetricus*	*Sphenolithus* spp.	*R. pseudoumbilicus*	*C. rugosus*	*A. delicatus*
C										
C										
F	R			R						
F										
C										
	R			R						
	C	F								
F	F	F						R		
C	F									
	C						R			
F	F			R						
C	F			F						
C	C			F						
F	F	R		F						
F	F			F		R				
C	F		F	F					cf.	
F	F			R	F	F				
C	F			F	F	F			cf.	
F	F		R	C	R	F	R		cf.	
F	F			F		F				
F	F		cf.	F		F			cf.	
F	F			F	F	C				
F	F			F	F	F	F		cf.	
F	F		R	F	F	C			cf.	
F	C			R	R	F	R			
F	F						C		cf.	
F	F			R		F	C	C		
C	F			R		R	C	C	F	
R	C		R	R		F	C	C	R	
F	C						C	C	F	R
F	C		F	F		R	C	C	F	R
F	F			F		R	C	C	F	
F	F			F			C	C	C	
C	F		R	F			C	C	R	
F	C		R	F		cf.	F	C	F	
F	R		R	C			F	C	R	R
R	F			F			C	C	R	R
	R		R	F			C	F	R	
	F		F	F			C	C	R	F
F	F		R	F			C	R	F	R
F	F			F			C	F	cf.	R
F	F			F			C	F	F	
R	F			F			F	C		
F	F			F			F		F	
F	F		R	F			F	F	F	
F	F			F			F		F	
F	F			F		cf.	F		F	F
	F			F			C			R
C	F		F	F			C	C		F
C	F			F		cf.	F	C		R
	C			C			C	C		R
F	C			F			C	C		R
	F			F			C	C		R
	F			F			C	A		

Table 13 (continued).

Zone (CN)	Core, section, interval (cm)	*A. primus*	*A. tricorniculatus*	*C. acutus*	*C. armatus*	*C. leptoporus*	*C. cristatus*	*C. telesmus*	*C. pelagicus*	*D. intercalaris*	*D. variabilis*
15 + 14b	2H-5, 60				C						
	2H-6, 54					C					
	2H-6, 120					C					
	2H-7, 20					C					
14a	2H-CC, 5					C					
	3H-1, 42					C	F	F			
	4H-1, 40					C					
	4H-5, 42					C					
	4H-5, 120					C	C				
	4H-6, 45					C					
13b	4H-6, 120					C					
	4H-7, 20					C					
	4H-7, 54					C	R				
	5H-1, 49					F					
	5H-3, 40					C					
	5H-3, 120					C	F	R			
	5H-4, 40					C	R	R			
	5H-6, 42					C					
	6H-1, 39					C	F				
	6H-3, 39					C	R				
	6H-3, 120					C	F		R		
	6H-4, 39					C	R		F		
	6H-5, 40					C			C		
	6H-6, 20					C			R		
	6H-6, 40					C			C		
13a	6H-CC, 5					C	F		F		
	7H-5, 40					F	R		C		
	8H-2, 120					C			C		
	8H-3, 43					C			F		
12d + c	8H-3, 120					C			C		
	8H-3, 140					C			C		
	8H-4, 69					C	R		C		
	9H-4, 60					C	F		C		
	10H-1, 60					C	R		C		
12b	10H-1, 135					C			C		
	10H-2, 60				cf.	C			C		
	10H-3, 60					C			C		
	10H-5, 60					C	R	F	C	R	
	11H-5, 60					C			C		
	12H-2, 120					C	R		F		
12aB	12H-3, 60					C			C		
	12H-5, 60					C	F		C	F	
	13H-1, 60				cf.	C	F		C	F	
	13H-7, 40					C	F		F		
	14H-3, 60				cf.	C	F	cf.	C		cf.
	14H-3, 120					C			F	R	
	14H-4, 60				cf.	C	F		C		R
	14H-4, 120					C	R	cf.	F	R	
12aA	14H-5, 60				F	C	F	F	F	F	F
	14H-CC, 3				F	C	F		F	F	
11	15H-1, 60				F	C			F		F
	15H-3, 60				F	C	F		F	F	R
	15H-7, 40				F	C	F	R	F	F	
	15H-7, 63	R	R		F	C	F		C		
	15H-CC, 13					C			C	F	F
	16H-1, 60				F	C	F		F	F	
	16H-4, 60				F	C			C	F	F
	17H-1, 50				R	C	R		C	F	F
	17H-1, 120					C			C	F	
10c	17H-2, 50	R				C			C	F	R
	17H-2, 120					C		R	C		C
	17H-5, 50	R			R	C				R	R
	18H-1, 50	R				C					F
	18H-3, 50	R				C			C		F
	18H-6, 50	R	R		R	C			F		C
	18H-7, 13				C	cf.		F	R		F
	18H-CC, 13				cf.	C			F		
	19H-1, 40	R				C			C	C	
	19H-1, 120				cf.	C			F		
	19H-3, 40			R		C			C		
	19H-3, 120			F		C			C	F	R
10b	19H-4, 40			R		C			F	F	F
	20H-3, 50			F		C			C	F	F
	20H-3, 120			F	cf.	C			C	F	R
10a	20H-4, 50	R	R			C			F	F	F
	20H-5, 50	R				C			F	F	F
	21H-3, 50	R	R			C			C	F	F
	21H-4, 50	R				C			C	F	F

fossil assemblages are difficult to interpret because of dilution by biosiliceous material. Among Pliocene discoasterids, *D. pentaradiatus* is very rare in the upper Pliocene, thus preventing the identification of Subzone CN12b (Zone NN17).

In the lower Pliocene and upper Miocene intervals (below 145 mcd; range chart in Table 16) preservation deteriorates, overgrowths affect discoasterids, and sometimes it was not possible to differentiate the species. Variations in the relative abundance of discoasterids, ceratolithids, and triquetrorhabdulids were observed, mostly in the upper Miocene interval.

The lower part of the Site 847 section was placed in Subzone CN9b, because of the presence of representatives of genus *Amaurolithus,* together with generally rare and overgrown *D. berggrenii* and *D. quinqueramus.*

In the lowermost part of the sequence, we observed strong reworking of lower Miocene nannofossils. These older forms (*Sphenolithus*

Table 13 (continued).

G. rotula	*H. carteri* gr.	*H. hyalina*	*Pontosphaera* spp.	*Reticulofenestra* spp.	*R. rotaria*	*R. claviger*	*Scyphosphaera* spp.	*Syracosphaera*	*Thoracosphaera*	*Umbilicosphaera* spp.
C	F	F	A							
	C	F		A						
cf.	C	R		A						
	C			A		R		F		
	C		F	A				F		
	C			A				F		
	C		F	C				F		
cf.	F		F	C						
	C		R	A						
	C		F	C				F		
	C		F	C				F		
	C		F	C						
	C			C						
F	C		F	C				F		
	F		F	F						
	F		F	F						
	C		F	F					F	
	C		F	A						
	C		F	C				F		
	F		F	C				F		
	C		F	C						
F	F		F	C						
	F		R	C				F	R	
	C			F						
	C		F	F						
	F			F						
	C			C					F	
	F			C				F		
	C			C				F		
	C		F	F				F		
	F		R	F				F		
	C		F	C				F		
	C		F	C					F	
	C		CF	F					R	
	C		F	F						
	C			C		R		F		
	C			A						
F	F			A						
F	C			A				R		
F	F			A				F		
F	F		F	A						
F	F			A						
C	C		F	A				F		
F	C		F	A				F		
C	C		F	A				F		
C	C			A						
F	C		F	A				F		
C	F		F	A				C		
F	F			A				F		
F	C			A				R		
F	F			A				F		F
R	C			A				R		F
F	C		F	A						
C	C			A				R		
F	C			A					R	
F	C		F	A						
R	C			A	C					
C	F			A	C				R	
C	F			A						R
F				A						
	F			A	F					
F				A	C					
F	C			A	C					
F	C		F	A	C			R		
F	C			A	C					
F			A	F	R		R			
F	F			A	F					
F	C			A	C					
F	C			A	F			R		
F	C			A	C					
F	C		F	A	C					
F	C		R	A	C					
C	F			A	C					
C	C			A	F		F			
	C		F	A	C		F			
C	C			A						
F	F			A						
	F			A						

conicus, S. dissimilis, S. belemnos-dissimilis, and *Helicosphaera intermedia*) are particularly abundant in the calcareous veneer scraped from the cherts that are the deepest samples retrieved at Site 847. The finding of lower Miocene reworked material in the sediments at Site 847 is particularly intriguing as it raises new questions regarding the complex tectonic history of an area with crust thought to be about 9 m.y. old (Hey, 1977).

Western Transect: Sites 848, 849, 850, 851, 852, and 853

The western transect sites were drilled at 110°W (Fig. 1), in an area where the equatorial current system is removed from the direct influence of the eastern boundary currents. Studies of the sedimentary sequences retrieved along this transect are designed to reconstruct the

Table 14. Distribution of calcareous nannofossil taxa in the Miocene interval at Site 846.

Zone (CN)	Core, section, interval (cm)	Depth (mbsf)	Depth (mcd)	Abundance	Preservation	Etching	Overgrowth	*D. brouweri*	*D. pentaradiatus*	*D. surculus*	*C. macintyrei*	*Sphenolithus* spp.
10a	21H-4, 50	192.5	219.45	A	M	1	1	F		F	R	C
	21H-4, 120	193.2	220.15	A	M	1	1			F	R	C
	21H-5, 50	194	220.95	A	G	1	0	R		F		A
9bC	21H-7, 50	197	223.95	A	G	1	0			F	R	C
	22H-3, 50	200.5	230.95	A	M	2	1	F		F		C
	23X-1, 50	207.7	241	A	M	2	1	F		F		A
	23X-3, 50	210	244	A	M	2	2	F		F		C
	23X-3, 120	210.7	244.7	A	M	1	2	R		R		C
9bB	23X-4, 50	211.5	245.5	A	M	2	2	F	R	F	R	C
	23X-5, 50	213	247	A	M	1	2	F		F		C
	23X-CC, 10	216.15	250.15	A	M	2	1	C		R		A
	24X-1, 40	216.6	252	A	G	1	0	F		F		C
	24X-3, 40	219.6	255	A	M	2	1	R		R	F	A
	24X-5, 40	22.6	258	A	M	1	1	C		F		C
	24X-7, 25	252.45	260.85	A	M	1	1	F				C
	25X-1, 50	226.2	261.3	A	G	1	0	C			F	C
	25X-2, 39	227.59	262.69	A	G	1	0	F		F		A
	25X-3, 40	229.1	264.2	A	M	1	1	C				C
9bA	25X-5, 16	231.86	266.96	A	G	1	0	F		R	F	C
	138-846D-											
	26X-1, 120	241	278.8	A	G	1	0	F		F		C
	26X-2, 120	242.5	276.3	A	M	1	2	F				C
	26X-3, 120	244	277.8	A	G	1	0	F				C
	26X-5, 120	247	280	A	M	1	1	F		R	C	C
	26X-6, 120	248.5	282.3	A	G	1	0	R		R	F	C
	26X-7, 23	249.03	282.83	A	G	1	0	C		F		C
	28X-3, 60	258.5	293.6	A	M	1	1	F			F	C
	29X-1, 60	264.8	299.9	A	M	1	1	F				C
9a	29X-2, 60	266.3	301.4	A	G	1	0	F				A
	29X-3, 60	267.8	302.9	A	G	1	0	F				A
	29X-4, 60	269.3	304.4	A	G	1	0	F				A
	29X-4, 120	269.9	305	C	G	1	0	R				A
	29X-5, 60	270.8	305.9	A	G	1	0	R				A
	29X-5, 120	271.4	306.5	A	M	1	1	F			R	A
8b	30X-1, 60	274.5	309.6	A	M	1	2	R				A
	30X-2, 60	276	311.1	A	M	1	2	R				A
	30X-3, 60	277.5	312.6	A	M	1	2	R				A
	30X-4, 60	279	314.1	A	M	1	2	R				A
	30X-7, 40	283.3	318.4	A	G	1	0					C
	31X-4, 60	288.6	323.7	A	M	1	2	F				A
	31X-7, 40	292.9	328	A	G	1	0	R			F	A
8a	32X-1, 60	293.7	328.8	C	M	1	1	cf.				A
	32X-2, 60	295.2	330.3	A	M	2	1			cf.		A
	32X-3, 60	296.7	331.8	A	M	2	1	F			F	A
	32X-4, 60	298.2	333.3	C	M	2	1				R	C
	32X-5, 60	299.7	334.8	C	M	2	1	R				C
	32X-5, 120	300.3	335.4	A	M	2	1				C	C
	32X-6, 60	301.2	336.3	C	M	2	1					C
	32X-6, 120	301.8	336.9	A	M	1	1	F		cf.		C
7	32X-7, 10	302.2	337.3	C	M	2	1				R	C
	33X-1, 60	303.4	338.5	A	M	1	1					F
	33X-4, 60	307.9	343	C	M	2	1					C
	33X-4, 120	308.5	343.6	C	M	2	1				R	C
	33X-5, 60	309.4	344.5	C	M	2	1					C
6	33X-5, 120	310	345.1	C	M	2	1				F	C
	33X-6, 60	310.9	346	C	M	2	1				R	C
	33X-6, 120	311.5	346.6	C	M	2	1				R	C
	33X-7, 34	312.14	347.24	C	M	2	1				R	C
	34X-2, 60			C	G	1	1				R	C
	34X-4, 60			C	G	1	1				R	C
	34X-7, 60			A	G	1	1				R	C
	35X-1, 120			A	G	0	0					C
	35X-2, 120			A	G	0	0					C
	35X-4, 120			A	G	0	1					C
	35X-6, 120			A	G	0	1					C
5b	36X-1, 36			A	G	0	1					C
	36X-4, 40			A	G	0	1					C
	36X-6, 68			A	G	0	1					C
	37X-1, 58			A	G	0	1					C
	37X-3, 26			A	G	0	1					C
	38X-2, 50			A	G	0	1					C
	38X-3, 50			A	G	0	1					C
	38X-5, 120	358.2	393.3	A	M	2	1					C
	38X-6, 50	359	394.1	A	M	2	1				R	C
5a	38X-6, 120	359.7	394.8	A	M	1	2					C
	38X-CC, 10	360.01	395.11	A	M	2	1					C
	40X-1, 40	370.7	405.8	A	M	2	1					C
	40X-2, 100	372.8	407.9	A	M	2	1					C
4	40X-3, 120	374.5	409.6	A	M	1	1					C
	40X-CC, 10	377.9	413	A	M	1	1					A
	41X-3, 60	383.5	418.6	A	M	1	1					C
	41X-CC, 9	386.77	421.87	A	M	1	1					C
	42X-1, 79	390.39	425.47	A	M	1	1					A
	42X-1, 113	390.73	425.83	A	M	1	1					A
3	42X-CC, 12	390.9	426	A	M	1	1					C
	43X-CC, 3	399.23	434.33	A	M	1	1					A
	44X-3, 60	412.5	447.6	A	M	2	1					A

Table 14 (continued).

R. pseudoumbilicus	*A. delicatus*	*A. primus*	*A. tricorniculatus*	*T. rugosus*	*D. quinqueramus*	*D. berggrenii*	*A. amplificus*	*D. loeblichii*	*M. convallis*
C	R	F		R					
C	F	F	F		F	F			
F					F	F			
C					F	R			
C			R		F	F			
C			A	R	F	R			
A			F		F	F			
C		R		F	C	F	R		
C	F				F	R	R		
C	F		F		R	F	R		
F	F	R	F		R	R	R		
F	F	F	R			R			
C	F	R				F			
C	R	R	R		R	R			
C	R	R				R			
	R		F			F			
C	cf.		F			C			
		cf.			F	C			
C		F				F			
F		R							
		F				F			
F		C		cf.	cf.	R			
		C		F	F	R			
	R	R		F	R	R			
						R			
						R		F	
					R	R			
						R		R	
									C
						R			C
								R	
						R			R
				R					R
					F			C	F
					cf.			C	F
					R			F	F
					R				F
F					F				
C									
C									
C									R
A									
A									cf.
C									cf.
C									
C				R					
C									
A				F					
C									
C									
C					cf.				
A									
C									
C				R					
A				R					
A				C					
A				C					
C				R					
C				R					
A				R					
A				R					
A				R					
A				F					
A				F					
A				C					
A				R					
A				F					
A				R					
A				F					
A									
A									
C									
F									
C									
F									
cf.									

Table 14 (continued).

Zone (CN)	Core, section, interval (cm)	*D. neohamatus*	*D. bollii*	*D. hamatus*	*C. miopelagicus*	*C. coalitus*	*D. kugleri*	*C. nitescens*	*C. floridanus*	*S. heteromorphus*	*H. ampliaperta*
10a	21H-4, 50										
	21H-4, 120										
	21H-5, 50										
9bc	21H-7, 50										
	22H-3, 50		R								
	23X-1, 50										
———	23X-3, 50										
	23X-3, 120		F								
9bB	23X-4, 50		cf.								
	23X-5, 50										
———	23X-CC, 10		cf.								
	24X-1, 40		R								
	24X-3, 40		cf.								
	24X-5, 40										
	24X-7, 25										
	25X-1, 50		cf.								
	25X-2, 39		R								
	25X-3, 40										
9bA	25X-5, 16										
	138-846D-										
	26X-1, 120										
	26X-2, 120										
	26X-3, 120										
	26X-5, 120										
———	26X-6, 120										
	26X-7, 23										
	28X-3, 60										
	29X-1, 60										
9a	29X-2, 60										
	29X-3, 60										
	29X-4, 60										
	29X-4, 120										
———	29X-5, 60										
	29X-5, 120										
8b	30X-1, 60	F									
	30X-2, 60	F									
———	30X-3, 60	F									
	30X-4, 60	F									
	30X-7, 40										
	31X-4, 60	C									
	31X-7, 40	R									
8a	32X-1, 60		F								
	32X-2, 60										
	32X-3, 60			cf.							
	32X-4, 60			cf.							
———	32X-5, 60		R	cf.							
	32X-5, 120			C							
	32X-6, 60			C							
	32X-6, 120			C							
7	32X-7, 10		cf.	R							
	33X-1, 60			C							
	33X-4, 60			R							
———	33X-4, 120			R							
	33X-5, 60		cf.								
6	33X-5, 120		R			R					
	33X-6, 60		R		C	R					
———	33X-6, 120		R		C	R					
	33X-7, 34		cf.		A						
	34X-2, 60		R		C						
	34X-4, 60		R		C						
	34X-7, 60		R		C						
	35X-1, 120		F		C		R				
	35X-2, 120		F		C		F				
	35X-4, 120		F		C		C				
	35X-6, 120		F		C		C				
5b	36X-1, 36		F		A		F				
	36X-4, 40		R		A						
	36X-6, 68		R		A		R				
	37X-1, 58		F		C		R				
	37X-3, 26		R		C						
	38X-2, 50				C						
	38X-3, 50		R		A						
	38X-5, 120				C				cf.		
———	38X-6, 50		cf.		A			R	cf.		
5a	38X-6, 120				C						
———	38X-CC, 10		cf.		C			F	F		
	40X-1, 40				C			R	F	F	
	40X-2, 100				C				F	A	
4	40X-3, 120				C			F	C	C	
	40X-CC, 10				C			C	C	C	
	41X-3, 60				C			R	F	F	
———	41X-CC, 9				C			C	F	C	
	42X-1, 79				A			C	R	A	F
	42X-1, 113				A			C	R	C	F
3	42X-CC, 12				C			F	R	A	R
	43X-CC, 3				A			F	F	A	F
	44X-3, 60				C			C	F	A	F

Table 14 (continued).

D. deflandrei	*D. signus*	*C. leptoporus*	*C. pelagicus*	*D. adamanteus*	*D. bellus* gr.	*D. calcaris*	*D. exilis*	*D. formosus*	*D. moorei*	*D. musicus*
		C								
		C								
		C	F							
		C	C				cf.			
		C	F							
		C	C				F			
		C	F							
		C	F				R			
		C	R	F						
		C		R			R			
		C	C	F						
		C	C	F			R			
		C	F	F			R			
		C	F	R						
		C	R	F						
		C								
		C	C							
		C	C							
		C	F							
		C	C							
		C	C							
		C	C			cf.				
		C	F							
		C	R		C					
		C	R	R	C					
		C	F	R	R					
		C	C							
		C	F			R				
		C	C							
		C	C			F				
		C	F		F	R				
		C	C			R				
		C	C	R	R	C				
		F	F	F	F	C				
		F	F	F	F	C				
		F	F	F	C	C				
		F	F	F	A	C				
		C	C	R	F					
		F	F		C					
		F	F	R			F			
			F	F						
			F				R			
		F	C	F						
		F	C		R					
				F			R			
		F			cf.		cf.			
		F			F					
		C		R	F					
		F	F		F					
		F		R	R					
		F	F		R		R			
		F	C		R		cf.			
		F	R	R	R		cf.			
		C	R	R	R	R	F			
		C	F	R		R	F			
		C	F	R			C		R	
		C	C	R			F		R	
		C	F	R			R			
		C	F	R			R			
		C	F	R			R			
		C	F	R			R			F
		C	F	R			R			F
		C	F	R			F			F
		C	F	R			R			F
		C	C	R			C		R	F
		C	C	R			C			R
		C	C	R			F			C
		C	F				R			A
		R	F				R			A
		R	F				F			C
		R	F	R			R			F
		F							R	F
		C						R		F
F				R					R	F
							F	F		F
								F		C
								F		F
								C		F
							R	F		C
F			R	R			R			F
		F		R						F
	C							C		C
C	C		R				F	F	R	C
C	F		cf.	F			F	C		C
A				R			F	R	R	C
A		F		R				A		F

Table 14 (continued).

Zone (CN)	Core, section, interval (cm)	*D. neorectus*	*D. pseudovariabilis*	*D. variabilis*	*G. rotula*	*H. carteri* gr.	*H. intermedia*	*Pontosphaera* spp.	*Reticulofenestra* spp.	*R. rotaria*
10a	21H-4, 50	R		F	F	F			A	C
	21H-4, 120			F	F	F			A	C
	21H-5, 50				F	C			A	F
9bc	21H-7, 50			F	C	F			A	F
	22H-3, 50			F		C			A	C
	23X-1, 50				F	F		R	A	C
———	23X-3, 50			F		F			A	F
	23X-3, 120			F	F	F			A	
9 bB	23X-4, 50			F	F	F			A	
	23X-5, 50			R		C			A	
———	23X-CC, 10			F	F	C		F	A	cf.
	24X-1, 40			R	C	C			A	cf.
	24X-3, 40					C			A	
	24X-5, 40			F		F			A	
	24X-7, 25			F	F	F			A	
	25X-1, 50			F	C	C			A	
	25X-2, 39				C	F			A	
	25X-3, 40				C	C			A	
9bA	25X-5, 16			C	C	C			A	
	138-846D-									
	26X-1, 120			F	C	C			A	
	26X-2, 120			C	C	F			A	
	26X-3, 120			C	F	F			A	
	26X-5, 120			F	C	F			A	
———	26X-6, 120			F	F	C			A	
	26X-7, 23			F	F	C			A	
	28X-3, 60			F	F	F			A	
	29X-1, 60			F	C	F			A	
9a	29X-2, 60				F	F		C	A	
	29X-3, 60			F	F	F			A	
	29X-4, 60			C		F			A	
	29X-4, 120			F		F			A	
———	29X-5, 60			C	F	C			A	
	29X-5, 120	cf.			F	C		F	A	
8b	30X-1, 60			F		F			A	
	30X-2, 60			F		F			A	
———	30X-3, 60			F		F			A	
	30X-4, 60			A		F			A	
	30X-7, 40			F	R	F			A	
	31X-4, 60	R	R		F	F			A	
	31X-7, 40			F	F	C			A	
8a	32X-1, 60				F	C		R	A	
	32X-2, 60		R	F	R	C			A	
	32X-3, 60			F	F	F		F	A	
	32X-4, 60			C	R			R	A	
———	32X-5, 60		F	F					A	
	32X-5, 120				R	C		R	A	
	32X-6, 60			F		F			A	
	32X-6, 120		F	F	F	C		R	A	
7	32X-7, 10			F		F		R	A	
	33X-1, 60					F		F	A	
	33X-4, 60			R		F			A	
———	33X-4, 120			R	C	C			A	
	33X-5, 60				F	F			A	
6	33X-5, 120			C		F		R	A	
	33X-6, 60			C	F	F			A	
———	33X-6, 120			C	C	F			A	
	33X-7, 34			F	C	F		R	A	
	34X-2, 60			R	F	F			C	
	34X-4, 60			R	F	F			C	
	34X-7, 60			F	F	F			C	
	35X-1, 120				R	C			A	
	35X-2, 120				R	C			A	
	35X-4, 120				R	C			A	
	35X-6, 120				R	C			A	
5b	36X-1, 36					C			A	
	36X-4, 40					C			A	
	36X-6, 68					C			A	
	37X-1, 58				R	C			A	
	37X-3, 26				F	A	F		A	
	38X-2, 50				R	A			A	
	38X-3, 50			cf.	R	C	F	R	A	
	38X-5, 120			cf.	F	C	F	F	A	
———	38X-6, 50			cf.	C	C	F	C	A	
5a	38X-6, 120			cf.	F	C	C	F	A	
———	38X-CC, 10			cf.	F	A	C	F	A	
	40X-1, 40			cf.	F	F			A	
	40X-2, 100					A			A	
4	40X-3, 120			cf.	C	C		R	A	
	40X-CC, 10				C	C		C	A	
	41X-3, 60			cf.	F	A		F	A	
———	41X-CC, 9			cf.		A		F	A	
	42X-1, 79				R	C		F	A	
	42X-1, 113				F	C		R	A	
3	42X-CC, 12				F	C		F	A	
	43X-CC, 3			cf.	R	F		F	A	
	44X-3, 60					C		C	A	

Table 14 (continued).

Thoracosphaera	*T. milowi*	*T. serratus*	*Umbilicosphaera* spp
R			
R			
			R
			F
			R
			F
			F
			F
			F
			F
			F
		F	
		R	
		C	
		F	
		F	
R		C	
		F	
R			
R			
	R		

Note: For an explanantion of the abundance and preservation codes, see the text. For genus names, see Appendix A.

development of the equatorial current system during late Neogene under the influence of global climatic change. All the western transect sites are located on crust generated at about 10 to 12 Ma. The sites lie about 900 km west of the East Pacific Rise, with the exception of the southernmost Site 848, which is located about 650 km away. Because sufficient time was saved during this part of the leg, because of favorable weather and drilling conditions, we were able to drill an extra site (Site 850) along the transect.

We report on six of the seven western transect sites. Site 848 lies south of the equator. Sites 849 and 850 lie within the equatorial divergence zone. Sites 851, 852, and 853 were drilled progressively north of the equator. We excluded from this report the northernmost Site 854 (for biostratigraphic results on nannofossils see *Initial Reports* volume).

Site 848

The sedimentary sequence drilled at this southernmost site of the western transect is almost 100 m thick, and extends to the uppermost part of middle Miocene. Excellent magnetostratigraphy was obtained in the Pleistocene–Pliocene interval (upper 46 m of the section) and in the lower part (the 20 m above the basement), which is middle–upper Miocene in age.

Our biostratigraphic work is based on closely spaced samples (10–40 cm) from Hole 848B and from five cores of Hole 848C. Nannofossil biostratigraphic results are summarized in Figure 7, and the events are listed in Table 7. Range charts are reported in Tables 17 and 18. Nannofossils are generally abundant and have variable preservation throughout the sequence. Poor nannofossil assemblages (in terms of abundance and preservation) were observed in the lower part of the section, and correspond to an interval with low sedimentation rates (4–6 m/m.y.) and enhanced dissolution (Mayer, Pisias, Janecek, et al., 1992).

Precise biostratigraphic assignment was difficult in some intervals because of the absence of marker species and to dissolution, which primarily effected discoasterids. Discoasterid identification was particularly vexing in the oldest sediments retrieved at Site 848, where overgrowths made the nannofossils almost unrecognizable. Furthermore, representatives of genus *Catinaster* are missing, thereby further complicating the biostratigraphy. In the lower part of the section, biostratigraphic control was provided by the highest occurrence of *C. miopelagicus* and lowest occurrence of *D. hamatus.* Poor preservation of discoasterids was observed within the entire Miocene interval. Notwithstanding the strong overgrowths, we detected the lowest occurrence of *D. neohamatus* and tentatively placed the boundary CN8a/CN8b at the lowest observed specimens of *D. loeblichii.* Even the CN8/CN9 boundary (B *D. berggrenii*) was placed with some difficulty, as the marker *D. berggrenii* was strongly overgrown, very rare, and scattered in the lower part of its range.

The consistent occurrence of ceratolithids in the uppermost Miocene and lower Pliocene is noteworthy. Specimens of genera *Amaurolithus* and *Ceratolithus* are unusually abundant in some levels and allowed us to define their biostratigraphic events. In the upper part of lower Pliocene (mainly within Zone CN11), we observed a strong reworking of middle–upper Miocene nannofossils such as *C. coalitus, M. convallis, D. berggrenii,* and *D. quinqueramus.* The same reworking was observed at Sites 850, 851, 852, and 853.

Site 849

The sedimentary sequence at Site 849 accumulated above a crust with an age of 11–12 Ma (Mayer, Pisias, Janecek, et al., 1992). As the site is located within the high productive equatorial divergence zone, it can provide important information about the development of oceanic conditions in this region during late Neogene. Four holes were drilled at this site, and a 320-m composite section was constructed from the recovered cores. This interval spans the time from the Pleistocene to the middle Miocene. The dominant lithology is diatom-nannofossil ooze with biosiliceous interbeds of variable thickness. The sedimentation rates at Site 849 are variable and follow a general pattern observed throughout the eastern equatorial Pacific (see Mayer, Pisias,

Table 15. Distribution of calcareous nannofossil taxa in the Pleistocene-upper Plicene interval at Site 847.

Zone (CN)	Core, section, interval (cm)	Depth (mbsf)	Depth (mcd)	Abundance	Preservation	Etching	Overgrowth	Small *Gephyrocapsa*	*E. huxleyi*	*P. lacunosa*	*G. oceanica*	*Gephyrocapsa* sp. 3
15	1H-2, 120	2.7	2.7	A	G	0	0	F	F		C	A
______	1H-3, 120	4.2	4.2	A	G	0	0	F	?		A	A
	1H-4, 120	5.7	5.7	A	G	0	0	R			A	C
	1H-5, 15	7.2	7.2	A	G	0	0	C			A	C
	2H-1, 120	7.7	7.83	A	G	0	0	F			A	F
14b	2H-3, 120	9.2	9.33	A	G	0	0	A			F	
	2H-4, 120	10.7	10.83	A	G	0	0	A			C	
	2H-5, 50	11.5	11.63	A	G	0	0	A			R	
______	2H-5, 120	12.2	12.33	A	G	0	0	A			C	
	2H-6, 51	12.99	13.14	A	G	0	0	A		F	R	
	2H-6, 120	13.68	13.83	A	G	0	0	A		C	F	
	2H-7, 24	14.22	14.37	A	G	0	0	A		C	R	
14a	3H-1, 50	16.5	16.85	A	G	0	0	A		C	R	
	3H-3, 50	19.5	19.85	A	G	0	0	A		A	F	F
	3H-7, 60	26.02	25.85	A	G	0	0	A		A	F	C
	4H-1, 60	26.1	28.93	A	G	0	0	A		A	R	F
	4H-1, 120	26.7	29.53	A	G	0	0	A		A	C	F
- - - - -	4H-2, 60	27.6	30.43	A	G	0	0	A		A	R	F
	4H-2, 120	28.2	31.03	A	G	0	0	A		A		*
	4H-3, 60	29.1	31.93	A	G	0	0	F		A	*	
	4H-3, 120	29.7	32.53	A	G	0	0	C		A		
	4H-4, 60	30.6	33.43	A	G	0	0	C		A		
	4H-5, 60	32.1	34.93	A	G	0	0	F		A		
	4H-7, 10	34.6	37.43	A	G	0	0	A		A		
	4H-7, 60	35.1	37.93	A	G	0	0	C		A		
	5H-1, 60	35.6	38.4	A	G	0	0	A		A		
	5H-1, 120	36.2	39	A	G	0	0	C		A	C	
13b	5H-2, 60	37.1	39.9	A	G	0	0	C		C	C	
	5H-2, 120	37.7	40.5	A	G	0	0	C		C	A	
	5H-3, 60	38.6	41.4	A	G	0	0	C		C	C	
	5H-5, 60	41.6	44.4	A	G	0	0	A		C	C	
	5H-7, 40	44.4	47.2	C	MG	1	0	A		F	A	
	5H-CC, 10	45.09	47.89	A	G	0	0	C		A	A	
	6H-1, 60	44.5	49.58	A	G	0	0	A		C	F	
	6H-1, 120	35.6	50.18	A	G	0	0	A		C	C	
	6H-2, 60	36.5	51.08	A	G	0	0	A		A	R	
	6H-3, 60	38	52.58	A	G	0	0	C		A	F	
- - - - -	6H-3, 120	38.6	53.18	A	G	0	0	A		A	R	
	6H-4, 60	39.5	54.08	A	G	0	0	C		A		
	6H-5, 60	41	55.58	A	G	0	0	F		C		
	7H-1, 60	54.6	61.35	A	G	0	0	C		A		
13a	7H-4, 60	59.1	65.85	A	G	0	0	F		A		
	7H-5, 60	60.6	67.35	A	G	0	0	C		C		
	7H-5, 120	61.2	67.95	A	G	0	0	R		C		
______	7H-6, 60	62.1	68.85	C	G	0	0	R		A		
	7H-6, 120	62.7	69.45	A	G	0	0	R		A		
	7H-7, 10	63.1	69.85	A	MG	1	0	R		A		
	7H-7, 40	63.4	70.15	A	MG	1	0			A		
	8H-1, 60	64.1	72.28	A	MG	1	1			A		
	8H-1, 120	64.7	72.88	A	G	0	0			A		
	8H-2, 60	65.6	73.78	A	MG	1	1			A		
	8H-2, 120	66.2	74.38	A	G	0	0			A		
12d	8H-3, 60	67.1	75.28	A	G	0	0			A		
+	8H-3, 120	67.7	75.88	A	MG	1	1			A		
12c	8H-4, 60	68.6	76.78	A	G	0	0			A		
	8H-4, 120	69.2	77.38	A	G	0	0			A		
	8H-5, 120	70.7	78.88	A	G	0	0			A		
	8H-6, 60	71.6	79.78	A	G	0	0			A		
	8H-6, 120	72.2	80.38	A	G	0	0			A		
	9H-1, 60	73.6	83.08	A	G	0	0			A		
	9H-1, 120	74.2	83.68	A	MG	1	0			A		
	9H-2, 60	75.1	84.58	A	MG	1	0			A		
	9H-2, 120	75.7	85.18	A	MG	1	0			A		
- - - - -	9H-3, 60	76.6	86.08	A	MG	1	0			A		
	9H-3, 120	77.2	86.68	A	MG	1	0			A		
	9H-4, 60	78.1	87.58	A	MG	1	0			A		
12b	9H-5, 60	79.6	89.08	A	MG	1	0			A		
	9H-6, 60	81.1	90.58	A	G	1	0			A		
______	9H-6, 120	81.7	91.18	A	MG	1	0			A		
	9H-7, 15	82.15	91.63	A	MG	1	0			C		
12aB	9H-7, 40	82.4	91.88	A	G	1	0			A		
	10H-2, 60	84.6	93.83	A	MG	1	0			A		
	10H-4, 60	87.6	96.83	A	G	0	0			A		

Janecek, et al., 1992). Sediment accumulation is particularly high in the latest Miocene/early Pliocene (as high as 100 m/m.y.). These high rates suggest that the site was within the highly productive equatorial divergence zone by that time.

The average sample spacing for nannofossil analysis at Site 849 was 60 cm (Hole 849B, five cores from Hole 849C, and from one core of Hole 849D). Because sedimentation rates varied, our 60-cm sample spacing translates in a range of temporal resolutions varying from 1 sample/0.04 m.y. to 1 sample/0.012 m.y. The nannofossil events we recognized are listed in Table 8, and the biostratigraphy is summarized in Figure 8.

Nannofossil preservation is generally moderate to good. Placoliths, mainly reticulofenestrids, are the most important component of the nannofossil assemblages. Within this group, we identified morphotypes with round outlines and central opening, labeled as "circular reticulofenestrids" in the figures (see "Taxonomic Notes" section,

Table 15 (continued).

large *Gephyrocapsa*	*H. sellii*	*C. macintyrei*	*D. brouweri*	*D. triradiatus*	*D. pentaradiatus*	*D. surculus*	*D. tamalis*	*D. asymmetricus*	*Sphenolithus*	*R. pseudoumbilicus*
		*								
C										
C										
C										
C										
C**										
*	R									
	R									
	R									
	R	R								
	C	F								
	A	F								
	C	F								
	C	C								
	C	F								
	F	C								
	C	F								
	A	C								
	F	C								
	A	F	*							
	R	F	C	F						
	F	F	F	R						
	R	C	F	*						
	A	F	C	*		*				
	F	A	A							
	R	F	F	*						
	R	C	C							
	R	F	C							
	R	R	A	*						
	R	R	C							
	R	*	C							
		C	A							
	R	F	C							
	R	F	R							
	*	F	F							
	F	C	C							
	F	F	F		*	*		R		
	F	F	C							
	R	C	F					R		
		F	A			R				
		F	F			F				
		F	F			F				
	R	F	F	*		F				
	F	F	A			R		*		
		F	A			*	R			
		C	C	*		F	F	F		
		R	C	*		F	R	F		
		F	C			F	F	F		

this chapter). At Site 849, these reticulofenestrids appear when the large morphotypes *R. pseudoumbilicus* reenter the stratigraphic record in Subzone CN9bA. The distribution of "circular reticulofenestrids" has also been checked at Sites 846, 847, and 850. At these sites, the distribution is also restricted to Subzone CN9b, up to levels corresponding to the lower range of *A. primus* and close to the lowest occurrence of *A. amplificus*.

Abundances of discoasterids at Site 849 fluctuate throughout the sequence and are generally low, as expected in an area of high productivity. Even ceratolithids are very rare and discontinuously distributed. Some biostratigraphic events were detected with difficulty, such as the lowest and highest occurrences of *A. amplificus* and the lowest occurrence of *D. hamatus*. Other markers are missing, such as *C. coalitus* and *C. calyculus*.

Table 15 (continued).

Zone (CN)	Core, section, interval (cm)	*C. leptoporus*	*C. cristatus*	*C. telesmus*	*C. pelagicus*	*D. intercalaris*	*D. variabilis*	*G. rotula*	*H. carteri*	*H. wallichii*	*Pontosphaera*
15	1H-2, 120	C		F						F	
———	1H-3, 120	A								C	
	1H-4, 120	A		R						C	
	1H-5, 15	A	R	R					F	C	
	2H-1, 120	C							R	R	
14b	2H-3, 120	C								F	
	2H-4, 120	A		R						F	
	2H-5, 50	C		R						C	
———	2H-5, 120	C		R						C	
	2H-6, 51	C								C	
	2H-6, 120	C		R						C	
	2H-7, 24	C								C	
14a	3H-1, 50	C									
	3H-3, 50	C								C	C
	3H-7, 60	C	F						F	F	C
	4H-1, 60	C	R						F	R	
	4H-1, 120	C							F		
———	4H-2, 60	C							C		F
	4H-2, 120	A	R						C		R
	4H-3, 60	C							C	F	F
	4H-3, 120	C							F		
	4H-4, 60	C							C	R	
	4H-5, 60	C							C		F
	4H-7, 10	A							C		
	4H-7, 60	C							F		F
	5H-1, 60	C							C		F
	5H-1, 120	C							C		
13b	5H-2, 60	C							C		F
	5H-2, 120	C							C		F
	5H-3, 60	C	R	R	R				C		C
	5H-5, 60	C			R				F		F
	5H-7, 40	F							F		
	5H-CC, 10	F	R	R					C		
	6H-1, 60	C			R				C		F
	6H-1, 120	C							F		
	6H-2, 60	C	R	R	R				C		
	6H-3, 60	C	F	R					C		C
———	6H-3, 120	C	F	F	R				C		
	6H-4, 60	C	C		F				C		R
	6H-5, 60	C	F		C				C		F
	7H-1, 60	C	R		F				C		F
13a	7H-4, 60	C	R		F				C		F
	7H-5, 60	C	F		F				C		
	7H-5, 120	C	R		C				C		F
———	7H-6, 60	C			F				F		C
	7H-6, 120	C	R		C				R		R
	7H-7, 10	C			F				C		R
	7H-7, 40	C	F		C				C	R	R
	8H-1, 60	C	F		C	*			A		R
	8H-1, 120	C	F		A	*			C		F
	8H-2, 60	C	F		C	*			C		R
	8H-2, 120	C			C				C		
12d	8H-3, 60	C			C				C		F
+	8H-3, 120	C	F		C				C		
12c	8H-4, 60	C			C				C		
	8H-4, 120	A			C	R			C		
	8H-5, 120	A			A				C		R
	8H-6, 60	C	F		C				C		F
	8H-6, 120	C			C				C		F
	9H-1, 60	C	F		C				C		F
	9H-1, 120	A	R		A				C		R
	9H-2, 60	C	R		F			F	F		C
	9H-2, 120	A	F		A				A		
———	9H-3, 60	C	R		F		*	R	A		F
	9H-3, 120	A	R		A	*		R	C		F
	9H-4, 60	C	F		C	R		F	C		F
12b	9H-5, 60	C	R		F	R	*	C	C		F
	9H-6, 60	C			C	R		F	C		F
———	9H-6, 120	A	R		C	R			C		F
	9H-7, 15	A	F		A	R			A		F
12aB	9H-7, 40	C	F		C	F		R	C		F
	10H-2, 60	C	F		F	C		F	C		F
	10H-4, 60	C	F		F	F		F	F		R

Within the oldest sediments retrieved at Site 849, we recorded the final range of common *D. kugleri*. This finding allows us to assign the lowermost part of the sequence to the middle part of Subzone CN5b.

Site 850

Site 850 was drilled just north of the equator, halfway between Sites 849 and 851. This location is suitable for investigating the narrow equatorial divergence zone. Unfortunately, the site was only drilled once, because of time pressures. The hole was cored with the APC to 74 mbsf and then cored with the XCB from there to the basement. The 400-m section recovered from this site spans the time interval from the Pleistocene to the middle Miocene. A brief interval with a strong magnetic signal was identified between 60 and 75 mcd, spanning the Subchron 2An.1r (Kaena) to the 2An–2Ar (Gauss–Gilbert) boundary. The sedimentary section at Site 850 represents a

Table 15 (continued).

Rhabdosphaera	*Reticulofenestra* spp.	*Scyphosphaera*	*Syracosphaera*	*Thoracosphaera*	*Umbilicosphaera*	Reworked
			C	R		
			F	R		
			C	F		
			R	R	C	
					C	
					C	
	C		C	R		
	C					
	F					
	F					
	F					
	C					
C	C					
C	F	R				
	C					
	C					
F	A					
R	C					
F	A					
	C					
	A					
F	A					
	F					
F	C					
F	C					
	C					
F	A					
F	A			F		
C	A	R				
F	C					
	A					
	C					
F	C					
	C		F			
	C		R			
C	C		F			
	A		C			
R	C		C			
F	A		C			
F	A		F			
F	A		F			
	A		F			
F	A		F			
C	A		F			
R	A		C			
R	A		C			
R	A		C			C
R	A		C			
F	A		F			
R	A		C			
	A		F			
F	A		A			
	A		F			
	A		A			
	A		F			
	A		A			
R	A		C			
F	A		F			
F	A		C			
F	A		F			
R	A		R			R
C	A		F			
	A					
F	A					
F	A					
F	A		R			
F	A		F			
F	A		F			
F	A		C			R
F	A		C			
F	A		C			
F	A		C			
R	A		F			

Notes: For an explanation of the abundance and preservation codes, see text. For genus names, see Appendix A. Single asterisk (*) = one specimen observed.

single lithologic unit of radiolarian and diatom-nannofossil ooze, with several layers of laminated diatom ooze and thinly bedded chert in the lower part of the section. The sedimentation pattern is similar to that reconstructed at Site 849 (Mayer, Pisias, Janecek, et al., 1992).

We took 6 to 12 samples per core from Hole 850B for nannofossil analysis. The resulting biostratigraphy is shown in Figure 9, and the nannofossil events are listed in Table 9. Nannofossils are abundant throughout the sequence and their preservation varies. Placoliths generally dominate the assemblages. Discoasterids and ceratolithids fluctuate in abundance and are very rare or absent in some intervals, as was seen at Site 849. A detailed nannofossil biostratigraphy in the upper Miocene and Pliocene intervals was difficult to generate on

Table 16. Distribution of calcareous nannofossil taxa in the lower Pliocene-upper Miocene interval at Site 847.

Zone (CN)	Core, section, interval (cm)	Depth (mbsf)	Depth (mcd)	Abundance	Preservation	Etching	Overgrowth	Small *Gephyrocapsa*	*H. sellii*	*P. lacunosa*	*C. macintyrei*	*D. brouweri*	*D. triradiatus*	*D. pentaradiatus*	*D. surculus*	*D. tamalis*	*D. asymmetricus*	*Sphenolithus* spp.	*R. pseudoumbilicus*	*C. rugosus*	*A. delicatus*	*A. primus*	*A. tricorniculatus*
	12H-1, 120	102.7	115.73	A	G	0	0		*	C	C	C		C	R	R	*			F			
12aB	12H-2, 60	103.6	116.63	A	G	0	0			C	C	C		F	F	*	R			R			
	12H-2, 120	104.2	117.23	A	MG	1	0			C	R	C	*	*			*			*			
	12H-3, 60	105.1	118.13	A	MG	1	1			A	C	C		F	F		*	*		F			
	12H-3, 120	105.7	118.73	A	G	0	0	F	R	C	A	R		F			*	C		F			
12aA	12H-4, 60	106.6	119.63	A	G	0	0	R	R	C	C	F		R	R			C		R			
	12H-4, 120	107.2	120.23	A	G	0	0	F	R	F	F	F		*			R	R		R			
	12H-5, 60	108.1	121.13	A	G	0	0	R		C	F	R		R	R			C		F			
	12H-5, 120	108.7	121.73	A	G	0	0	F		F	A	C	*	*	R	*	*	C	C	F			
	12H-6, 63	109.63	122.66	A	G	0	0	R		F	F	R			R		*	C	A	R			
	12H-6, 120	110.23	123.26	A	G	0	0	R	R	R	A	R			*			A	A	F			
	12H-7, 14	110.67	123.7	A	MG	1	0	R			F	C		R	R		R	F	A	F			
	12H-7, 60	111.13	124.16	A	G	0	0			R	F	F		F	R		*	C	C	R			
	13H-1, 70	111.7	125.7	A	G	0	0				F	F		R	R		F	C	C	R			
	13H-2, 60	113.1	127.1	A	G	0	0				F	C			R		F	C	C				
11B	13H-4, 150	117	131	A	G	0	0				F	F					*	A	A	F			
	13H-5, 60	117.6	131.6	A	G	0	1				F	F		F	R		F	C	C	R	*		
	14H-1, 60	121.1	136.58	A	MG	1	1				F	C		R	F			C	C	F			
	14H-2, 124	123.24	138.72	A	G	0	0		R		F	F	R	F	R			A	A	R			
	14H-3, 60	124.1	139.58	A	G	0	0				F	F		F	F		F	A	A	R			
	14H-3, 124	124.74	140.22	A	G	0	0				C	C	R		R		F	A	A	R			
	14H-4, 124	126.24	141.72	A	G	0	0				C	F			F			A	A				
	14H-5, 60	127.1	142.58	A	G	0	0				F	A		F	F		F	C	C	*		*	
11a ?	14H-5, 124	127.74	143.22	A	MG	1	1				A	F		C	R			A	A	F			
	14H-6, 60	128.6	144.08	A	MG	1	1				F	C		F	F		*	A	C	R		*	
	14H-6, 124	129.24	144.72	A	M	1	2				C	F		*				A	A	R			
	14H-7, 50	130	145.48	A	MG	1	1				F	F		F	F			F	F	R		*	
	15H-2, 60	132.1	148.05	A	MG	1	1				F	C		R	F			F	F	R		R	
	15H-4, 60	135.1	151.05	A	MG	1	1				F	F		F	C			F	R	R			
	15H-6, 62	138.12	154.07	A	MG	1	1				C	F		R	F			F	C	R		*	
	15H-7, 49	139.49	155.44	A	MG	0	2				R	C		C	F			A	R	R		*	
	16H-1, 140	140.9	157.35	A	MG	0	2				F	A		C	C			C	F	C		R	
10c	16H-5, 60	144.6	161.05	A	MG	1	1				F	F		F	F			C	C	F	F	R	
	16H-6, 60	146.1	162.55	A	MG	0	1				F	F		R	R			C	F	R	R	F	
	17H-1, 60	146.4	165.75	A	MG	1	2				F	F		F	F			C	F			R	
	17H-2, 60	147.9	167.25	A	MG	1	1				F	F		F	F			A	F				
	17H-3, 60	149.4	168.75	A	G	0	0				F	F		F	F			C		R		R	
	17H-4, 60	150.9	170.25	A	G	0	1				F	F		F	F			A		F		*	
	17H-5, 60	152.4	171.75	A	G	0	1				F	F		R	F		*	F		R	*		
	17H-5, 123	153.03	172.38	A	M	1	2				C	C			R			C	R	R	R	R	
	17H-6, 60	153.9	173.25	A	MG	1	1				F	F		R	F			C				R	
	17H-6, 123	154.53	173.88	A	MG	1	2				C	C			C			A					
	17H-7, 154.85	174.2	A	MG	I					F	F		R	F		*	C				R		R
	18H-2, 60	157.6	176.95	A	MG	1	1				F	F		F	F		*	C					
10b	18H-3, 60	159.1	178.45	A	MG	1	1				C	F		F	F		*	C					
	18H-4, 60	160.6	179.95	A	MG	0	1				F	C			F			A					
	18H-5, 60	162.1	181.45	A	MG	1	1				C	F			F			C	C			*	
	18H-6, 60	163.6	182.95	A	MG	1	1				F	A			F			C	C				
	18H-7, 3	164.53	183.88	A	G	0	1				F	C		F	R		R	A	A				
	18H-7, 15	164.65	184	A	MG	0	2				C	C			F			C	R				
	19H-1, 60	165.3	184.65	A	MG	1	2				F	F			F			C	C				
	19H-1, 123	165.93	185.28	A	G	0	0				R	F		F	R		*	C	F				
	19H-2, 123	167.43	186.78	A	MG	1	1				C	F		C	R			C	C			*	
10a	19H-5, 123	168.93	188.28	A	MG	0	2				R	C		C	F			A	A			*	
	19H-7, 5	169.25	188.6	A	MG	0	2				C	F		F	R			A	F			*	
	19H-7, 40	169.6	188.95	A	MG	1	1				F	F		R	F			C	C		*		
	20X-1, 60	174.5	193.85	A	MG	1	2					F			F			A	C				
	20X-1, 122	175.12	194.47	A	MG	0	2				R	C		F	C			A	A				
	20X-2, 60	176	195.35	A	MG	1	1					R		R	F			A	C				
	20X-2, 122	176.62	195.97	A	G	0	0				C			*	*			A	C			R	
	20X-3, 60	177.5	196.85	A	MG	1	1				F	F		R	R			C	C				
	20X-3, 93	177.83	197.18	A	G	0	1				F	C		R	C			C	C				
	20X-4, 60	179.01	198.36	A	MG	1	1							R	R			C	C				
	20X-4, 123	179.64	198.99	A	MG	1	1				R	C		C	C			A	A			*	
	20X-5, 60	180.51	199.86	A	MG	1	2					R			F			C	C				
	20X-6, 60	182.01	201.36	A	MG	1	2				F	F			R			C	C				
	21X-1, 60	184.1	203.45	A	MG	1	1					R			F			A	C				
	21X-2, 60	185.6	204.95	A	G	1	0				F	R			F			A	C		*		
	21X-3, 60	187.1	206.45	A	M	0	2				R	cf						AA	C				
	21X-4, 60	188.6	207.95	A	G	0	1				F	R			F			A	A				
	21X-5, 60	190.1	209.45	A	MG	0	2				F	R			cf			A	A				
9b	21X-6, 60	191.6	210.95	A	MG	0	2				F	R			F			A	C				
	21X-7, 40	192.9	212.25	A	MG	0	2				F	R			F			A	A				
	22X-1, 60	193.8	213.15	A	M	0	2				R	R			cf			A	A				
	22X-2, 123	195.93	215.28	A	MG	0	2				F	C						A	A				
	22X-3, 60	196.8	216.15	A	G	0	1					R			R			AA	C				
	22X-4, 123	198.93	218.28	A	M	1	2				C	R			R			A	C				
	22X-5, 60	199.8	219.15	A	MG	0	2				F	F			F			AA	C			*	
	22X-6, 123	201.93	221.28	A	MG	0	2				R	cf			*			AA	A				
	23X-1, 60	203.4	222.75	A	MG	0	2				F	cf			F			A	A			*	

Table 16 (continued).

Zone (CN)	Core, section, interval (cm)	*C. acutus*	*C. armatus*	*T. rugosus-rioensis*	*D. quinqueramus-berggrenii*	*A. amplificus*	*M. convallis*	*C. leptoporus*	*C. cristatus*	*C. pelagicus*	*Dictyococcites*	*D. bellus*	*D. decorus*	*D. intercalaris*	*D. tressilifer*	*D. variabilis*	*G. rotula*	*H. carteri*	*Pontosphaera*	*Reticulofenestra*	Circular *Reticulofenestra*	*Rhabdosphaera*	*Scyphosphaera*	*Syracosphaera*	Reworked	*S. conicus*	*S. dissimilis*	*S. dissimilis-belemnos*	*C. coalitus*	Miocene forms
	12H-1, 120							A	R				F	R			F	F	R	A										
12aB	12H-2, 60							C	*						R	R	C	C	F	A				F						
	12H-2, 120							F	R					F			R	F	R	A				F						
	12H-3, 60		*					C	R					R		R	F	C		A				F						
	12H-3, 120							A	C							*	F	C	F	A				C					X	
12aA	12H-4, 60							A						R		R	F	F	C	A		R		R						
	12H-4, 120							A	F							*	F	A	R	A				R						
	12H-5, 60		*					C								F	C	C		A										X
	12H-5, 120							A	R				*				F	A	R	A				R						X
	12H-6, 63						C						F		F	F	C	R	A											
	12H-6, 120				R			A					R			R	C	C		A										X
	12H-7, 14							A	R							C	R	R		A									X	X
	12H-7, 60							A	F	R				R		F		C		A				R						
	13H-1, 70							C		R				R		R	F	C		A				R						
	13H-2, 60							C		R				R		F	R	F		A										
11B	13H-4, 150							A	R					*	*	*	R	C		A										
	13H-5, 60							C	*	F				R		C		C		A										
	14H-1, 60							C		F				*		F	F	C	R	A	C		R	R						
	14H-2, 124				F			A			*				*	F	F	C		A	F									X
	14H-3, 60							A		F	R			F		C		F		A	F									
	14H-3, 124							A		R	F					F	F	A		A	F									
	14H-4, 124				C			A		*	F				R	C	F	A		A	F									X
	14H-5, 60							C		R	F					F	F	C		A										
11a ?	14H-5, 124				C			A		R	F					*	F	C		A	R									X
	14H-6, 60							C		C	F			R		F	F	C	R	A	C			R						
	14H-6, 124							A		F	R						C	C		A			R							
	14H-7, 50							C		F	R			*			F	F	R	A	C			R						
	15H-2, 60							C			R			F		R	C	C	R	A	C									
	15H-4, 60							C		R	R			F			F	C	F	A	C									
	15H-6, 62							C								R	F	C	R	A	C			F						
10c	15H-7, 49							A			F					R	C	C	R	A	C			F						X
	16H-1, 140							C		F	F					F	F	C	R	A	C		R	R						
	16H-5, 60							C		C	F			R		R		C		A	C			R						
	16H-6, 60							C			R						R	C		A	C									
	17H-1, 60							F		R	F			F		*	R	C	R	A	F			F						
	17H-2, 60							C		F	C						C	C		A	F									
	17H-3, 60							C		C	F			R		F	F	F		A	C									
	17H-4, 60	R						C		F	R						F	F		A	F									
	17H-5, 60	*	*					C		F	F			R			F	F		A	F									
	17H-5, 123							A		A	F			F		R	F	F		A	F		R							
	17H-6, 60	R						A		R	F			R		R	R	F		A	C									
	17H-6, 123	F						A		F	A			R			F	C		A	F		R							
	17H-7, 154.85						C		C	A			R			F	C	R	A	F			R							
	18H-2, 60	R						C		F				R			F	C		A	C		R							
10b	18H-3, 60							C		C				F		F	F	C		A	C			F						
	18H-4, 60	F						A		R	A			R			F	C		A	C		F	F						
	18H-5, 60	F						C		F				R			C	F		A	C									
	18H-6, 60	F						C		C				F		R	C	F		A	C		R	R						
	18H-7, 3	F						A			R			R			F	R		A	C									
	18H-7, 15							C		R				F		R	F	R		A	C									
	19H-1, 60							C		R	F			R		*	R	F		A	F									
	19H-1, 123					cf		C		R	F			*			F			A	F									
	19H-2, 123				*			C		C	A						C	C	F	A										
	19H-5, 123							A		F	A					R	R	C		A										
10a	19H-7, 5							A		*	A			R			C	C		A										
	19H-7, 40							C		C	A			R			F	F		A										
	20X-1, 60							C		F	A			R			F	F		A										
	20X-1, 122							C		A	A			F		R	C	F		A										
	20X-2, 60				*			C		F	A			R		*				A										X
	20X-2, 122				*			A		F	A					R	F	R		A										
	20X-3, 60			*				C		F	C					F	C	C		A										
	20X-3, 93				*			C		C	C			R		R	F	R		A										
	20X-4, 60				F			C		C	C						F	C		A										
	20X-4, 123				C			C		R	R						F	R		A										
	20X-5, 60				F			C		F	R						F	R		A										
	20X-6, 60				C			F		F	F					F	F	F		A										
	21X-1, 60			R	C			C		F	F					F	F	F		A										
	21X-2, 60				F			F		F	C						F	F		A										
	21X-3, 60				F			C		F	C					F	F	F		A										X
	21X-4, 60				C			C		F	C					F	F	F		A										
9b	21X-5, 60				F			C		R	C			cf		C	F	F		A										
	21X-6, 60				F			C		F	C			R		F	F	F		A										
	21X-7, 40			cf	F			C		R	C			R		F	F	F		A										
	22X-1, 60			R	F			C		F	C					F	F	R		A										
	22X-2, 123			R	C			C		R	C						F	F		A										
	22X-3, 60			F	R			F		C	C						F	C		A										
	22X-4, 123			R	cF			A		C	C						C	R		A						X	X			
	22X-5, 60				F			C		C	A						F	F		A										
	22X-6, 123			R	R			C		R	R			F		F	C	R		A						X				X
	23X-1, 60		R	C			C		F	F						F	R		A											

Table 16 (continued).

Zone (CN)	Core, section, interval (cm)	Depth (mbsf)	Depth (mcd)	Abundance	Preservation	Etching	Overgrowth	Small *Gephyrocapsa*	*H. sellii*	*P. lacunosa*	*C. macintyrei*	*D. brouweri*	*D. triradiatus*	*D. pentaradiatus*	*D. surculus*	*D. tamalis*	*D. asymmetricus*	*Sphenolithus* spp.	*R. pseudoumbilicus*	*C. rugosus*	*A. delicatus*	*A. primus*	*A. tricorniculatus*
	23X-4, 123	207.03	226.38	A	MG	0	2					cf		*	cf			A	A			cf	
	23X-7, 40	210.7	230.05	A	M	1	2				C							A	A				
	24X-1, 122	213.72	233.07	A	M	0	2				*							AA	C				
	24X-4, 122	218.22	237.57	A	M	0	2				R	cf			F			AA	A			*	
9b	24X-7, 40	221.9	241.25	A	M	1	2					F						A	F				
	25X-3, 60	225.8	245.15	A	M	1	2				R							C	F				
	25X-4, 60	227.3	246.65	A	M	1	2					F						C	C			*	
	25X-5, 60	228.8	248.15	A	M	0	2					F						A	C				
	25X-6, 60	230.3	249.65	A	M	0	2											AA	C				
	25X-7, 40	231.6	250.95	A	M	0	2					F						AA	C				
	26X-CC	232.04	251.39	R	P	0	3											*					
	27X-CC	241.54	260.89	C	M						R												

Notes: For an explanation of the abundance and preservation codes, see text. For genus names, see Appendix A. Single asterisk (*) = one specimen observed

board because of the scarcity of some marker species. We could not locate some Pliocene events precisely (i.e., T *A. primus* and B common *D. asymmetricus*) or place the relative zonal boundaries. With the careful shore-based work of this study, however, we were able to substantially improve the upper Miocene biostratigraphy and recognized all the conventional and some secondary events (Fig. 9).

In the lower part of Site 850, we did not detect the lowest occurrence of *C. coalitus;* therefore, we were not able to discriminate Zone CN6 as we had at Site 849. In the assemblages of the lowermost Cores 138-850B-41X and -42X, we recognized the interval with common *D. kugleri,* which terminates at the top of Core 138-850B-41X. This finding indicates that the oldest sediments retrieved at Site 850 can be assigned to the middle part of Subzone CN5b.

Site 851

Site 851 is located beneath the highly productive surface waters along the northern edge of the South Equatorial Current, on top of crust generated at about 11–12 Ma. The upper 150 m of the site were triple APC cored, and the remainder was double XCB cored to basement.

The 390-mcd section spans the time interval from the Pleistocene to the middle Miocene. The sedimentary section is considered a single lithologic unit composed of foraminifer-nannofossil ooze and diatom-nannofossil ooze. A clear paleomagnetic record for the Pleistocene and part of the Pliocene (top 80 mcd) was obtained at this site. This record, together with the biostratigraphy, provided high-quality age control points for reconstructing sedimentation rates. The sedimentation rate pattern is typical of pelagic sedimentation in this region of the equatorial Pacific (Mayer, Pisias, Janecek, et al., 1992). There is a drop in the sedimentation at around 10 to 8 Ma. This drop is associated with an increase in dissolution. This event was observed in all the other Leg 138 sites that penetrated to this point.

We sampled Hole 851B, two cores of Hole 851C, and five cores of Hole 851E, at a spacing that averages 40 cm. Nannofossils are abundant and generally well preserved throughout the sequence. They provide a detailed and well-constrained biostratigraphy, as summarized in Figure 10. The nannofossil events recognized are listed in Table 10.

The abundance of discoasterids in the upper Pliocene interval is particularly low. *D. tamalis* and *D. surculus* become extinct concomitantly, and *D. pentaradiatus* is virtually absent in Zone CN12, whereas it is common to abundant in underlying intervals (particularly in Cores 138-851B-8H to -12H).

In the upper Miocene, discoasterids are abundant and well preserved, as is the entire nannofossil assemblage. Common reworked forms from Zones CN9 and CN6 and Subzone CN5b are present in some levels of the upper Pliocene, within Subzone CN12a and Zone CN11. Poorly preserved assemblages were observed in the upper middle Miocene interval (within Zones CN6 and CN7), corresponding to the interval of increased dissolution and low sedimentation rates outlined above.

Close to the appearance level of *C. coalitus* (bottom of CN6), discoasterids are very rare and fluctuate in abundance throughout the middle Miocene interval. The presence of common to abundant *D. kugleri* in the lowermost part of the Site 851 sequence (Fig. 10) allows us to assign it to Subzone CN5b. This feature in the distribution of *D. kugleri* is correlatable between eastern transect Sites 844, 845, and 846 and western transect Sites 851 and 850. The bottom and top of common *D. kugleri,* calibrated at Site 845 as occurring in the lower part of Chron 5r, provide an age constraint for the basal sediments of Site 850 and 851, which accumulated after 11.8–11.9 Ma.

Site 852

Site 852 was drilled to provide material to study the interaction between the south Equatorial Current and the North Equatorial Countercurrent during the late Neogene. The site is located near the boundary between the two currents, north of the equator. Based on plate reconstructions, the site ever passed beneath the equatorial divergence. A continuous sedimentary record for the upper Pleistocene through the uppermost middle Miocene was recovered from four holes (852A–852D) drilled at Site 852. A single lithologic unit was described, composed of a mixture of foraminifer-nannofossil ooze, with some oxide-rich beds, and radiolarian-nannofissil ooze. Because this site is located north of the high-productivity zone, the microfossil constituents differ from the more equatorial sites and the sedimentation rates are lower at Site 852. A good magnetic stratigraphy was obtained from the Pliocene to the lower upper Miocene in Holes 852B and 852C.

In this study, we sampled Hole 852B and the lowermost cores of Holes 852C and 952D at an average spacing of 40 cm. Calcareous mannofossils are abundant and generally well or moderately well preserved throughout the entire sequence. They provide a detailed and well-constrained biostratigraphy. The nannofossil events recognized at Site 852 are reported in Table 11 and illustrated in Figure 11.

In the Pleistocene and Pliocene, nannofossils are well preserved and abundant. In this interval, we observed reworked nannofossils from the upper Miocene Zone CN9 to CN6 (NN11 to NN9). In the Pliocene and uppermost Miocene, discoasterids and ceratolithids are common or abundant. The upper Miocene discoasterid assemblage is

Table 16 (continued).

Zone (CN)	Core, section, interval (cm)	*C. acutus*	*C. armatus*	*T. rugosus-rioensis*	*D. quinqueramus-berggrenii*	*A. amplificus*	*M. convallis*	*C. leptoporus*	*C. cristatus*	*C. pelagicus*	*Dictyococcites*	*D. bellus*	*D. decorus*	*D. intercalaris*	*D. trestilifer*	*D. variabilis*	*G. rotula*	*H. carteri*	*Pontosphaera*	*Reticulofenestra*	Circular *Reticulofenestra*	*Rhabdosphaera*	*Scyphosphaera*	*Syracosphaera*	Reworked	*S. conicus*	*S. dissimilis*	*S. dissimilis-belemnos*	*C. coalitus*	Miocene forms
	23X-4, 123			cf			C		F	AA			R			C	F		A											
	23X-7, 40		F	F			C		C	C						C			A											
	24X-1, 122		R	R			C			A						C	R		A						X					
	24X-4, 122			A			A		*	A					F	A	F		A						X					
	24X-7, 40		R	R			C		F	A					F	F			A											
	25X-3, 60			F			C		F	A					F	C			A											
9b	25X-4, 60			F			C		C	A			R		F	R			A											
	25X-5, 60		R	F			F		C	A					F	C	C		A						X					
	22X-4, 123		R	cf			A		C	C						C	R		A						X	X				
	22X-5, 60			F			C		C	A						F	F		A											
	25X-6, 60			cf			C		C	A						C	F		A											
	25X-7, 40						C		C							F	R		A						X	X				
	26X-CC																R		R						X	X	X			
	27X-CC			cf					A	A									A											

particularly rich and diverse; *D. quinqueramus* and *D. berggreni* are common throughout their stratigraphic range. Discoasterids in the upper part of middle Miocene (in Zones CN6 and CN7) show moderate overgrowth. Between 10.5 and 8.5 Ma, we observed strong dissolution of the nannofossil assemblage, and some samples were barren. This interval coincides with a time of very low sedimentation rates (as low as 3 m/m.y.) and is well correlated as a dissolution event among the Leg 138 sites that penetrated to this point in the stratigraphic record.

In samples from the lowermost part of Site 852, we recorded common specimens of *Catinaster coalitus* and *D. calcaris* and the highest occurrence of *C. miopelagicus.* These events allowed us to place this interval in Subzone CN6.

Site 853

Site 853 is presently located beneath the region dominated by the Northern Equatorial Countercurrent (NECC). The site was drilled to recover a sedimentary record suitable for studying fluctuations of the NECC and the influence of the Northern Hemisphere trade winds. A continuous section from the upper Pleistocene through the upper part of the upper Miocene was recovered from the five holes cored at Site 853. The sedimentary section is about 73 m thick. It is composed of clayey nannofossil oozes with levels containing abundant foraminifers and iron and manganese oxides in the upper part, and some levels of almost pure nannofossil ooze. Siliceous microfossils are virtually absent, except in the upper Pliocene and Pleistocene intervals, suggesting low-productivity conditions. Site 853 was never located beneath the equatorial divergence during its sedimentary history (Mayer, Pisias, Janecek, et al., 1992). The excellent polarity record together with the calcareous nannofossil biostratigraphy provides a well-constrained stratigraphy.

For this study, we sampled Hole 853B and the lowermost core of Hole 853D at an average spacing of 50 cm. Nannofossils are generally abundant or common throughout the section, and show good to moderately good preservation. The nannofossil events recognized at Site 853 are reported in Table 12 and are summarized in Figure 12.

Within the Pliocene interval, and mainly in lower Zone CN12 and in Zone CN11, we observed assemblages with rare and poorly preserved nannofossils, together with common reworked forms from the upper Miocene (Zones CN9, CN7, and CN6). This observation was also made at Sites 851 and 852. The mixture of reworked and in situ nannofossils in these Pliocene assemblages made difficult the recognition of some extinction events of long-ranging forms (like *A. primus, R. pseudoumbilicus, S. abies,* and *S. neoabies*), which are commonly present in upper Miocene assemblages.

Ceratolithids and discoasterids are generally common and abundant throughout the Pliocene and upper Miocene section, reflecting the relatively low-productivity conditions at this site, far from the equator. The lowermost part of the Site 852 sequence is placed in Zone CN8. In this interval, the nannofossil assemblage is characterized by abundant and slightly overgrown discoasterids, among which *D. neohamatus* and the *D. bellus* group dominate. Common *M. convallis* and abundant *S. abies* and *S. neoabies* are also observed.

SUMMARY AND CONCLUSIONS

We presented a chronostratigraphic classification of the calcareous nannofossil biostratigraphy of Leg 138 sediments from the Pleistocene to the late early Miocene. Most of the zonal boundaries of the standard zonations of Okada and Bukry (1980) and Martini (1971) are recognized in these eastern equatorial Pacific sediments.

The biostratigraphic classification of the Pleistocene was augmented with the biozonation proposed by Gartner (1977) and by a recent biochronologic study of low- and mid-latitude, deep-sea sequences (Raffi et al., 1993). As we used only standard light microscope techniques, we did not recognize the appearance of *Emiliania huxleyi* (CN15/CN14b and NN21/NN20 boundaries) or the beginning of its dominance in the upper Pleistocene interval.

Detailed biostratigraphic classification in Pliocene Zones CN12, CN11, and CN10 (Zones NN18 to NN12) was difficult at some sites because of the scattered occurrence or absence of the primary and secondary species of discoasterids and ceratolithids. At these sites, we found that discoasterids and ceratolithids were unreliable as biostratigraphic markers in much of the Pliocene and in some intervals of the middle and late Miocene because of their highly variable distributions and generally low abundances or absences, in some cases. This is particularly evident in the sedimentary sequences of sites located beneath the equatorial divergence zone and/or influenced by upwelling (in the western transect Sites 849, 850, and 851 and in the eastern transect Sites 844, 845, and 846). The rare and discontinuous occurrences of discoasterids are associated with high surface-water productivity, thus supporting the results of Chepstow-Lusty et al. (1989, 1992), who showed that discoasterid abundances are influenced by varying productivity pressure.

In the Miocene interval, we recognized the zonal boundaries as defined by Martini (1971) and Bukry (1973) at all sites, with some exceptions: (1) the boundary CN7a/CN7b; (2) the base of Zone CN6 (NN8) at western transect Sites 849 and 850; and (3) the top of CN7 (NN9) at eastern transect Site 845. This was because of the sporadic occurrence or absence, and the different stratigraphic ranges, of the defining markers (*C. coalitus, C. calyculus,* and *D. hamatus*). The

Table 17. Distribution of calcareous nannofossil taxa in the Pleistocene-Pliocene interval at Site 848.

Zone (CN)	Core, section, interval (cm)	Depth (mbsf)	Depth (mcd)	Abundance	Preservation	Etching	Overgrowth	*P. lacunosa*	small *Gephyrocapsa*	*G. oceanica*	*G. omega*	large *Gephyrocapsa*	*H. sellii*
	138-848A-												
	1H-1, 60	0.6	0.8	A	G	0	0		C	A	C		
15 + 14b	1H-2, 60	2.1	2.3	A	G	0	0		C	A	C		
	1H-3, 60	3.6	3.8	A	G	0	0		A	C	R		
______	1H-4, 60	5.1	5.3	A	G	0	0		A	R	R		
	1H-5, 60	6.6	6.8	A	G	0	0	F	A	R	*		
	1H-6, 60	8.1	8.3	A	G	0	0	A	A	R	R		
	138-848B-												
	2H-3, 60	5.8	8.6	A	G	0	0	C	A	C	F		
14a	2H-4, 60	7.3	10.1	A	G	0	0	A	A	C	R		
	2H-5, 60	8.8	11.6	A	G	0	0	C	A	C	R		
	2H-6, 60	10.1	12.9	A	G	0	0	C	C	F	R		
	2H-7, 70	11.9	14.7	A	G	0	0	A	C	A	C		
	3H-1, 60	12.3	16.25	A	G	0	0	A	C	F	R		
------	3H-1, 70	12.4	16.35	A	G	0	0	A	F	R	R		
	3H-1, 80	12.5	16.45	A	G	0	0	A	C				
	3H-1, 120	12.9	16.85	A	G	0	0	A	F				
	3H-2, 60	13.8	17.75	A	G	0	0	A	C				
	3H-3, 60	15.3	19.25	A	G	0	0	A	F				
	3H-3, 120	15.9	19.85	A	G	0	0	A	F	F		F	
	3H-4, 40	16.6	20.55	A	G	0	0	A	C	A		C	
13b	3H-4, 80	17	20.95	A	G	0	0	A	C	A		F	
	3H-4, 120	17.4	21.35	A	G	0	0	A	C	C		R	
	3H-5, 40	18.1	22.05	A	G	0	0	A	C	A		F	
	3H-5, 80	18.5	22.45	A	G	0	0	C	A	A		F	
	3H-5, 120	18.9	22.85	A	G	0	0	F	C	C		R	*
	3H-6, 40	19.6	23.55	A	G	0	0	A	C	A			
	3H-6, 80	20	23.95	A	G	0	0	C	C	A			
	144-848C-												
	3H-5, 20	21.2	24.2	A	G	0	0	C	F	F			R
------	3H-5, 40	21.4	24.4	A	G	0	0	A	R	C			R
	3H-5, 50	21.5	24.5	A	G	0	0	A	F				
	3H-5, 60	21.6	24.6	A	G	0	0	A	F				C
	3H-5, 90	21.9	24.9	A	G	0	0	A	C				A*
	3H-5, 100	22	25	A	MG	1	0	A	C				A*
13a	3H-5, 120	22.2	25.2	A	G	0	0	A	C				A
	3H-5, 140	22.4	25.4	A	G	0	0	A	C				C
	3H-6, 20	22.7	25.7	A	MG	1	0	A	F				C
	3H-6, 50	23	26	A	G	0	0	A	F				A*
	3H-6, 80	23.3	26.3	A	MG	1	0	A	F				C
______	3H-6, 120	23.7	26.7	A	G	0	0	A	F				A
	3H-7, 10	24.1	27.1	A	G	0	0	A	F				C
	3H-7, 20	24.2	27.2	A	G	0	0	A	F				C
	3H-7, 30	24.3	27.3	A	G	0	0	A	F				C
	3H-7, 40	24.4	27.4	A	G	0	0	A	R				C
12 d	3H-7, 50	24.5	27.5	A	G	0	0	A					C
+	3H-7, 60	24.6	27.6	A	G	0	0	A					F
12c	4H-3, 40	24.6	28.95	A	G	0	0	A					F
	4H-3, 120	25.4	29.75	A	G	0	0	A					R
______	4H-4, 40	26.1	30.45	A	G	0	0	A					R
	4H-4, 80	26.5	30.85	A	MG	0	0	A					R
12b	4H-4, 120	26.9	31.25	A	G	0	0	A					R
______	4H-5, 23	27.43	31.78	A	G	0	0	A					R
	4H-5, 85	28.05	32.4	A	G	0	0	A					C
	4H-5, 120	28.4	32.75	A	G	0	0	C					R
	4H-6, 20	28.9	33.25	A	G	0	0	C					R
12aB	4H-6, 120	29.9	34.25	A	G	0	0	C					R
	4H-6, 145	30.15	34.5	A	G	0	0	C					
	4H-7, 20	30.4	34.75	A	G	0	0	C					R
______	4H-7, 50	30.7	35.05	A	MG	0	0	F					F
12aA	5H-1, 42	31.12	36.77	A	G	0	0	R					C
______	5H-1, 95	31.65	37.3	A	MG	1	0	R					R
11b	5H-1, 120	31.9	37.55	A	MG	1	0						F
---?---	5H-2, 50	32.7	38.35	A	MG	1	0						
	5H-2, 120	33.4	39.05	A	G	0	0						R
11a	5H-2, 127	33.47	39.12	A	G	0	0						
______	5H-3, 62	34.32	39.97	A	G	0	0						
	5H-3, 120	34.9	40.55	A	G	0	0						
	5H-4, 40	35.6	41.25	A	G	0	0						
	5H-4, 120	36.4	42.05	A	MG	0	1						
	5H-5, 40	37.1	42.75	A	MG	1	0						
	5H-5, 120	37.9	43.55	C	MG	1	1						
10c	5H-6, 40	38.6	44.25	A	G	0	0						
	5H-6, 120	39.4	45.05	A	MG	0	1						
	5H-7, 45	40.15	45.8	A	G	0	0						
	6H-1, 75	40.95	46.65	A	G	0	0						
	6H-2, 35	42.05	47.75	A	G	0	0						
	6H-2, 75	42.45	48.15	A	MG	0	1						
	6H-3, 35	43.55	49.25	A	G	0	1						
	6H-3, 75	43.95	49.65	A	MG	1	1						
______	6H-4, 35	45.05	50.75	A	MG	1	1						
10b	6H-4, 75	45.45	51.15	A	G	0	1						
______	6H-5, 35	46.55	52.25	A	MG	0	1						
10a	6H-5, 75	46.95	52.65	A	MG	0	1						

Table 17 (continued).

C. macintyrei	*D. brouweri*	*D. triradiatus*	*D. pentaradiatus*	*D. surculus*	*D. tamalis*	*D. asymmetricus*	*Sphenolithus*	*R. pseudoumbilicus*	*C. rugosus*	*A. primus*	*A. tricorniculatus*
*											
	*	*									
*											
F											
C											
C											
F											
C											
A			*								
C											
A											
C											
C											
C											
A	F			*							
C	R										
A	R	R		*							
A	F	R									
C	F	R									
A	F	R	*								
C	C	F				*					
C	A										
C	A	*				F					
C	C		*	R		*		*			
A	C			*	*	*					
C	C		R	R		R					
A	C			R	F	C					
C	A		F	R	F	C			F		
C	C		R	C		F			R		
C	F			F		R			F		
C	F			F	R	F			C		
C	C			C	R	R			A		
A	A			F	R	R		*	C		
C	C				R	F	F		R		
F	F			*		*	R		R		
C	C				*	R		F	R		
F	A			R		*	*	C	R		
F	C	*	R				F	A	F		
F	A	*	C	F			A	A	A		
F	F		F	C			A	A	R	R	
F	A*	R		C		R	C	C	F	R	
R	A		R	C			A	C	C	R	R
R	F			R		*	C	F	R	F	
F	A		F	C		*	R	A	R	R	
	F		R								
R	A		R	A			F	C	C	R	
R	C		R				R	F	R	R	
	C		R	C			R	F	F	R	
R	F		F	F			R	C	F	R	
R	C			A			R	R	F	R	
	A			A			F	R	R		
	A		C	A			F	R		R	
			R	A			C	F	R	R	
	F		R	C			R	R	R	R	
	C			C			R	C		R	
R	A			F			F	F			
	C		R	R			C	F		R	

Table 17 (continued).

Zone (CN)	Core, section, interval (cm)	*C. acutus*	*T. rugosus/rioensis*	*D. quinqueramus*	*C. leptoporus*	*C. cristatus/telesmus*	*C. pelagicus*	*C. radiatus*	*D. decorus*	*D. intercalaris*	*D. pansus*
	138-848A-										
	1H-1, 60				C	F		C			
15 + 14b	1H-2, 60				C	R		F			
	1H-3, 60				C	R		F			
———	1H-4, 60				C	F		R			
	1H-5, 60				C	R		R			
	1H-6, 60			C	F		C				
	138-848B-										
	2H-3, 60				C	R		C			
14a	2H-4, 60				C	R		C			
	2H-5, 60				C	R		R			
	2H-6, 60				A	F		F			
	2H-7, 70				C	R					
	3H-1, 60				A			R			
- - - - - -	3H-1, 70				A	R		F			
	3H-1, 80				A	R		F			
	3H-1, 120				A			R			
	3H-2, 60				A			F			
	3H-3, 60				A	F					
	3H-3, 120				A	R		F			
	3H-4, 40				A	F		C			
13b	3H-4, 80				A	C		F			
	3H-4, 120			*	A	R		R			
	3H-5, 40				A	F		C			
	3H-5, 80				A	R		C			
	3H-5, 120				A	R		F			
	3H-6, 40				C	F		C			
	3H-6, 80				A	F		F			
	144-848C-										
	3H-5, 20				C	F		F		*	
- - - - - -	3H-5, 40				C	F		C			
	3H-5, 50				C	F		F			
	3H-5, 60				C	R		C			
	3H-5, 90				A	A		F			
	3H-5, 100				C	F		F			
13a	3H-5, 120				A	C	R	C			
	3H-5, 140				A	C		C			
	3H-6, 20				A	C		C			
	3H-6, 50				C	C		F			
	3H-6, 80				C	A		C			
———	3H-6, 120				A	C		C			
	3H-7, 10				A	F		C			
	3H-7, 20				A	C		C			
	3H-7, 30				A	C		F			
	3H-7, 40				A	A	R	F			
12d	3H-7, 50				A	C	F	C			
+	3H-7, 60				A	C	F	C			
12c	4H-3, 40				A	A	C	F			
	4H-3, 120				A	F	C	R			
———	4H-4, 40				A	F	C	R		*	
	4H-4, 80				A	C	F	R		*	
12b	4H-4, 120				A	C	F	F			
———	4H-5, 23				A	A	F	F			
	4H-5, 85				A	A	C	F			
	4H-5, 120				A	C	F	C			
	4H-6, 20				A	F	F	F		R	
12aB	4H-6, 120				A	F	A	F			
	4H-6, 145				A	C	R	F		R	
	4H-7, 20				A	C	R	R		R	
———	4H-7, 50				A	C		C	*	F	
12aA	5H-1, 42				A	A		R			
———	5H-1, 95				A	C		F			
11b	5H-1, 120				A	F		R			
- -?-?- -	5H-2, 50				A	C		F			
	5H-2, 120			A	C		R			*	
11a	5H-2, 127				A	F		F		R	
———	5H-3, 62				A	R		C		R	*
	5H-3, 120				A	R		F			
	5H-4, 40				A	F		F			
	5H-4, 120				A			R		R	
	5H-5, 40				A			R		R	
	5H-5, 120				C						
10c	5H-6, 40				A						
	5H-6, 120				A						
	5H-7, 45				C						
	6H-1, 75				A		C				
	6H-2, 35	R			A		C			F	
	6H-2, 75	R			A		F			F	
	6H-3, 35	R			A		R			F	
	6H-3, 75	R			A		C	R			
———	6H-4, 35	C			A		C				
10b	6H-4, 75	F			A		F				
———	6H-5, 35	C	*		A		R				
10a	6H-5, 75	*	F		A		F				

Table 17 (continued).

D. tristellifer	*D. variabilis*	*G. rotula*	*H. carteri* gr.	*H. wallichii*	*Pontosphaera*	*Reticulofenestra*	*Rhabdosphaera*	*Syracosphaera*	*Thoracosphaera*	*Umbilicosphaera*	Reworked
			F	C	C	C	C				
			R	C		F	F				
				F			R				
				F			R				
			F	C							
		F	C		A	R					
			R	F		A	R				
			C	C		C	R				
			F	C	R	F	R				
			R	C				F		C	
				R		F		F		F	
			F	F	R	A		C		C	
			R	R		A		C		C	
		R		F		A		R	R	F	
						A		R		R	
			C	A		A		C		C	
			R	F	R	C		R	R	C	
			F	R		C				C	
			A	C	F	F		F		A	
			A	C	F	F		F		A	
			R	C		C				C	
			C	A	F	C		C		F	
			C	C	F	A		A		C	
			F	C	C	A		C		C	
	*		F	C	F	C		C		C	
			F	F	F	C		F		C	
			F	R	F	C		F		C	
			F			A		F		F	
			C			A		R			
			C			A		R			
			C			C		F		F	
			C			C		R	R	R	
			C		R	A		C		F	
	**		A		F	A		C	R	F	
			C		R	A		C		F	
			F		F	A		F		F	
			F		R	A		C	R	F	
			C		R	A		C			
	*		C			A		C		R	
			C			A		F		R	
	*		F			A		C			
			R			A		F			
			F			A		C			
			R			A		A			
			C			A		C			
			F			A		C			
			C			A		C			
	*		F			A		C			
		R	C			A		A			
	*		F			A		C			
			C			A		C			
			C			A		C			
		F	C			A		C			
		F	C			A		C			
		R	F			A		F			
			C			A		C			
	R		F			A		C			
	F		A			A					
	R		F			C					
			C			A		C			
	R		R			A		R			
F		R			A						
C	C		F			A		F			
C	R		F			A		F			
F	F		R			A		F			
	A	R	F			A					
A	C		C			A					
R	A	R	C			A					
R	R	R				A					
	A		F			A					
	R		R			A					
	C		R			A					
	C		R			A					
	C		R			A					
	F					A					
	C		R			A					
	C		F			A					
	R	F	R			A					
	A					A					
	F		F			A	C				
	R		F			A	C				

Notes: For an explanation of the abundance and preservation codes, see text. For genus names, see Appendix A. Single asterisk (*) = one specimen observed. A* = dominant species (50%).

Table 18. Distribution of calcareous nannofossil taxa in the Miocene interval at Site 848.

Zone (CN)	Core, section, interval (cm)	Depth (mbsf)	Depth (mcd)	Abundance	Preservation	Etching	Overgrowth	*C. macintyrei*	*D. brouweri*	*D. triradiatus*	*D. pentaradiatus*	*D. surculus*
	138-848B-											
	6H-6, 35	48.05	53.75	A	MG	0	1	R	A		F	C
10a	6H-6, 75	48.45	54.15	A	G	0	0	R	F			C
	6H-7, 40	49.6	55.3	A	MG	0	1	R	C		R	C
———	7H-1, 50	50.2	56.9	A	MG	0	2		C			C
	7H-1, 95	50.65	57.35	A	MG	0	1	R	F			A
	7H-2, 35	51.55	58.25	A	MG	0	2		C			A
	7H-2, 120	52.4	59.1	A	G	0	1	R	R			C
	7H-3, 35	53.05	59.75	A	MG	0	2	*	F	*	R	A
9bC	7H-3, 120	53.9	60.6	A	MG	0	2		F			C
	138-848C-											
	7H-1, 25	53.25	61	A	MG	0	2	R	F			F
	7H-1, 100	54	61.75	A	MG	0	2	R	C		F	R
———	7H-2, 25	54.75	62.5	A	MG	0	2		C			R
	7H-2, 50	55	62.75	A	MG	0	2		C			R
	7H-3, 50	56.5	64.25	A	M	1	2	R	C	*		R
	7H-3, 100	57	64.75	A	M	1	2	*	C			R
	7H-4, 25	57.75	65.5	A	M	1	2	F	A			R
9bB	7H-4, 100	58.5	66.25	A	MG	0	1	F	A*			R
	7H-5, 25	59.25	67	A	MG	0	1	F	A*	**		
	7H-5, 100	60	67.75	A	MG	0	1	F	A			
	7H-6, 25	60.75	68.5	A	MG	0	1	F	A*			*
	7H-6, 100	61.5	69.25	A	G	0	1	R	F			R
	7H-6, 125	61.75	69.5	A	MG	0	1	F	F			*
———	7H-6, 145	61.95	69.7	A	MG	0	1	F	C			R
	7H-7, 20	62.2	69.95	A	MG	0	2	F	C			R
	7H-7, 50	62.5	70.25	A	M	1	2	F	C			R
	8H-1, 80	63.3	72.4	A	M	1	2	F	A			F
	8H-1, 140	63.9	73	A	M	1	2	F	A			F
	8H-2, 80	64.8	73.9	A	M	1	2	F	A			F
9bA	8H-2, 140	65.4	74.5	A	M	1	2	F	C			R
	8H-3, 40	65.9	75	A	M	1	2	F	C			
	8H-3, 100	66.5	75.6	A	M	1	2	C	C			F
	8H-4, 20	67.2	76.3	A	M	1	2	F	C		*	R
	8H-4, 100	68	77.1	A	M	1	2	C	C			C
	8H-5, 20	68.7	77.8	A	M	1	2	R	A	*		*
	8H-5, 140	69.9	79	A	M	1	2	F	C			F
———	8H-6, 80	70.8	79.9	A	M	1	2	R	A			F
	8H-6, 140	71.4	80.5	A	M	1	2	R	C			*
	8H-7, 40	71.9	81	A	M	1	2	F	C			R
	9H-2, 119	84.89	94.49	A	M	1	2	F	C			R
	9H-3, 50	72.2	81.8	A	M	1	2	C	C			*
9a	9H-3, 100	72.7	82.3	A	M	1	2	C	C			
	9H-3, 119	72.89	82.49	A	M	1	2	C	F			
	9H-4, 40	73.6	83.2	A	MG	1	1	C	C			R
	9H-4, 100	74.2	83.8	A	MG	1	1	F	A			
	9H-5, 36	75.06	84.66	A	MG	1	1	R	A			*
—?—	9H-5, 119	75.89	85.49	A	M	1	2	X	C			
8b	9H-6, 40	76.6	86.2	A	MG	1	1	X	R			
	9H-6, 119	77.39	86.99	A	MG	1	1	X	R			
	10H-1, 40	78.6	89.2	A	MG	1	1		C			
	10H-1, 120	79.4	90	A	MG	1	1	X	C	*		
8a	10H-2, 47	80.17	90.77	A	MG	1	1	X	A			
	10H-2, 120	80.9	91.5	A	M	2	2		F			
	10H-3, 46	81.66	92.26	A	MP	2	2	X	F			
	10H-3, 108	82.28	92.88	A	M	2	2		C			
———	10H-3, 126	82.46	93.06	A	M	2	2	X	F			
	10H-4, 10	82.8	93.4	A	M	2	2		F			
	10H-4, 40	83.1	93.7	A	M	1	2	X	R			
	10H-4, 85	83.55	94.15	A	M	1	2		F			
	10H-4, 150	84.2	94.8	A	MG	1	1	X	F			
7	10H-5, 40	84.6	95.2	A	MG	1	2	X	R			
	10H-5, 120	85.4	96	A	MG	1	1	X	R			
	10H-6, 40	86.1	96.7	A	MG	1	2					
	10H-6, 120	86.9	97.5	A	MG	1	2	X	F			
	10H-7, 10	87.3	97.9	A	MG	1	2	X	R			
	10H-7, 20	87.4	98	A	MG	1	1	X	*			
———	10H-7, 60	87.8	98.4	A	MG	1	1	X	F			
	11H-1, 20	87.9	100.25	A	MG	1	2	X				
	11H-1, 50	88.2	100.55	A	MG	1	2		R			
	11H-1, 115	88.85	101.2	A	M	1	2	X	R			
	11H-2, 35	89.55	101.9	A	MG	1	2	X	R			
6	11H-2, 120	90.4	102.75	A	MG	1	2					
	11H-3, 40	91.1	103.45	A	MG	1	1	X	R			
	11H-3, 120	91.9	104.25	A	MG	1	1					
	11H-4, 40	92.6	104.95	A	M	1	2	X				
	11H-5, 20	93.9	106.25	A	M	1	2	X				
	11H-5, 50	94.2	106.55	A	M	1	2	X				

Notes: For an explanation of the abundance and preservation codes, see text. For genus names, see Appendix A. Single asterisk (*) = one specimen observed. A* = dominant species (50%). X = species present, but not quantitatively evaluated.

Table 18 (continued).

D. asymmetricus	*Sphenolithus*	*R. pseudoumbilicus*	*A. delicatus*	*A. primus*	*A. tricorniculatus*	*C. acutus*	*T. rugosus/rioensis*	*D. quinqueramus* gr.	*A. amplificus*	*D. loeblichii*
	C	A	F	R	R	*				
	C	A	C	F						
	C	A	C	C			R			
	C	A	F	C			*	*		
	C	A	F	F				R		
	C	C	F	C			*	C		
	C	C	R	R				R		
	C	A	R	R				C		
	C	C						A		
	A	C	F	F				F		
	A	R	C	C				F		*
	A	R	R	R				R		
	A	R	F	R			F	R	R	
	A	R	C	F	*		R	R	*	
*	A	R	C	C			F		F	
	A	*	C	F	*			R	C	
F	A	R	C	C	R			R	*	
R	A	R	C	C	*			R	*	
*	C		F	F				R	F	
R	C		C	C			C	R	R	
	C		F	F				A	R	
	C		R	F				A	F	
*	C		R	C			R	A	R	
	C		F	C			F	A		
	A		R	R			R	A		
*	F	*						*		
	F	*								
F	F	*	F	C				R		
*	A	*	C	A	*					
*	C		C	A						
*	A		F	R			R	*		
F	A		R	*			R	R		
F	A			R			R			
F	A		*	R			F	R		
	A			R			R			
	C			A			F	*		
	C						C	F		
	C						A	R		
	C						A	R		
	A						C	F		
	A						C	C		
	C						C			
	C	*					F			R
	A						C			C
	A									A
	A						X			R
	X						X			R
	X						X			
	X	C					X			
	X	F					X			
	F	C					X			
	F	R					X			
	F	R					X			
	F	F					X			
	C	F					X			
	F	F					X			
	F	F					X			
	F	F					X			
	X	C					X			
	X	C					X			
	X	C					X			
	X	C					X			
	X	F					X			
	X	C					X			
	X	C					X			
	X	A					X			
	X	A					A			
	X	A					C			
	X	A					C			
	X	C					C			
	X	C					X			
	X	C					X			
	X	F					X			
	X	R					X			
	X	R					X			
	X	R					X			

Table 18 (continued).

Zone (CN)	Core, section, interval (cm)	*M. convallis*	*D. neohamatus*	*D. hamatus*	*C. miopelagicus*	*C. coalitus*	*D. exilis*	*C. leptoporus*	*C. pelagicus*	*Discoaster* in class	*D. adamanteus*
	138-848B-										
	6H-6, 35							A	F	R	
10a	6H-6, 75							C	C	*	
	6H-7, 40							A	C	R	
———	7H-1, 50							A	C	F	
	7H-1, 95							A	C	R	
	7H-2, 35							A	C	F	
	7H-2, 120							A	A	R	
	7H-3, 35							A	A	F	
9bC	7H-3, 120									C	
	138-848C-										
	7H-1, 25								F	F	
	7H-1, 100									C	*
———	7H-2, 25										
	7H-2, 50										
	7H-3, 50							C	C	C	
	7H-3, 100							C	C	C	R
	7H-4, 25							C	C	C	R
9bB	7H-4, 100							C	C	*	R
	7H-5, 25							C	C	F	*
	7H-5, 100							C	C	R	R
	7H-6, 25							C	C		*
	7H-6, 100							C	C		*
	7H-6, 125							C	C		*
———	7H-6, 145							C	C		*
	7H-7, 20							C	C	R	R
	7H-7, 50							C	C	F	R
	8H-1, 80							F	C	A	R
	8H-1, 140							F	C	C	F
	8H-2, 80							C	C	C	*
9bA	8H-2, 140							C	C	C	
	8H-3, 40							C	C	C	
	8H-3, 100							C	C	C	*
	8H-4, 20							C	A	A	
	8H-4, 100							C	F	C	
	8H-5, 20							C	C	C	*
	8H-5, 140							C	C	C	
———	8H-6, 80							C	C	A	
	8H-6, 140							C	C	C	*
	8H-7, 40		cf					C	C	A	*
	9H-2, 119		cf					C	C	C	R
	9H-3, 50		*					C	C	A	R
9a	9H-3, 100							C	C	A	*
	9H-3, 119							C	C	F	
	9H-4, 40							C	C	C	
	9H-4, 100		R					C	C		
	9H-5, 36							C	C	C	
———	9H-5, 119	*	R					X	X	A	
8b?	9H-6, 40	R						X	X		*
	9H-6, 119								X	R	
	10H-1, 40		C					X	X	R	
	10H-1, 120	F	R					X	X	R	
8a	10H-2, 47	R	C					X	X	R	
	10H-2, 120	R						X	X		
	10H-3, 46		R					X	X	C	
	10H-3, 108							X	X	C	
———	10H-3, 126		R					X	X	F	
	10H-4, 10							X	X		
	10H-4, 40			*				X	X		
	10H-4, 85			R					X	R	
	10H-4, 150		*	F				X	X	F	
7	10H-5, 40			R					X	R	
	10H-5, 120			R				X	X	C	
	10H-6, 40			R				X	C	C	
	10H-6, 120			*				X	C	C	
	10H-7, 10							X	X	C	
	10H-7, 20			R		*		X	X	C	
———	10H-7, 60							X	X	C	
	11H-1, 20				F			X	X	F	
	11H-1, 50				C		F	X	X	C	
	11H-1, 115				A		cf	X	X	C	
	11H-2, 35				A			X	X	C	
6	11H-2, 120				A			X	X	C	
	11H-3, 40				A			X	X	C	
	11H-3, 120				A			X	X	C	
	11H-4, 40				A			X	X	C	
	11H-5, 20				A			X	X	C	
	11H-5, 50				A			X	X	C	

Notes: For an explanation of the abundance and preservation codes, see text. For genus names, see Appendix A. Single asterisk (*) = one specimen observed. A* = dominant species (50%). X = species present, but not quantitatively evaluated.

Table 18 (continued).

D. bellus gr.	*D. calcaris*	*D. hamatus-bellus*	*D. intercalaris*	*D. moorei*	*D. prepentaradiatus*	*D. variabilis*	*H. carteri* gr.	Reticulofenestrids	*T. extensus*	
			R			C		A		
						A		A		
						A		A	R	
						C		A		
						C		A		
						C	R	A		
						F	C	A		
						C	A	A		
C								C	C	A
			*			A	C	A		
			F			F	C	A		
							C	A		
							C	A		
			R	*		F	F	A		
*			R			C	C	A		
			R			C	F	A		
						R	F	A		
						C	R	A		
			R			F	R	A		
			F			R	F	A		
			*			C	F	A		
			*			C	F	A		
			R	*	*	C	F	A	R	
			R			A	F	A	R	
			R			C	C	A		
			R			C		A		
			F	*		A	F	A		
*			R			A	F	A		
			*	*		C	F	A		
			R			C	F	A		
			*			F	C	A		
*			R			C	C	A		
						C	F	A		
						**	F	A		
			*	R		F	F	A		
				*		C	R	A		
			*			R	F	A		
R			*	*		C	F	A		
			F			F		A		
			*			F	F	A		
R			R			F	F	A		
			*			F		C		
R				*		C	F	C		
F			*	R		A	C	C		
A				*		C	F	A		
C			*			C		R		
A*						C				
A*						R		*		
C						*		A		
?						F		A		
R						R		A		
R						F		A		
F								A		
cf								A		
						R		C		
R				*		C		A		
C						R		A		
C		*		*		C		A		
A		C				C		A		
R				*		F		A		
A		*		*		F		A		
A						R		A		
F		*				R		A		
R						F		A		
F				*		F		A		
C								C		
R				*		C		A		
	*					C		A		
	R					cf		A		
								A		
								A		
								A		
								A		
								A		
								A		
								A		

lowest occurrence of *C. coalitus* was directly calibrated to the magnetostratigraphy at Site 845 as occurring in the lower part of Chron 5n.2n (age estimate of 10.7 Ma).

Moreover, in the Miocene interval, we discussed supplementary events that improve upon the biostratigraphic resolution provided by the standard zonations.

In the upper Miocene interval, the stratigraphic relationship of the lowest and highest occurrences of *A. amplificus* relative to the events B *A. primus* and T *D. quinqueramus* allowed us to divide further a rather long time interval (about 1.7 m.y.), corresponding to Subzone CN9b, into three distinguishable biostratigraphic subunits. The lowest and highest occurrences of *A. amplificus* were calibrated to the magnetostratigraphy at Sites 844, 845, 852, and 853 as occurring at the bottom and top of Chron 3An, respectively, and are isochronous with the occurrence of *A. amplificus* in the western equatorial Indian Ocean (Rio et al., 1990a). In the interval between lower Subzone CN9b and Zone CN8, we observed a significant turnover within the placoliths, corresponding to the temporary and almost complete disappearance of large specimens (>7 µm) of *R. pseudoumbilicus.* This interval seems to have a wide geographical extent, as it has also been observed in the western equatorial Indian Ocean (Young, 1990; Rio et al., 1990a) at a similar stratigraphic level. This turnover is thought to reflect oceanographic-climatic instability (Rio et al., 1990a).

In the middle Miocene interval, the following additional events were recorded within Zone CN5 (from the top): T *C. nitescens,* T *C. premacintyrei,* B *T. rugosus,* T *D. signus,* and T *C. floridanus.* The T *C. floridanus* event is easily detected in Leg 138 material and is recorded above the highest occurrence of *S. heteromorphus* and well below the lowest occurrence of *D. kugleri.* This finding supports the contention that the final range of *C. floridanus* is biogeographically controlled, as shown by Olafsson (1991) and Fornaciari et al. (1993). The lowest occurrence of *D. kugleri* was recognized and used to place the boundary between Subzones CN5b and CN5a by means of a quantitative analysis on closely spaced samples. This marker species is generally rare and scattered in most of its range, except for a brief interval in which *it* is common and continuously distributed. This interval with common and typical *D. kugleri* is correlatable between all different sequences and was calibrated as occurring within Chron 5r (estimated age interval: 11.3–11.9 Ma) at Site 845. At this same site, the other nannofossil events of Zone CN5 have also been calibrated to the magnetostratigraphic record.

In the lower Miocene interval, corresponding to the uppermost part of Zone CN3, we detected the acme end of *D. deflandrei* and the lowest occurrence of *D. signus,* which have similar stratigraphic positions in the western equatorial Indian Ocean (Rio et al., 1990a).

TAXONOMIC NOTES

A complete list of taxa considered in the present study is reported in Appendix A. We followed the taxonomic concepts explained in Rio et al. (1990a); concepts concerning the most important taxa are summarized below. Species representatives of genera *Dictyococcites, Pontosphaera, Rhabdosphaera, Scyphosphaera, Syracosphaera, Toracosphaera,* and *Umbilicosphaera* are grouped under the single genus epithet in the range charts.

Gephyrocapsids

Rio (1982) and Rio et al. (1990b) have shown that gephyrocapsids can be consistently used for biostratigraphic purposes, and Raffi et al. (1993) and Rio et al. (in press) have shown that they provide an accurate and precise tool for correlation in early Pleistocene sequences. In the material studied, the taxonomic concepts followed for recognition in light microscope of gephyrocapsids are those summarized in Raffi et al. (1993). They discriminate within the group the following biometrically based taxonomic entities:

1. Gephyrocapsids <4 µm in size, "small *Gephyrocapsa* spp.";
2. Gephyrocapsids ≥4 µm and ≤5.5 µm in size, with an open central area, "medium *Gephyrocapsa* spp.";
3. Gephyrocapsids >5.5 µm in size, labeled "large *Gephyrocapsa* spp."

Within the medium-sized gephyrocapsids, there are morphotypes with an open central area and a bridge nearly aligned with the short axis of the placolith, similar to *G. oceanica* as intended by many authors. These gephyrocapsids are comparable to *G. omega* Bukry (= syn. *G. parallela* Hay and Beaudry) and make up a large proportion of the medium-sized gephyrocapsid stock that reappeared in the lower Pleistocene after the interval of temporary disappearance of medium-sized forms.

Reticulofenestrids

Within reticulofenestrids, we distinguished the following species and groups: "circular reticulofenestrids," *Reticulofenestra* spp., and *R. pseudoumbilicus.*

To "circular reticulofenestrids," we ascribed forms that are 5–8.5 µm in size, with a circular outline and relatively large central opening, known as *R. rotaria* Theodoridis or *R. pseudoumbilicus* var. *rotaria* Young. These reticulofenestrids seem restricted to late Miocene.

Reticulofenestra spp. includes the small-sized reticulofenestrids *R. haqii, R. minuta,* and *R. minutula.*

For distinguishing *R. pseudoumbilicus,* we followed taxonomic concepts of Raffi and Rio (1979) and Backman and Shackleton (1983), and considered adding to this species reticulofenestrids larger than 7 µm. In the eastern equatorial Pacific, *R. pseudoumbilicus* appears at the boundary between Zones CN4 and CN5, and has low abundance in its lower range. It becomes a dominant element of nannofossil assemblages in Zone CN5. These reticulofenestrids virtually disappears from the stratigraphic record for a long interval in the late Miocene. The Pliocene extinction of large *R. pseudoumbilicus* is a clear event in the Leg 138 material, which occurs in the upper part of Chron 2Ar (late Gilbert), as it does in other areas (Backman and Shackleton, 1983; Rio et al., 1990a, 1990b).

Calcidiscus

We ascribed to *C. macintyrei* species only circular *Calcidiscus* specimens equal to or larger than 11 µm, using the "10-µm size" as a break point to make the distinction between *C. leptoporus* and *C. macintyrei* (see discussion in Fornaciari et al., 1990). Following this taxonomic concept, in the equatorial Indian Ocean (Fornaciari et al., 1990), the first appearance of *C. macintyrei* occurs within Zone CN5, at a higher stratigraphic level than that indicated by Bukry (1978). In the middle Miocene of the eastern equatorial Pacific, *C. macintyrei* is very rare and discontinuously present in the lower part of its range.

Elliptical *Calcidiscus* referred to *Calcidiscus premacintyrei* are consistently present in Zones CN3 and CN4, and become extinct in the upper part of Subzone CN5a.

Discoasterids

Discoasterids recorded in the sediments of Leg 138 show variable distribution and preservation patterns between the different sites and at different stratigraphic intervals. Rich and well-preserved discoasterid assemblages have been observed mainly at sites located out of the equatorial divergence zone and out of the influence of upwelling. Overgrown discoasterids were recorded in the Miocene interval, making the identification of the different species difficult and sometimes impossible, particularly within the lower and middle Miocene nannofossil assemblages.

Pliocene Discoasterids

Pliocene discoasterid species were identified following concepts outlined in Backman and Shackleton (1983). In this time interval, the assemblages are dominated by *Discoaster brouweri. D. pentaradiatus* is common or abundant in the early Pliocene; *Discoaster surculus, D. variabilis, D. decorus, D. tristellifer,* and, overall, *D. tamalis* and *D. asymmetricus* are subordinate.

Late–early Miocene through late Miocene Discoasterids

The massive six-rayed forms, which characterize discoasterid assemblages in the early and middle Miocene, were replaced by slender forms with bifurcated and pointed tips in the late Miocene. This turnover in the discoasterid assemblages, which took place gradually within the late–middle Miocene, is particularly evidenced by the appearance in the stratigraphic record of five-rayed discoasterids. The species of five-rayed discoasterids observed in the eastern equatorial Pacific are the *D. bellus* group, *D. hamatus, D. berggrenii, D. quinqueramus* and *Discoaster* sp. 1 (sensu Rio et al., 1990a).

Specimens belonging to *Discoaster bellus* gr. are characterized by small size (6–8 µm) and poorly developed central area. Morphotypes with intergrade morphologic features between *D. bellus* and *D. hamatus* and between *D. bellus* and *D. berggrenii* are included in the group.

Discoaster hamatus is characterized by five long rays with a spine extending and bending sharply near the tips (Plate 1, Fig. 1). Specimens relatively thin and smaller (8–10 μm in size) than standard have been observed in the material studied.

To *D. berggrenii,* we ascribed forms even with a poorly developed central knob, with a distinct central area, following Rio et al. (1990a). In the material studied, *D. berggrenii* appears and becomes extinct earlier than *D. quinqueramus,* according to Bukry (1971); in the range charts, the two species were lumped together because intergrades between typical *D. berggrenii* and *D. quinqueramus* are commonly recorded. Large specimens of *D. quinqueramus* (about 16 μm) were observed in the final range of the species. Small five-rayed discoasterids, which are common and continuously distributed up to the highest occurrence of *D. quinqueramus,* are referred to as *Discoaster* sp. 1 (Plate 2, Fig. 5). This form is smaller in size than *D. berggrenii* and *D. quinqueramus* (6–8 μm vs. 8–15 μm) and has a poorly developed central area with a very small knob (see Rio et al., 1990a, pl. 2, fig. 9).

The six-rayed species of slender discoasterids with pointed tips considered here are *D. braarudii, D. brouweri, D. intercalaris, D. neohamatus, D. neorectus,* and *Discoaster* sp. 2 (sensu Rio et al., 1990a). *D. braarudii* and *D. neorectus* are found with rare and scattered specimens; the medium-sized *D. intercalaris* is rather common, but it occurs discontinuously. The first and rare *D. brouweri* appears in the upper part of Subzone CN5, and becomes common and continuously distributed in Zone CN7. In the eastern equatorial Pacific, within Subzones CN9a and CN9b (lower part), we observed a large discoasterid (20–30 μm in size) morphologically similar to *D. brouweri* and referred to as *Discoaster* sp. 2 (Plate 2, Figs. 6–7), which was observed by Rio et al. (1990a) in the equatorial Indian Ocean. In the material studied, it is rare and discontinuous, and does not provide a meaningful biostratigraphic signal.

D. neohamatus was easily recognized, even in overgrown assemblages. The feature of its long pointed rays is a "spine" at tips, which sharply bends in one direction; it can be recognized even in strongly overgrown specimens. It is less protruding in specimens found in the terminal range of the species, where intergrade forms between *D. brouweri* and *D. neohamatus* were observed.

Among slender discoasterids with bifurcating rays, we considered the groups of five-rayed (*D. moorei, D. pentaradiatus,* and *D. prepentaradiatus*) and six-rayed (*D. bollii, D. calcaris, D.* aff. *calcaris, D. challengeri, D. exilis, D. icarus, D. loeblichii, D. pansus, D. perclarus, D. pseudovariabilis, D. surculus, D. subsurculus, D. signus, D. tuberi,* and *D. variabilis*) discoasterids. The four-rayed species *D. blackstockae* is found only in spot samples with single specimens.

D. moorei is easily recognized by its asymmetrical rays, even in overgrown assemblages, and it is distributed scattered and in low abundances from Zones CN3 to CN6. *D. prepentaradiatus* was distinguished from *D. pentaradiatus* for the poorly developed central area and for the shape of its arms, which are shorter and bend downward and lack birefringence. *D. pentaradiatus* shows a certain degree of morphologic variability, consisting in arms more or less slender and bifurcations more or less developed.

Among six-rayed bifurcating discoasterids, some species are not easily differentiated because many intergrading forms exist. The classifications of *D. variabilis* and *D. surculus* take into account their high degree of variability in morphologic features. *D. perclarus* and *D. icarus* are found to be very rare and scattered. Typical *D. calcaris* (Plate 1, Fig. 2) is common and has restricted range in intervals close (just below) the lowest occurrence of *D. hamatus. D.* aff. *calcaris* is a discoasterid observed and described by Rio et al. (1990a; see pl. 7, figs. 4–6) in the equatorial Indian Ocean. We found this form as rare and scattered within Subzone CN5b. We could not distinguish *D. signus* and *D. tuberi,* the observed specimens having often the tips of bifurcated rays broken. Therefore, we designated with a single species epithet, *D. signus,* those discoasterids with characteristic central prominent knob, recognizable even in strongly overgrown assemblages.

The middle Miocene discoasterid assemblage is characterized by six-rayed forms belonging to *D. musicus* (= *D. sanmiguelensis*) and *D. kugleri* group, having a broad central area of variable size, larger than the length of the rays; species circumscription within this group is sometimes difficult when overgrowth is present. In the material studied, *D. kugleri* (Plate 1, Figs. 3–5) is present with typical specimens having a flat central area that lacks the large star-shaped knob of *D. musicus* specimens.

Another middle Miocene form observed is the small discoasterid *D. adamanteus,* recognized even in strongly overgrown assemblages, where, on the contrary, it was difficult to distinguish species like *D. aulakos, D. variabilis,* and *D. exilis.* The same problems of identification arose in the early Miocene interval, in which discoasterids are generally poorly preserved. Distinction within *D. dilatus–D. extensus* group proved impossible, whereas the *D. deflandrei* group was discriminated, sometimes with difficulty. This group dominates the assemblages of the upper part of the early Miocene.

Ceratolithids

The horseshoe-shaped nannofossils belonging to the Ceratolithaceae family are a minor but distinctive component of the assemblages during the latest Miocene and early Pliocene. In the Leg 138 material, ceratolithids are present with variable abundances and are found overall at sites located north of the equatorial zone. In these sequences, qualitative observations on rich and well-preserved assemblages helped to clarify the phylogenetic relationship of the group. Appearance and extinction events of members of the ceratolithid group provide meaningful biostratigraphic signals in the late Neogene (summarized below, listed in stratigraphic succession).

Late Miocene ceratolithid events are as follows:

1. B (bottom occurrence of) *A. primus,*
2. B *A. delicatus,*
3. B *A. amplificus,* and
4. T (top occurrence of) *A. amplificus.*

Early Pliocene ceratolithid events are as follows:

5. B *C. acutus,*
6. B *C. armatus,*
7. B *C. rugosus,*
8. T *C. acutus,*
9. T *C. armatus,* and
10. T *A. primus, A. delicatus,* and *A. tricorniculatus.*

The first representative of the group is the species *A. primus,* within which two morphotypes can be distinguished. The primitive specimens are comparable with the holotype (see Bukry and Percival, 1971, pl. 1, fig. 12), have a thick arch, and evolve rapidly to more delicate crescent-shaped forms, which occur together with another delicate species, *A. delicatus.* In the material studied, the distinction between these two morphotypes is clear but does not seem to be stratigraphically useful, as they occur closely one after the other.

An interesting finding in some Leg 138 successions was the observation of transitional forms between *Triquetrorhabdulus rugosus–T. extensus* and *A. primus,* observed close to the appearance level of ceratolithids. The presence of such intergrading forms (Plate 3, Figs. 3, 4, and 6) confirms previous suggestions of a phylogenetic relationship between *Triquetrorhabdulus* and *Amaurolithus* (Gartner, 1967; Perch-Nielsen, 1977, 1985). A similar phylogenetic relationship was documented also at higher levels, where we observed nannofossils with transitional morphological features between *T. extensus* and *A. amplificus* (Plate 3, Figs. 7–8) just below the appearance of *A. amplificus.* Gartner and Bukry (1975) pointed out that the robust and asymmetrical *A. amplificus* could be related to *A. primus* and *A. delicatus,* although such a relationship is unclear. The presence of the intergrading forms indicates that *A. amplificus* probably evolved directly from *Triquetrorhabdulus.* These intergrading forms are also present within the range of typical *A. amplificus* and in the equatorial Indian Ocean (Rio et al., 1990a). The stratigraphic range of *A. amplificus* in the eastern equatorial Pacific is restricted to Chron 3An, as in the equatorial Indian Ocean (Rio et al., 1990a; Raffi et al., this volume).

A. tricorniculatus, an asymmetrical delicate ceratolithid with a pronounced apical spine, occurs discontinuously with rare specimens in sediments of the investigated sections; intergrade forms between *A. primus, A. delicatus,* and *A. tricorniculatus* are rather common.

Similar intergrading between different species was observed among the birefringent ceratolithids *C. acutus, C. armatus, C. rugosus, C. cristatus,* and *C. telesmus.* Therefore, species assignments and recognition of some events were sometimes difficult, and were also hindered by overgrowth problems. For this reason, we could not confidently recognize the events B *C. armatus* and T *C. armatus;* the event T *C. acutus* was also difficult to detect.

We point out the finding of forms that seem related to ceratolithids (shown in Plate 4, Figs. 5–7). These are birefringent rod-shaped forms, similar to species of the lower Cretaceous genus *Ceratolithina* (see Perch-Nielsen, 1988), and were found as rare and scattered in the lower part of Zone CN7 (NN9). Similar forms were also observed by one of us (I.R.) at Sites 710 and 714 in the western equatorial Indian Ocean in the same stratigraphic interval.

Triquetrorhabdulids

Species ascribed to the genus *Triquetrorhabdulus* observed in Leg 138 Miocene sediments are *T. extensus, T. milowii, T. rugosus,* and *T. serratus.*

T. rioensis and *T. farnsworthii* were included in the taxonomic unit *T. rugosus,* as *T. rioensis* has the same stratigraphic distribution as *T. rugosus,* and *T. farnsworthii* was considered a well-preserved morphotype of *T. rugosus,* common in the upper part of its range. *T. extensus* was found in the upper Miocene interval together with intergrade forms between *Amaurolithus* species (see above).

T. milowii was found to be rare and sporadic. *T. serratus* is common in the lower and middle Miocene interval, and disappears within Subzone CN5a, just above the appearance of *T. rugosus.*

Helicoliths

Helicolith nannofossils, which are not solution resistant, occur continuously in most of the Leg 138 sequences. Helicoliths are missing or represented by strongly etched specimens in the intervals where dissolution affects nannofossil assemblages, as in the upper Miocene and lower Pliocene intervals at Sites 844 and 845.

The species recognized are listed in Appendix A. Among them, we included into the group of *H. carteri* specimens with slightly variable morphology. In the late early Miocene, *H. ampliaperta* is generally rare but clearly distinguishable within the helicolith assemblage dominated by *H. intermedia,* recorded up to Zone CN5, and *H. granulata.*

Sphenoliths

Sphenoliths are a major constituent of the Miocene and early Pliocene nannofossil assemblages of the eastern equatorial Pacific. We observed characteristic high-abundance intervals (blooms) of these nannoliths in the Leg 138 sequences. The simultaneous extinction of *S. abies* and *S. neoabies* in the Pliocene (Backman and Shackleton, 1983) provides a useful event; the two species have been grouped together with *S. moriformis* and *S. compactus* (as *Sphenolithus* spp.) in the range charts, as differentiations among these species are not always clear. The typical spined sphenolith *S. heteromorphus* is abundant in the material studied, and its extinction event provides a neat biostratigraphic signal in the middle Miocene.

ACKNOWLEDGMENTS

We would like to thank J. Backman and D. Rio for their critical reviews, comments, and suggestions, which improved the quality of this paper. Special thanks go to J.W. Farrell and A. Sposato for the help given in some phases of this work. Funding for this study was provided by CNR Grant No. AI91.00913.05 to I. Raffi.

REFERENCES[*]

Aguirre, E., and Pasini, G., 1985. The Pliocene-Pleistocene boundary. *Episodes,* 8:11–120.

Aubry, M.-P., 1984. *Handbook of Cenozoic Calcareous Nannoplankton* (Book 1): *Ortholithae (Discoasters):* New York (Micropaleontology Press).

————, 1988. *Handbook of Calcareous Nannoplankton* (Book 2): *Ortholithae (Catinasters, Ceratoliths, Rhabdoliths):* New York (Micropaleontology Press).

————, 1989. *Handbook of Cenozoic Calcareous Nannoplankton* (Book 3): *Ortholithae (Pentaliths and Others). Heliolithae (Fasciculiths, Sphenoliths, and Others):* New York (Micropaleontology Press).

————, 1990. *Handbook of Cenozoic Calcareous Nannoplankton* (Book 4): *Heliolithae (Helicoliths, Cribriliths, Lopadoliths, and Others):* New York (Micropaleontology Press).

Backman, J., and Pestiaux, P., 1987. Pliocene *Discoaster* abundance variations, Deep Sea Drilling Project Site 606: biochronology and paleoenvironmental implications. *In* Ruddiman, W.F., Kidd, R.B., Thomas, E., et al., *Init. Repts. DSDP,* 94 (Pt. 2): Washington (U.S. Govt. Printing Office), 903–910.

Backman, J., Schneider, D.A., Rio, D., and Okada, H., 1990. Neogene low-latitude magnetostratigraphy from Site 710 and revised age estimates of Miocene nannofossil datum events. *In* Duncan, R.A., Backman, J., Peterson, L.C., et al., *Proc. ODP, Sci. Results,* 115: College Station, TX (Ocean Drilling Program), 271–276.

Backman, J., and Shackleton, N.J., 1983. Quantitative biochronology of Pliocene and early Pleistocene calcareous nannofossils from the Atlantic, Indian and Pacific oceans. *Mar. Micropaleontol.,* 8:141–170.

Bergen, J.A., 1984. Calcareous nannoplankton from Deep Sea Drilling Project Leg 78A: evidence for imbricate underthrusting at the Lesser Antillian active margin. *In* Biju-Duval, B., Moore, J.C., et al., *Init. Repts. DSDP,* 78 (Pt. 1): Washington (U.S. Govt. Printing Office), 411–445.

Berggren, W.A., Kent, D.V., and Van Couvering, J.A., 1985. The Neogene: Part 2. Neogene geochronology and chronostratigraphy. *In* Snelling, N.J. (Ed.), *The Chronology of the Geological Record.* Geol. Soc. London Mem., 10:211–260.

Bukry, D., 1971. *Discoaster* evolutionary trends. *Micropaleontology,* 17:43–52.

————, 1973. Low-latitude coccolith biostratigraphic zonation. *In* Edgar, N.T., Saunders, J.B., et al., *Init. Repts. DSDP,* 15: Washington (U.S. Govt. Printing Office), 685–703.

————, 1975. Coccolith and silicoflagellate stratigraphy, northwestern Pacific Ocean, Deep Sea Drilling Project Leg 32. *In* Larson, R.L., Moberly, R., et al., *Init. Repts. DSDP,* 32: Washington (U.S. Govt. Printing Office), 677–701.

————, 1978. Biostratigraphy of Cenozoic marine sediment by calcareous nannofossils. *Micropaleontology,* 24:44–60.

————, 1991. Paleoecological transect of western Pacific Ocean late Pliocene coccolith flora. Part I: Tropical Ontong-Java Plateau at ODP 806B. *Open-File Rep.—U.S. Geol. Surv.,* 91-552:1–35.

Bukry, D., and Percival, S.F., 1971. New Tertiary calcareous nannofossils. *Tulane Stud. Geol. Paleontol.,* 8:123–146.

Cande, S.C., and Kent, D.V., 1992. A new geomagnetic polarity time scale for the Late Cretaceous and Cenozoic. *J. Geophys. Res.,* 97:13917–13951.

Channell, J.E.T., Rio, D., and Thunell, R.C., 1988. Miocene/Pliocene boundary magnetostratigraphy at Capo Spartivento, Calabria, Italy. *Geology,* 16:1096–1099.

Chepstow-Lusty, A., Backman, J., and Shackleton, N.J., 1989. Comparison of upper Pliocene *Discoaster* abundance variations from North Atlantic Sites 552, 607, 658, 659 and 662: further evidence for marine plankton responding to orbital forcing. *In* Ruddiman, W.F., Sarnthein, M., et al., *Proc. ODP, Sci. Results,* 108: College Station, TX (Ocean Drilling Program), 121–141.

Chepstow-Lusty, A., Shackleton, N.J., and Backman, J., 1992. Upper Pliocene *Discoaster* abundance from the Atlantic, Pacific, and Indian oceans: the significance of productivity pressure at low latitudes. *Mem. Sci. Geol.,* 44:357–373.

Cita, M.B., and Premoli Silva, I., 1968. Evolution of the planktonic foraminiferal assemblages in the stratigraphical interval between the type-Langhian and the type-Tortonian and biozonation of the Miocene of Piedmont. *G. Geol.,* 35:1–23.

Ellis, C.H., 1982. Calcareous nannoplankton biostratigraphy—Deep Sea Drilling Project Leg 60. *In* Hussong, D.M., Uyeda, S., et al., *Init. Repts. DSDP,* 60: Washington (U.S. Govt. Printing Office), 507–535.

Fornaciari, E., Backman, J., and Rio, D., 1993. Quantitative distribution patterns of selected lower to middle Miocene calcareous nannofossils from the Ontong Java Plateau. *In* Berger, W.H., Kroenke, L.W., Mayer, L.A., et al., *Proc. ODP, Sci. Results,* 130: College Station, TX (Ocean Drilling Program), 245–256.

Fornaciari, E., Raffi, I., Rio, D., Villa, G., Backman, J., and Olafsson, G., 1990. Quantitative distribution patterns of Oligocene and Miocene calcareous nannofossils from the western equatorial Indian Ocean. *In* Duncan, R.A., Backman, J., Peterson, L.C., et al., *Proc. ODP, Sci. Results,* 115: College Station, TX (Ocean Drilling Program), 237–254.

Gartner, S., 1967. Calcareous nannofossils from Neogene of Trinidad, Jamaica, and Gulf of Mexico. *Univ. Kansas Paleontol. Contrib.,* 29.

————, 1977. Calcareous nannofossil biostratigraphy and revised zonation of the Pleistocene. *Mar. Micropaleontol.,* 2:1–25.

————, 1992. Miocene nannofossil chronology in the North Atlantic, DSDP Site 608. *Mar. Micropaleontol.,* 18:307–331.

Gartner, S., and Bukry, D., 1975. Morphology and phylogeny of the coccolithophycean family Ceratolithaceae. *J. Res. U.S. Geol. Surv.,* 3:451–465.

Gartner, S., and Chow, J., 1985. Calcareous nannofossil biostratigraphy, Deep Sea Drilling Project Leg 85, eastern equatorial Pacific. *In* Mayer, L., Theyer, F., Thomas, E., et al., *Init. Repts. DSDP,* 85: Washington (U.S. Govt. Printing Office), 609–619.

[*] Abbreviations for names of organizations and publication titles in ODP reference lists follow the style given in *Chemical Abstracts Service Source Index* (published by American Chemical Society).

Hagelberg, T., Shackleton, N., Pisias, N., and Shipboard Scientific Party, 1992. Development of composite depth sections for Sites 844 through 854. *In* Mayer, L., Pisias, N., Janecek, T., et al., *Proc. ODP, Init. Repts.*, 138 (Pt. 1): College Station, TX (Ocean Drilling Program), 79–85.
Hey, R., 1977. Tectonic evolution of the Cocos-Nazca spreading center. *Geol. Soc. Am. Bull.*, 88:1404–1420.
Hilgen, F.J., 1991a. Astronomical calibration of Gauss to Matuyama sapropels in the Mediterranean and implication for the Geomagnetic Polarity Time Scale. *Earth Planet. Sci. Lett.*, 104:226–244.
————, 1991b. Extension of the astronomically calibrated (polarity) time scale to the Miocene-Pliocene boundary. *Earth Planet. Sci. Lett.*, 107:349–368.
Hilgen, F.J., and Langereis, C.G., 1988. The age of the Miocene-Pliocene boundary in the Capo Rossello area (Sicily). *Earth Planet. Sci. Lett.*, 91:214–222.
Loeblich, A.R., and Tappan, H., 1966. Annotated index and bibliography of the calcareous nannoplankton. *Phycologia*, 5:81–215.
————, 1968. Annotated index and bibliography of the calcareous nannoplankton II. *J. Paleontol.*, 42:584–598.
————, 1969. Annotated index and bibliography of the calcareous nannoplankton III. *J. Paleontol.*, 43:568–588.
————, 1970a. Annotated index and bibliography of the calcareous nannoplankton IV. *J. Paleontol.*, 44:558–574.
————, 1970b. Annotated index and bibliography of the calcareous nannoplankton V. *Phycologia*, 9:157–174.
————, 1971. Annotated index and bibliography of the calcareous nannoplankton VI. *Phycologia*, 10:315–339.
————, 1973. Annotated index and bibliography of the calcareous nannoplankton VII. *J. Paleontol.*, 47:715–759.
Martini, E., 1971. Standard Tertiary and Quaternary calcareous nannoplankton zonation. *In* Farinacci, A. (Ed.), *Proc. 2nd Int. Conf. Planktonic Microfossils Roma:* Rome (Ed. Tecnosci.), 2:739–785.
Mayer, L., Pisias, N., Janecek, T., et al., 1992. *Proc. ODP, Init. Repts.*, 138 (Pts. 1 and 2): College Station, TX (Ocean Drilling Program).
Mayer, L.A., Shipley, T.H., and Winterer, E.L., 1986. Equatorial Pacific seismic reflectors as indicators of global oceanographic events. *Science*, 233:761–764.
Mazzei, R., Raffi, I., Rio, D., Hamilton, N., and Cita, M.B., 1979. Calibration of late Neogene calcareous plankton datum planes with the paleomagnetic record of Site 397 and correlation with Moroccan and Mediterranean sections. *In* von Rad, U., Ryan, W.B.F., et al., *Init. Repts. DSDP*, 47 (Pt. 1): Washington (U.S. Govt. Printing Office), 375–389.
Okada, H., and Bukry, D., 1980. Supplementary modification and introduction of code numbers to the low-latitude coccolith biostratigraphic zonation (Bukry, 1973; 1975). *Mar. Micropaleontol.*, 5:321–325.
Olafsson, G., 1989. Quantitative calcareous nannofossil biostratigraphy of upper Oligocene to middle Miocene sediment from ODP Hole 667A and middle Miocene sediment from DSDP Site 574. *In* Ruddiman, W., Sarnthein, M., et al., *Proc. ODP, Sci. Results*, 108: College Station, TX (Ocean Drilling Program), 9–22.
————, 1991. Quantitative calcareous nannofossil biostratigraphy and biochronology of early through late Miocene sediments from DSDP Hole 608. *Medd. Stockholms Univ. Inst. Geol. Geok.*, 285.
Parker, M.E., Clark, M., and Wise, S.W., Jr., 1985. Calcareous nannofossils of Deep Sea Drilling Project Sites 558 and 563, North Atlantic Ocean: biostratigraphy and the distribution of Oligocene braarudosphaerids. *In* Bougault, H., Cande, S.C., et al., *Init. Repts. DSDP*, 82: Washington (U.S. Govt. Printing Office), 559–589.
Perch-Nielsen, K., 1977. Albian to Pleistocene calcareous nannofossils from the western South Atlantic, DSDP Leg 39. *In* Supko, P.R., Perch-Nielsen, K., et al., *Init. Repts. DSDP*, 39: Washington (U.S. Govt. Printing Office), 699–823.
————, 1985. Cenozoic calcareous nannofossils. *In* Bolli, H.M., Saunders, J.B., and Perch-Nielsen, K. (Eds.), *Plankton Stratigraphy:* Cambridge (Cambridge Univ. Press), 427–554.
————, 1988. New Lower Cretaceous calcareous nannofossil species from England. *INA Newsl.*, 10:30–36.
Proto Decima, F., Medizza, F., and Todesco, L., 1978. Southeastern Atlantic Leg 40 calcareous nannofossils. *In* Bolli, H.M., Ryan, W.B.F., et al., *Init. Repts. DSDP*, 40: Washington (U.S. Govt. Printing Office), 571–634.
Raffi, I., Backman, J., Rio, D., and Shackleton, N.J., 1993. Plio-Pleistocene nannofossil biostratigraphy and calibration to oxygen isotopes stratigraphies from Deep Sea Drilling Project Site 607 and Ocean Drilling Program Site 677. *Paleoceanography*, 8:387–408.
Raffi, I., and Rio, D., 1979. Calcareous nannofossil biostratigraphy of DSDP Site 132—Leg 13 (Tyrrhenian Sea—Western Mediterranean). *Riv. Ital. Paleontol. Stratigr.*, 85:127–172.
Ramsay, A.T.S., 1972. Aspects of the distribution of fossil species of calcareous nannoplankton in North Atlantic and Caribbean sediments. *Nature*, 236:67–70.
————, 1977. Sedimentological clues to paleoceanography. *In* Ramsay, A.T.S. (Ed.), *Oceanic Micropaleontology* (Vol. 2): New York (Academic Press), 1371–1453.
Ramsay, A.T.S., Schneidermenn, N., and Finch, J.W., 1973. Fluctuations in the past rates of carbonate solution at Site 149: a comparison with other ocean basins and an interpretation of their significance. *In* Edgar, N.T., Saunders, J.B., et al., *Init. Repts. DSDP*, 15: Washington (U.S. Govt. Printing Office), 805–811.
Rio, D., 1982. The fossil distribution of coccolithophore genus *Gephyrocapsa* Kamptner and related Plio-Pleistocene chronostratigraphic problems. *In* Prell, W.L., Gardner, J.V., et al., *Init. Repts. DSDP*, 68: Washington (U.S. Govt. Printing Office), 325–343.
Rio, D., Backman, J., Raffi, I., in press. Calcareous nannofossil biochronology and the Pliocene/Pleistocene boundary: the Neogene/Quaternary boundary. *Final Rep. IGCP Project*, 41.
Rio, D., Fornaciari, E., and Raffi, I., 1990a. Late Oligocene through early Pleistocene calcareous nannofossils from western equatorial Indian Ocean (Leg 115). *In* Duncan, R.A., Backman, J., Peterson, L.C., et al., *Proc. ODP, Sci. Results*, 115: College Station, TX (Ocean Drilling Program), 175–235.
Rio, D., Raffi, I., and Villa, G., 1990b. Pliocene-Pleistocene calcareous nannofossil distribution patterns in the Western Mediterranean. *In* Kastens, K.A., Mascle, J., et al., *Proc. ODP, Sci. Results*, 107: College Station, TX (Ocean Drilling Program), 513–533.
Rio, D., Sprovieri, R., and Di Stefano, E., 1994. The Gelasian stage: a proposal of a new chronostratigraphic unit of the Pliocene series. *Riv. It. Paleontol. Strat.*, 100:103–124.
Rio, D., Sprovieri, R., and Fornaciari, E., 1990. Remarks on the middle/late Miocene boundary. *IX R.C.M.N.S. Congr., Barcelona, Abstr. Volume*, 283.
Rio, D., Sprovieri, R., and Thunell, R., 1991. Pliocene–lower Pleistocene chronostratigraphy: a re-evaluation of Mediterranean type sections. *Geol. Soc. Am. Bull.*, 103:1049–1058.
Roth, P.H., 1974. Calcareous nannofossils from the northwestern Indian Ocean, Leg 24, Deep Sea Drilling Project. *In* Fisher, R.L., Bunce, E.T., et al., *Init. Repts. DSDP*, 24: Washington (U.S. Govt. Printing Office), 969–994.
————, 1983. Jurassic and Lower Cretaceous calcareous nannofossils in the western North Atlantic (Site 534): biostratigraphy, preservation, and some observations on biogeography and paleoceanography. *In* Sheridan, R.E., Gradstein, F.M., et al., *Init. Repts. DSDP*, 76: Washington (U.S. Govt. Printing Office), 587–621.
Roth, P.H., and Thierstein, H., 1972. Calcarcous nannoplankton: Leg 14 of the Deep Sea Drilling Project. *In* Hayes, D.E., Pimm, A.C., et al., *Init. Repts. DSDP*, 14: Washington (U.S. Govt. Printing Office), 421–485.
Takayama, T., 1970. The Pliocene-Pleistocene boundary in the Lamont Core V-21-98 and at Le Castella, Southern Italy. *J. Mar. Geol.*, 6:70–77.
Takayama, T., and Sato, T., 1987. Coccolith biostratigraphy of the North Atlantic Ocean, Deep Sea Drilling Project Leg 94. *In* Ruddiman, W.F., Kidd, R.B., Thomas, E., et al., *Init. Repts. DSDP*, 94 (Pt. 2): Washington (U.S. Govt. Printing Office), 651–702.
Tauxe, L., Opdyke, N.D., Pasini, G., and Elmi, C., 1983. The paleomagnetism of the Vrica section (Calabria, Italy): the proposed Pliocene/Pleistocene Boundary-stratotype section. *Nature*, 304:125–129.
Thierstein, H.R., Geitzenauer, K., Molfino, B., and Shackleton, N.J., 1977. Global synchroneity of late Quaternary coccolith datum levels: validation by oxygen isotopes. *Geology*, 5:400–404.
Young, J.R., 1990. Size variation of Neogene *Reticulofenestra* coccoliths from Indian Ocean DSDP Cores. *J. Micropaleontol.*, 9:71–85.
Zijderveld, J.D.A., Zachariasse, J.W., Verhallen, P.J.J.M., and Hilgen, F.J., 1986. The age of the Miocene-Pliocene boundary. *Newsl. Stratigr.*, 16:169–181.

Date of initial receipt: 12 April 1993
Date of acceptance: 31 December 1993
Ms 138SR-112

APPENDIX A

Calcareous Nannofossils Considered in This Chapter (in Alphabetic Order of Generic Epithets)

Amaurolithus amplificus (Bukry and Percival, 1971) Gartner and Bukry, 1975
Amaurolithus delicatus Gartner and Bukry, 1975
Amaurolithus primus (Bukry and Percival, 1971) Gartner and Bukry, 1975
Amaurolithus tricorniculatus (Gartner, 1967) Gartner and Bukry, 1975
Calcidiscus leptoporus (Murray and Blackman, 1898) Loeblich and Tappan, 1978
Calcidiscus macintyrei (Bukry and Bramlette, 1969) Loeblich and Tappan, 1978
Calcidiscus premacintyrei Theodoridis, 1984
Catinaster calyculus Martini and Bramlette, 1963
Catinaster coalitus Martini and Bramlette, 1965
Ceratolithus acutus Gartner and Bukry, 1974
Ceratolithus armatus Müller, 1974
Ceratolithus cristatus Kamptner, 1950
Ceratolithus rugosus Bukry and Bramlette, 1968
Ceratolithus telesmus Norris, 1965
Coccolithus miopelagicus Bukry, 1971
Coccolithus pelagicus (Wallich, 1877) Schiller, 1930
Coccolithus radiatus Kamptner, 1955
Coronocyclus nitescens (Kamptner, 1963) Bramlette and Wilcoxon, 1967
Cyclicargolithus floridanus (Roth and Hay in Hay et al., 1967) Bukry, 1971
Discoaster adamanteus Bramlette and Wilcoxon, 1967
Discoaster asymmetricus Gartner, 1969
Discoaster aulakos Gartner, 1967
Discoaster bellus Bukry and Percival, 1971
Discoaster berggrenii Bukry, 1971
Discoaster blackstockae Bukry, 1973
Discoaster bollii Martini and Bramlette, 1963
Discoaster braarudii Bukry, 1971
Discoaster brouweri Tan (1927) emend. Bramlette and Riedel, 1954
Discoaster calcaris Gartner, 1967
Discoaster challengeri Bramlette and Riedel, 1954
Discoaster decorus (Bukry, 1971) Bukry, 1973
Discoaster deflandrei Bramlette and Riedel, 1954
Discoaster exilis Martini and Bramlette, 1963
Discoaster hamatus Martini and Bramlette, 1963
Discoaster icarus Stradner, 1973
Discoaster intercalaris Bukry, 1971
Discoaster kugleri Martini and Bramlette, 1963
Discoaster loeblichii Bukry, 1971
Discoaster misconceptus Theodoridis, 1984 = *Discoaster pentaradiatus*
Discoaster moorei Bukry, 1971
Discoaster musicus Stradner, 1959
Discoaster neohamatus Bukry and Bramlette, 1969
Discoaster neorectus Bukry, 1971
Discoaster pansus (Bukry and Percival, 1971) Bukry, 1973
Discoaster pentaradiatus Tan (1927) emend. Bramlette and Riedel, 1954
Discoaster perclarus Haq in Haq et al., 1967
Discoaster prepentaradiatus Bukry and Percival, 1971
Discoaster pseudovariabilis Martini and Worsley, 1971
Discoaster quinqueramus Gartner, 1969
Discoaster sanmiguelensis Bukry, 1981 = *Discoaster musicus*
Discoaster signus Bukry, 1971
Discoaster subsurculus Gartner, 1967
Discoaster surculus Martini and Bramlette, 1963
Discoaster tamalis Kamptner, 1967
Discoaster triradiatus Tan, 1927
Discoaster tristellifer Bukry, 1976
Discoaster tuberi Filewicz, 1984
Discoaster variabilis Martini and Bramlette, 1963
Geminilithella rotula (Kamptner, 1956) Backman, 1980
Gephyrocapsa oceanica Kamptner, 1943
Gephyrocapsa omega Bukry, 1973
Gephyrocapsa parallela Hay and Beaudry, 1973
Helicosphaera ampliaperta Bramlette and Wilcoxon, 1967
Helicosphaera carteri (Wallich, 1877) Kamptner, 1954
Helicosphaera carteri var. *wallichii* (Lohmann) Theodoridis, 1984
Helicosphaera hyalina Gaarder, 1970
Helicosphaera intermedia Martini, 1965
Helicosphaera sellii Bukry and Bramlette, 1969
Minylitha convallis Bukry, 1973
Orthorhabdus serratus Bramlette and Wilcoxon, 1967 = *Triquetrorabdulus serratus*
Pseudoemiliania lacunosa (Kamptner, 1963) Gartner, 1969
Reticulofenestra haqii Backman, 1978
Reticulofenestra minuta Roth, 1970
Reticulofenestra minutula (Gartner, 1967) Haq and Berggren, 1978
Reticulofenestra pseudoumbilicus (Gartner, 1967) Gartner, 1969
Sphenolithus abies Deflandre in Deflandre and Fert, 1954
Sphenolithus heteromorphus Deflandre, 1953
Sphenolithus moriformis (Brönnimann and Stradner, 1960) Bramlette and Wilcoxon, 1967
Sphenolithus neoabies Bukry and Bramlette, 1969
Triquetrorhabdulus extensus Theodoridis, 1984
Triquetrorhabdulus farnsworthii (Gartner, 1967) Perch-Nielsen, 1985 = *Triquetrorhabdulus rugosus*
Triquetrorhabdulus milowii Bukry, 1971
Triquetrorhabdulus rioensis Olafsson, 1989
Triquetrorhabdulus rugosus Bramlette and Wilcoxon, 1967
Triquetrorhabdulus serratus (Bramlette and Wilcoxon, 1967) Olafsson, 1989

APPENDIX B

Definition, Occurrence, and Remarks for the Three Biostratigraphic Units That Divide Okada and Bukry (1980) Subzone CN9b

CN9bA. *Amaurolithus primus* Subzone

Definition: Top - lowest occurrence of *Amaurolithus amplificus*; bottom - lowest occurrence of *A. primus*.

Occurrence: The type locality is Hole 853B from Sample 138-853B-7H-2, 147 cm, to -6H-4, 65 cm. Other occurrences are recorded at Leg 138 Sites 844, 845, 846, 848, 849, 850, 851, and 852, and at Leg 115 Sites 707, 709, 710, 711, and 713.

CN9bB. *Amaurolithus amplificus* Subzone

Definition: Top - highest occurrence of *A. amplificus*; bottom - lowest occurrence of *A. amplificus*.

Remarks: Bergen (1984) indicated that *A. amplificus* became extinct within the upper part of CN9b in sediments from the tropical Atlantic Ocean. Similar distribution range for *A. amplificus* has been observed by Rio et al. (1990a) in the equatorial Indian Ocean, where it was calibrated to the polarity time scale and corresponded to Chron 3An. This same stratigraphic position for *A. amplificus* is recorded in the eastern equatorial Pacific.

Occurrence: The type locality is Hole 853B from Sample 138-853B-6H-4, 27 cm, to -5H-5, 120 cm. Other occurrences are recorded at Leg 138 Sites 844, 846, 848, 849, 850, 851, and 852, and at Leg 115 Sites 707, 709, 710, 711, and 713.

CN9bC. *Amaurolithus delicatus* Subzone

Definition: Top - highest occurrence of *Discoaster quinqueramus*; bottom - highest occurrence of *A. amplificus*.

Occurrence: The type locality is Hole 852B from Sample 138-852B-7H-CC to -7H-3, 140 cm. Other occurrences are recorded at Leg 138 Sites 844, 846, 848, 849, 850, 851, and 853, and at Leg 115 Sites 707, 709, 710, 711, and 713.

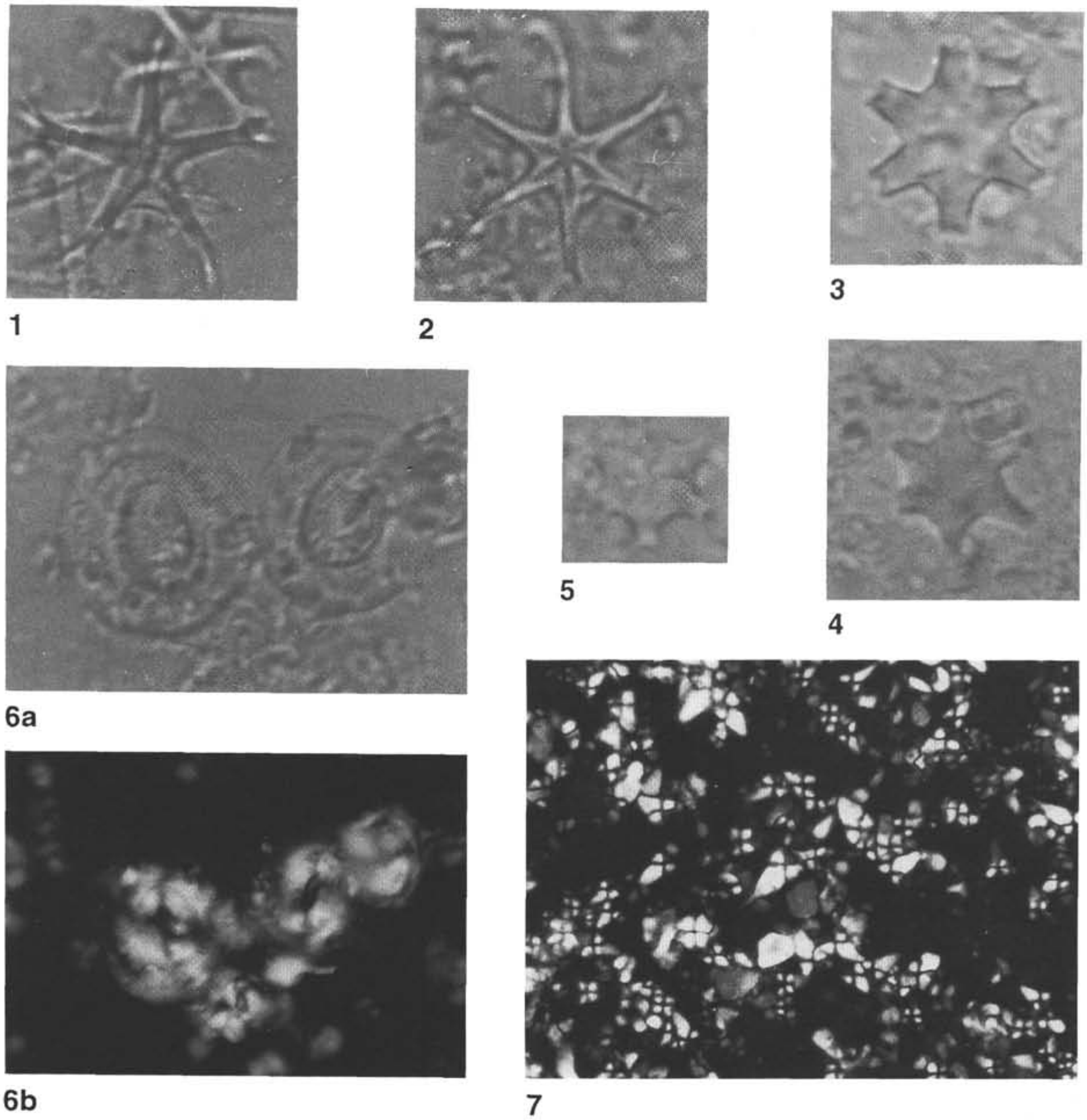

Plate 1. **1.** *Discoaster hamatus* Martini and Bramlette; ×2000. Sample 138-845A-15H-5, 149 cm; parallel light. **2.** *Discoaster calcaris* Gartner; ×2000. Sample 138-845A-16H-1, 120 cm; parallel light. **3–5.** *Discoaster kugleri* Martini and Bramlette; ×2000. Sample 138-846B-35X-3, 120 cm; parallel light. **6.** *Coccolithus miopelagicus* Bukry; ×2000. Sample 138-846B-35X-3, 120 cm; (a) parallel light; (b) crossed nicols. **7.** Acme in abundance of *Sphenolithus heteromorphus* Deflandre; ×1400. Sample 138-845A-31X-CC; crossed nicols.

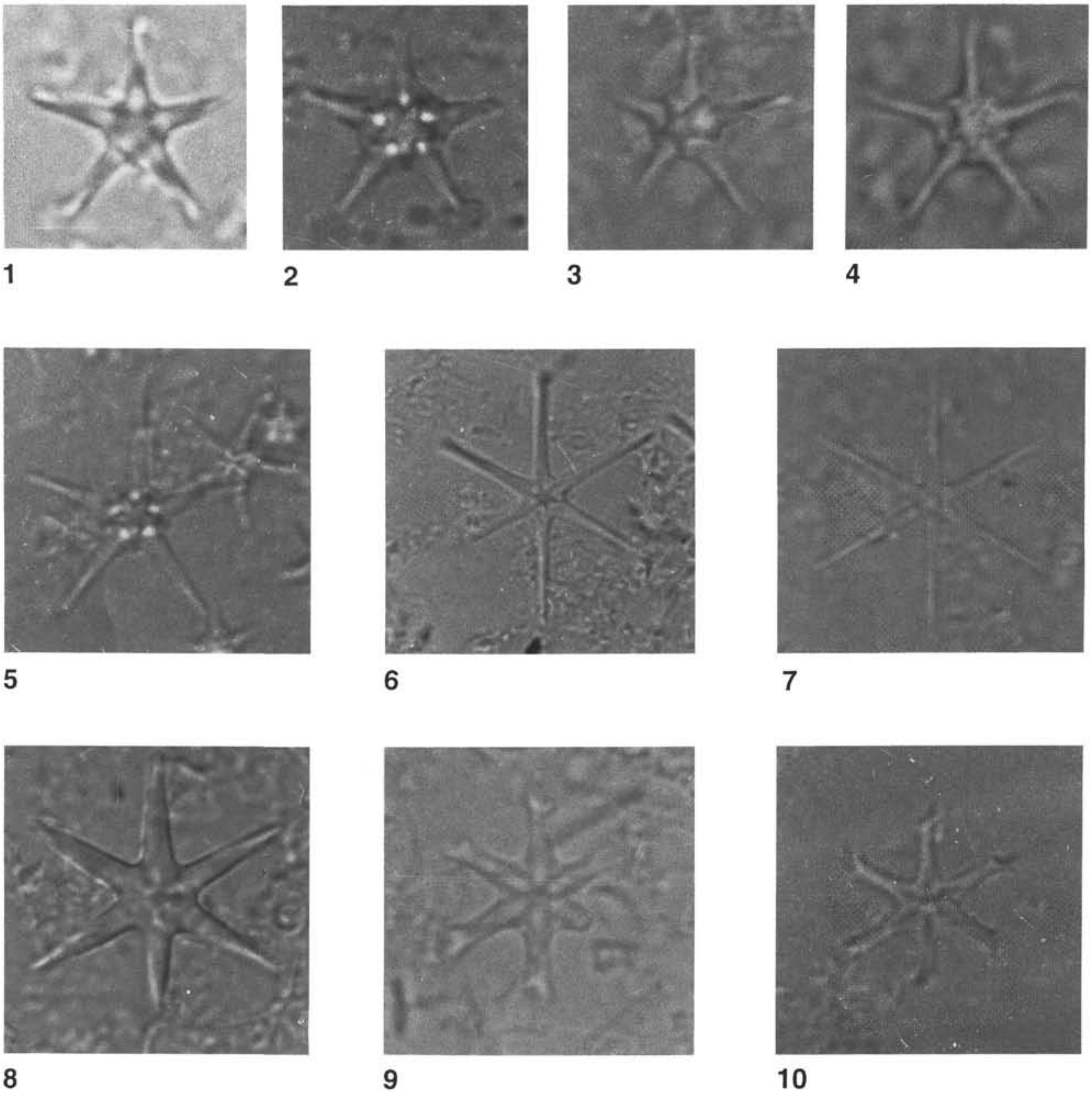

Plate 2. All specimens at parallel light. **1.** *Discoaster berggrenii* Bukry (primitive form); ×2000. Sample 138-853D-7H-4, 60 cm. **2.** *Discoaster berggrenii* Bukry; ×2400. Sample 138-844B-5H-2, 29 cm. **3.** *Discoaster berggrenii–Discoaster quinqueramus* intergrade; ×2000. Sample 138-853D-7H-1, 30 cm. **4.** *Discoaster quinqueramus* Gartner; ×2000. Sample 138-853D-7H-1, 30 cm. **5.** *Discoaster quinqueramus* Gartner (left) and *Discoaster* sp. 1 (right); ×2000. Sample 138-853B-6H-3, 65 cm. **6, 7.** *Discoaster* sp. 2; ×2000; (6) Sample 138-853B-7H-2, 147 cm; (7) Sample 138-853D-7H-1, 30 cm. **8.** *Discoaster neorectus* Bukry; ×2000. Sample 138-853D-7H-1, 30 cm. **9, 10.** *Discoaster loeblichii* Bukry; ×2000; (9) Sample 138-846B-30X-2, 60 cm; (10) Sample 138-853B-7H-4, 30 cm.

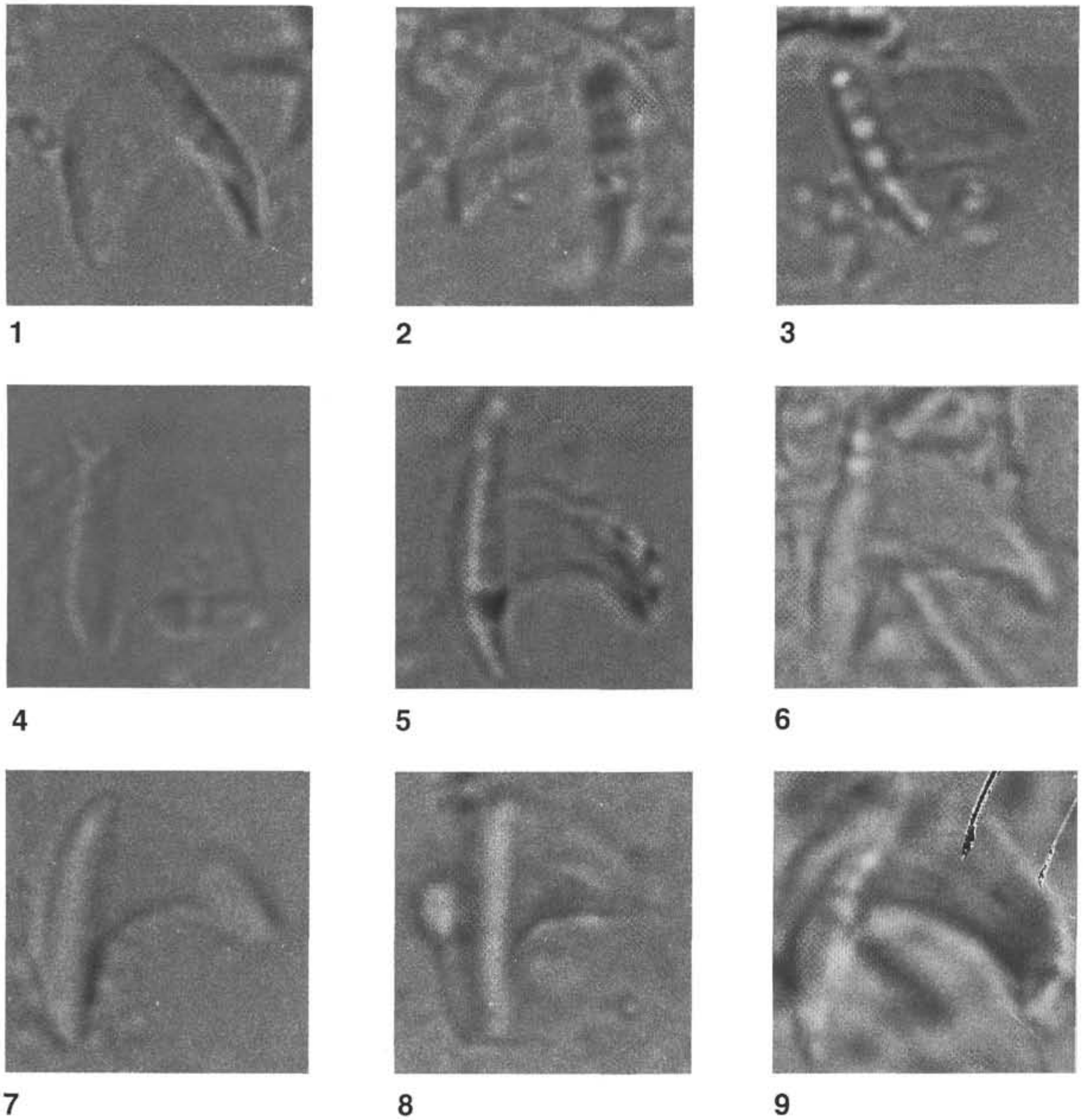

Plate 3. All specimens ×4000, parallel light. **1, 2, 5.** *Amaurolithus primus* (Bukry and Percival); (1, 2) Sample 138-853B-7H-3, 30 cm; (5) Sample 138-853B-7H-2, 147 cm. **3, 4, 6.** *Triquetrorhabdulus–Amaurolithus* intergrade. Sample 138-853B-7H-2, 147 cm. **7, 8.** *Triquetrorhabdulus extensus–Amaurolithus amplificus* intergrade; (7) Sample 138-853B-6H-4, 27 cm; (8) Sample 138-844B-5H-2, 129 cm. **9.** *Amaurolithus amplificus* (Bukry and Percival). Sample 138-844B-5H-2, 129 cm.

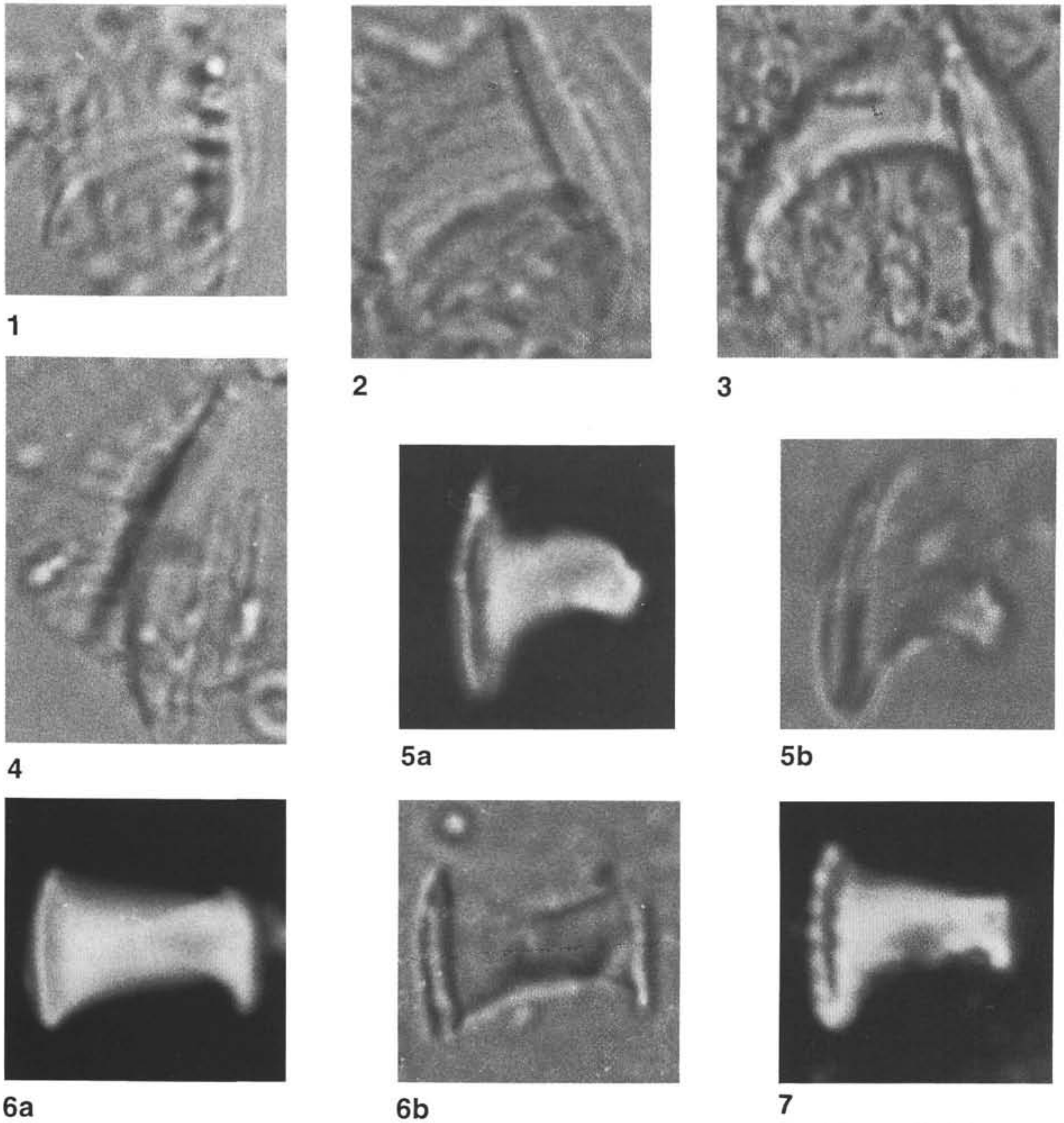

Plate 4. **1.** *Amaurolithus primus* (Bukry and Percival); ×4000. Sample 138-853B-7H-2, 147 cm; parallel light. **2.** *Triquetrorhabdulus extensus–Amaurolithus amplificus* intergrade; ×4000. Sample 138-853B-6H-4, 65 cm; parallel light. **3.** *Amaurolithus amplificus* (Bukry and Percival). Sample 138-853B-5H-6, 25 cm; parallel light. **4.** *Triquetrorhabdulus extensus* Theodoridis; ×4000, lateral view. Sample 138-844C-4H-1, 50 cm. **5–7.** *Ceratolithus*(?); (5) Sample 138-845B-15H-2, 145 cm; (6,7) Sample 138-845B-15H-2, 100 cm; (5a, 6a, 7) crossed nicols; (5b, 6b) parallel light.